MLC E0891

EVALUATION OF SHUTTLE SOLID ROCKET BOOSTER CASE MATERIALS

(NASA-CR-120160) EVALUATION OF SHUTTLE SOLID ROCKET BOOSTER CASE MATERIALS. CORROSION AND STRESS CORROSION (McDonnell-Douglas Astronautics Co.) 100 p HC $8.00 CSCL 21H G3/28 N74-20400 Unclas 16800

by

L.J. Pionke
K.C. Garland

28 December 1973

Prepared under Contract NAS8-27270

"Corrosion and Stress Corrosion Susceptibility of Several High Temperature Materials"

for the period
19 May 1972 to 19 October 1973
by
McDonnell Douglas Astronautics Company
St. Louis, Missouri
for
NATIONAL AERONAUTICS AND SPACE ADMINISTRATION
George C. Marshall Space Flight Center
Alabama 35812

Copy No. 166

FOREWC ɹD

This report was prepared by McDonnell Douglas Astronautics Company - East (MDAC-E) under NASA-MSFC Contract NAS-8-27270, Corrosion and Stress Corrosion Susceptibility of Several High Temperature Alloys.

The work reported herein describes the results of the second study year, which was concerned with the evaluation of two candidate Shuttle Solid Rocket Booster case materials. The work conducted during the first study year was concerned with the evaluation of candidate materials for a metallic Shuttle Thermal Protection System and is reported in McDonnell Douglas Report No. MDC E0609. Both programs were conducted under the direction of Mr. J. G. Williamson of the Metallic Materials Branch, Materials Division of the George C. Marshall Space Flight Center, National Aeronautics and Space Administration. Mr. L. J. Pionke was the Program Study Manager for MDAC-E; Mr. K. C. Garland conducted the laboratory testing and assisted in data analysis and preparation of the final report. The authors wish to gratefully acknowledge the assistance of J. W. Davis and J. J. Slavic, who contributed in many ways throughout the program.

ABSTRACT

Two candidate alloys for the Shuttle Solid Rocket Booster (SRB) case were tested under simulated service conditions to define subcritical flaw growth behavior under both sustained and cyclic loading conditions. The materials evaluated were D6AC and 18 Ni maraging steel, both heat treated to a nominal yield strength of 1380 MN/m^2 (200 ksi).

The sustained load tests were conducted by exposing precracked, stressed specimens of both alloys to alternate immersion in synthetic sea water. It was found that the corrosion and stress corrosion resistance of the 18 Ni maraging steel were superior to that of the D6AC steel under these test conditions. It was also found that austenitizing temperature had little influence on the threshold stress intensity (K_{TH}) of the D6AC.

The cyclic tests were conducted by subjecting precracked surface-flawed specimens of both alloys to repeated load/thermal/environmental profiles which were selected to simulate the SRB missions. It was found that liner removal operations that involve heating to 589°K (600°F) caused a decrease in cyclic life of D6AC steel relative to those tests conducted with no thermal cycling (i.e., load cycling at room temperature). It was also found that a decrease in the cyclic life of 18 Ni maraging steel occurred upon intermittent exposure to synthetic sea water during load/temperature cycling, relative to those tests conducted in the absence of sea water.

NOMENCLATURE

a	=	Crack depth of a semielliptical surface flaw
α	=	Proof test factor (proof ÷ maximum operating pressure)
B_n	=	Net thickness for MWOL specimens
c	=	Crack length in a MWOL specimen
$2c$	=	Crack length of a semielliptical surface flaw
c_1	=	Distance between centerline of load application and point at which displacement measurements were taken (MWOL specimens)
D_{CL}	=	Deflection of MWOL specimen, measured at centerline of load application
D_{End}	=	Deflection of MWOL specimen, measured at knife edges attached to end of specimen
d	=	Diameter of a cylindrical pressure vessel
E	=	Elastic modulus
G	=	Crack extension force (also, the strain energy release rate)
K	=	Stress intensity factor
K_f	=	Stress intensity at termination of fatigue precracking
K_i	=	Stress intensity at test initiation
K_{Ic}	=	Plane strain fracture toughness or critical stress intensity
K_{IE}	=	Apparent fracture toughness
K_{TH}	=	Threshold stress intensity in a particular environment
MEOP	=	Maximum expected operating pressure
P	=	Applied load
P_i	=	Internal pressure for a pressure vessel
P_Q	=	Secant intercept load as specified in ASTM 399-70T, Section 9.1.1
Q	=	Flaw shape parameter for a surface crack = $\phi^2-0.212\ (\sigma/\sigma_{ys})^2$

Φ = Complete elliptic integral of the second kind having modulus k defined as

$$k = (1 - a^2/c^2)^{1/2}$$

R = Ratio of minimum to maximum applied stress in a fatigue cycle.

S = Compliance (reciprocal of stiffness)

t = Wall thickness of a pressure vessel

σ_G = Cross section fracture stress

σ_{MEOP} = Stress associated with the maximum expected operating pressure of a pressure vessel

σ_{ys} = Yield stress

TABLE OF CONTENTS

TABLE OF CONTENTS (CONT'D)

LIST OF PAGES

Title Page

i thru vi

1 - 94

1.0 INTRODUCTION

Current plans for the Space Shuttle require the use of twin solid propellant rockets to boost the Orbiter to an altitude near 45.72 km (150,000 ft). After separation, these boosters will be recovered at sea and refurbished for subsequent reuse. The employment of such Solid Rocket Boosters (SRB's) on the Space Shuttle has imposed two important demands on current solid propellant rocket technology -- reliability and reuse capability. In this instance, emphasis is being placed on obtaining maximum reliability, since the SRB will be used as a booster for a manned vehicle. At the same time, a maximum reuse capability is being demanded of the solid rocket motor case, a requirement that is unusual in the history of solid rocket technology. This demand for reusability is based on economic considerations because substantial cost savings accrue over the lifetime of the Shuttle if the SRB cases can be recovered, cleaned and reused. Since the SRB's will be recovered from the ocean after each mission, both of these requirements are complicated by the fact that the Shuttle SRB's will be exposed to sea water environments for extended periods of time prior to recovery and cleaning.

The primary objective of this program was to assess the adequacy of candidate SRB case materials by predicting service life based on tests conducted under simulated service conditions. Such a prediction requires a knowledge of the specific sizes of defects present in the structure prior to its being placed into service. This program determined the size of the defects which would cause failure (i.e. the critical size) and the manner in which subcritical flaws would grow to critical size. Such subcritical flaw growth characteristics were defined by alternate immersion exposure to synthetic sea water under a sustained load and fatigue testing under cyclic stress/temperature conditions that approximate those expected during service. The latter tests also included an investigation of corrosion-fatigue interaction resulting from exposure to synthetic sea water.

2.0 BACKGROUND

2.1 Estimated Booster Service Conditions

Although the final design configuration of the Shuttle SRB and the details of its mission have not as yet been finalized, preliminary design information is available (References 1 and 2).

This information, summarized in Figure 2-1, indicates that each case will be required to complete a minimum of 10 missions. Significant loads are applied to the case only during proof testing and actual operation. The loads imposed on the case during splashdown and recovery are as yet undetermined.

Most preliminary design studies have been conducted using D6AC steel as the baseline material. For such an SRB case, it is projected that the initial proof test following fabrication will be carried out at pressures 1.15 times a maximum expected operating pressure (MEOP) of 6900 N/m^2 (1000 psi). Subsequent proof tests, conducted prior to each flight, are to be carried out at pressures of 1.05 MEOP (Reference 2).

Five distinct temperature cycles will also be associated with each mission, as indicated in Table 2-1. The maximum temperature experienced by the case is expected to occur during refurbishment, when the case is heated to 589°K (600°F) for a maximum period of up to 12 hours. Heating of the case to this temperature represents one method proposed for removal of the elastomeric liner that bonds the propellant to the case and protects the case from the burning solid propellant. The temperature reached by the case during the pressurized portion of the SRB flight cycle is not expected to exceed 339°K (150°F).

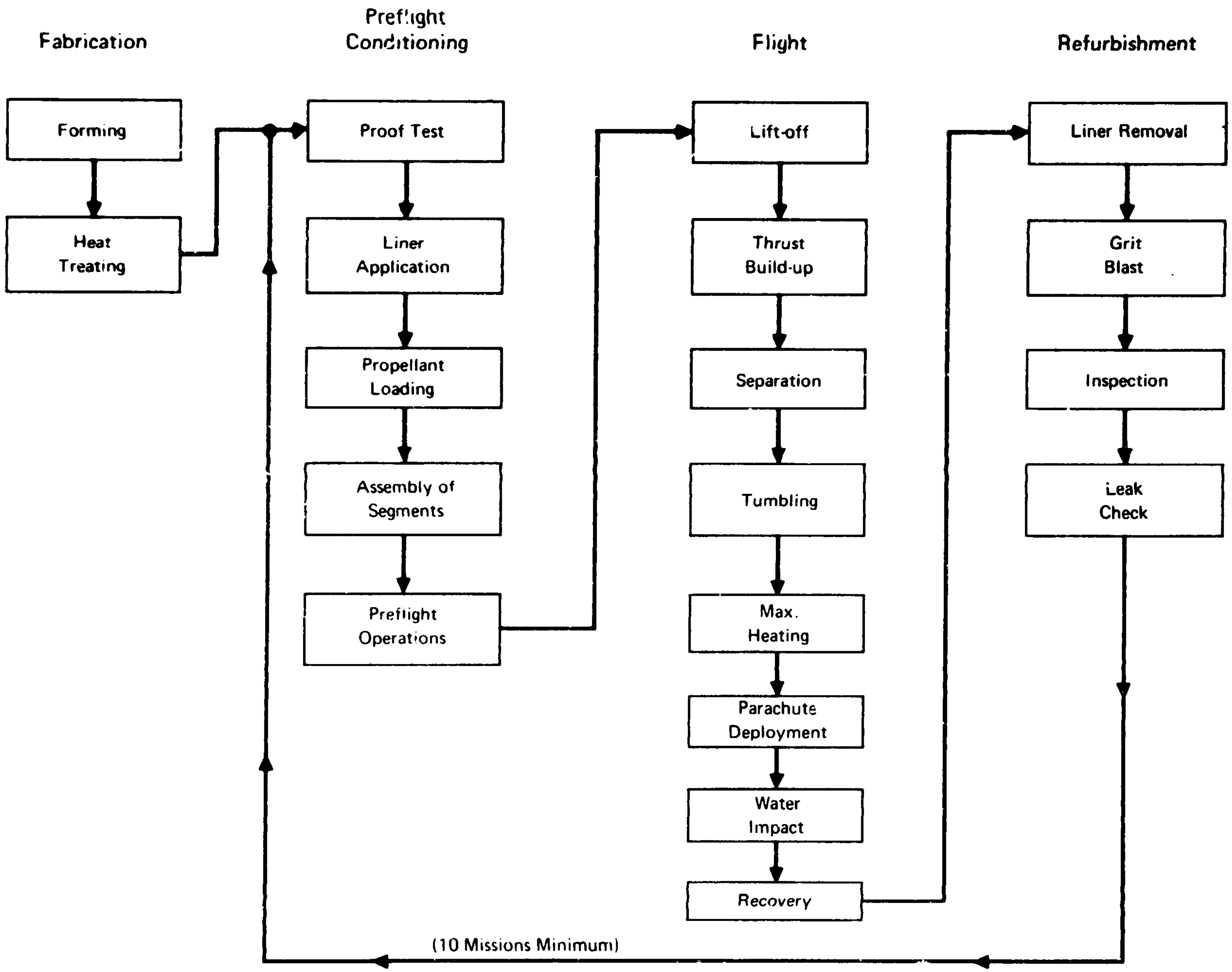

FIGURE 2-1
EXPECTED SRB SERVICE LIFE EVENTS

GP73 3377 23

TABLE 2-1 THERMAL HISTORY ASSOCIATED WITH AN SRB MISSION			
EVENT	TEMPERATURE °K	°F	DURATION
Liner Application	477	400	4 hours
Coating	339	150	4 hours
Propellant Cure	333	140	7 days
In-flight Heating *	455	360	5 minutes
Liner Removal	589	600	12 hours

* Maximum value, after thrust termination

2.2 Candidate Case Materials

Many different types of steels have been used for solid rocket motor cases. Those of particular interest for the Shuttle SRB are the maraging steels and the quenched and tempered low alloy medium carbon steels.

Maraging steels are of interest for rocket motor case applications for a number of reasons. These steels combine a high strength-to-weight ratio with good fracture toughness and weldability. Also attractive is the simple heat treatment required for these steels. The ductile martensite obtained after annealing at 1116°K (1550°F) allows these alloys to be readily formed and welded, after which a simple aging treatment produces full strength. Such a simple aging operation on large diameter rocket motor cases is more attractive than the quench and temper operations required for low alloy steels, particularly because distortion and processing problems are minimized. Maraging steels are, however, much more expensive than the low alloy steels.

The term "maraging steel" encompasses alloys with a range of compositions, as shown in Table 2-2. The maraging steels contemplated for use in rocket motor case applications have focused largely on the various grades of the 18 percent nickel alloys containing cobalt, molybdenum, and titanium. An 18 percent nickel 200 grade maraging steel was selected for use on a joint Air Force - NASA Program in 1962 to fabricate a 660 cm (260 inch) diameter booster (Reference 3). The goal of the program was achieved by the successful static test firing of two short length motors in late 1965 and early 1966.

The low alloy medium carbon steels that have been used in the missile industry include AISI 4130, 4340, D6AC, and AMS 6435, all of which have had a history of successful use at high strength levels; their compositions are listed in Table 2-3. These alloys have been used extensively in such missiles as Spartan, Pershing, Polaris, Minuteman, and Titan IIIC strap-ons. These steels generally are quenched to a fully martensitic structure which is tempered to improve ductility and toughness as well as to adjust the strength to the required level.

TABLE 2-2 COMPOSITIONS OF MARAGING STEEL

	C	Mn	Si	Ni	Co	Mo	Ti	Al	Cr	Other
18 Ni, 200 Grade	.03	.10	.10	17.0-19.0	7.0-8.5	4.0-4.5	0.10-0.25	0.05-0.15	--	--
18 Ni, 250 Grade	.03	.10	.10	17.0-19.0	7.0-8.5	4.6-5.2	0.3-0.5	0.05-0.15	--	--
18 Ni, 300 Grade	.03	.10	.10	18.0-19.0	8.5-9.5	4.7-5.2	0.6-0.8	0.05-0.15	--	--
Almar 362	.03	.30	.20	6.5	-	-	0.80	-	14.5	--
Unimar Cr-2	.03	.30	.40	10.25	-	-	0.30	0.70	11.5	--
IN-736	.02	.08	.08	10.0	-	2.0	0.20	0.30	10.0	--
Custom 450	.05	.50	.50	6.25	-	0.75	-	-	15.5	.40 Cb, 1.50 Cu
Custom 455	.03	.25	.25	8.50	-	-	1.20	-	11.75	.30 Cb, 2.25 Cu

TABLE 2-3

COMPOSITIONS OF VARIOUS HIGH STRENGTH LOW ALLOY STEELS

Alloy Content	AISI 4130	AISI 4340	D6AC	AMS 6434 (V-modified AISI) 4335)
C	.30	.40	.45	.34
Mn	.50	.70	.75	.70
Si	.28	.28	.30	.27
Ni	-	1.82	.50	1.80
Cr	.95	.80	1.00	.8
Mo	.20	.25	1.00	.35
V	-	-	.08	.20
Cu	-	-	-	.35
Total:	2.23	4.25	4.08	4.81

2.3 Materials Selected for Evaluation

One maraging steel and one low alloy steel were selected for evaluation under this program. A 200 grade 18 Ni maraging steel was selected for evaluation because of the success achieved on the 660 cm (260 inch) diameter booster program. The low alloy D6AC steel was selected because of its low cost, good performance in past applications, and the availability of information from recent design studies which used this alloy for baseline analysis.

For evaluation of sustained load flaw growth behavior, two distinct heat treatments of D6AC steel were selected, in addition to the standard heat treatment of 18 Ni maraging steel. These heat treatments were selected because recent data (Reference 4) on the fracture toughness of D6AC steel indicate that improved toughness values are obtained for a given strength level if the austenitizing temperature is increased from 1158°K (1625°F) to 1200°K (1700°F). Both heat treatments used the same 872°K (1110°F) tempering temperature to produce an ultimate strength of 1350-1550 MN/m^2 (195 - 225 ksi).

For evaluation of the cyclic flaw growth behavior, one heat treatment of each alloy was selected. Besides the standard heat treatment of 18 Ni maraging steel, the D6AC steel austenitized at 1200°K (1700°F) was selected because slightly better resistance to sustained load flaw growth was observed for such material during the first three weeks of testing.

2.4 Alloy Procurement

Because this study involved the evaluation of materials for a solid rocket motor case, the D6AC steel was obtained from Ladish as 9.53 x 305 x 914 mm (.375 x 12 x 36 inch) segments sectioned from a ring-rolled Titan IIIC rocket motor case. The starting material for this case was vacuum arc remelted; its forming history is summarized in Figure 2-2.

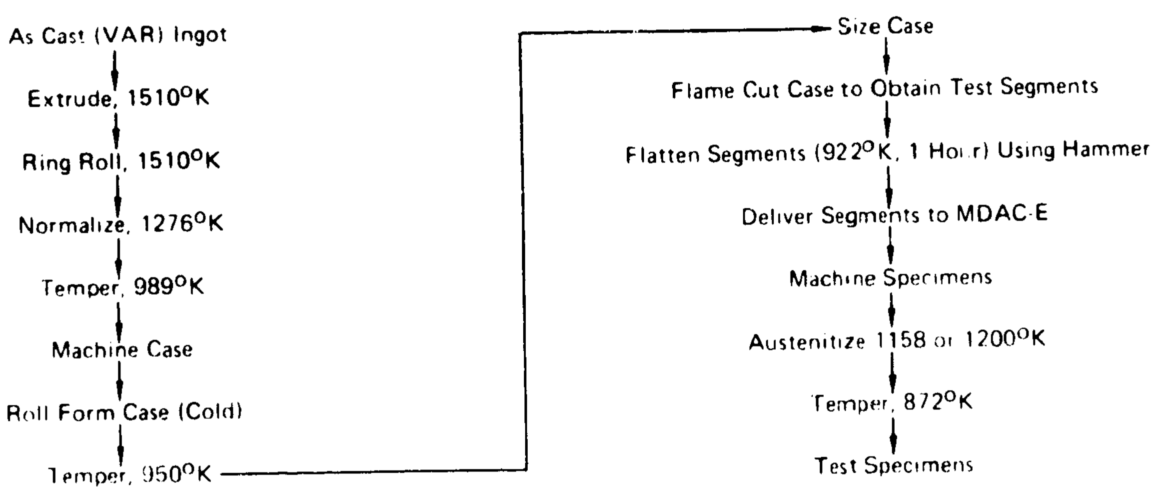

FIGURE 2-2
THERMAL/MECHANICAL PROCESSING HISTORY FOR D6AC STEEL

The 18 Ni grade 200 maraging steel was obtained from Allegheny-Ludlum as hot rolled and annealed plates having the dimensions 15.9 x 1520 x 762 mm (.625 x 60 x 30 inches). The starting material for this plate was vacuum induction melted and vacuum arc remelted.

To insure that the material used would be representative of current manufacturing technology, all of the material was procured to applicable specifications and the material suppliers were required to submit certified test reports covering chemistry and mechanical properties. A summary of the suppliers' certification is presented in Table 2-4.

TABLE 2-4. SUMMARY OF SUPPLIERS CERTIFICATION

	D6AC	18 Ni Maraging
SUPPLIER:	Ladish	Allegheny-Ludlum
ORIGIN:	Latrobe Heat No. C150006-1 Ladish Cylinder No. 334	Heat No. W28047
Melting Practice:	VAR	VIM/VAR
As-Received Condition	Normalized and Tempered	Mill Annealed
Applicable Specification:	UTC-4MDS-20701	ASTM-A538-72A
Analysis, % by Weight:		
C	.46	.019
O	*	.0013
N	*	.0040
Mn	.82	.022
P	.008	.009
S	.003	.002
Si	.18	.03
Ni	.56	18.00
Cr	1.03	-
Mo	.94	4.00
V	.08	-
Co	-	7.80
Ti	-	0.20
Al	-	0.08
Zr	*	0.01
B	*	0.003
Fe	Balance	Balance

*Not analyzed

3.0 TEST SPECIMEN PREPARATION

3.1 Selection of Test Specimen Geometry

The smooth tensile specimen shown in Figure 3-1 was used for determining baseline mechanical properties. Different types of specimens were selected for the evaluation of stress corrosion and fatigue properties; both contained fatigue precracks, primarily because such cracks are representative of the defects that are introduced in structural components during normal manufacturing processes such as forming and welding. Such defects can escape detection during routine inspection procedures and subsequently lead to failure when the component is subject to proof-test or service loads (Reference 5). The use of precracked specimens, then, will provide the basis for an efficient design of the SRB vehicle combined with a high degree of reliability and confidence.

The specimen configuration selected for the evaluation of stress corrosion susceptibility under the present program is shown in Figure 3-2. The modified wedge opening loading (MWOL) specimen configuration was selected for alternate immersion testing because of its testing economy and because there is a considerable amount of past experience available, as summarized in Reference 6. The MWOL specimen is self-stressed which eliminates the need for a tensile machine during environmental testing. A bolt maintains the crack-opening-displacement (COD) at a constant value throughout the test; as the crack propagates, the force decreases, leading to eventual crack arrest. This arrested crack length and the known COD value define the threshold stess intensity (K_{TH}) below which slow crack growth will not occur. This behavior is contrasted with that observed for a constant load test in Figure 3-3.

The MWOL specimen configuration used in the present study was side-grooved in an attempt to prevent the formation of shear lip and to confine all crack

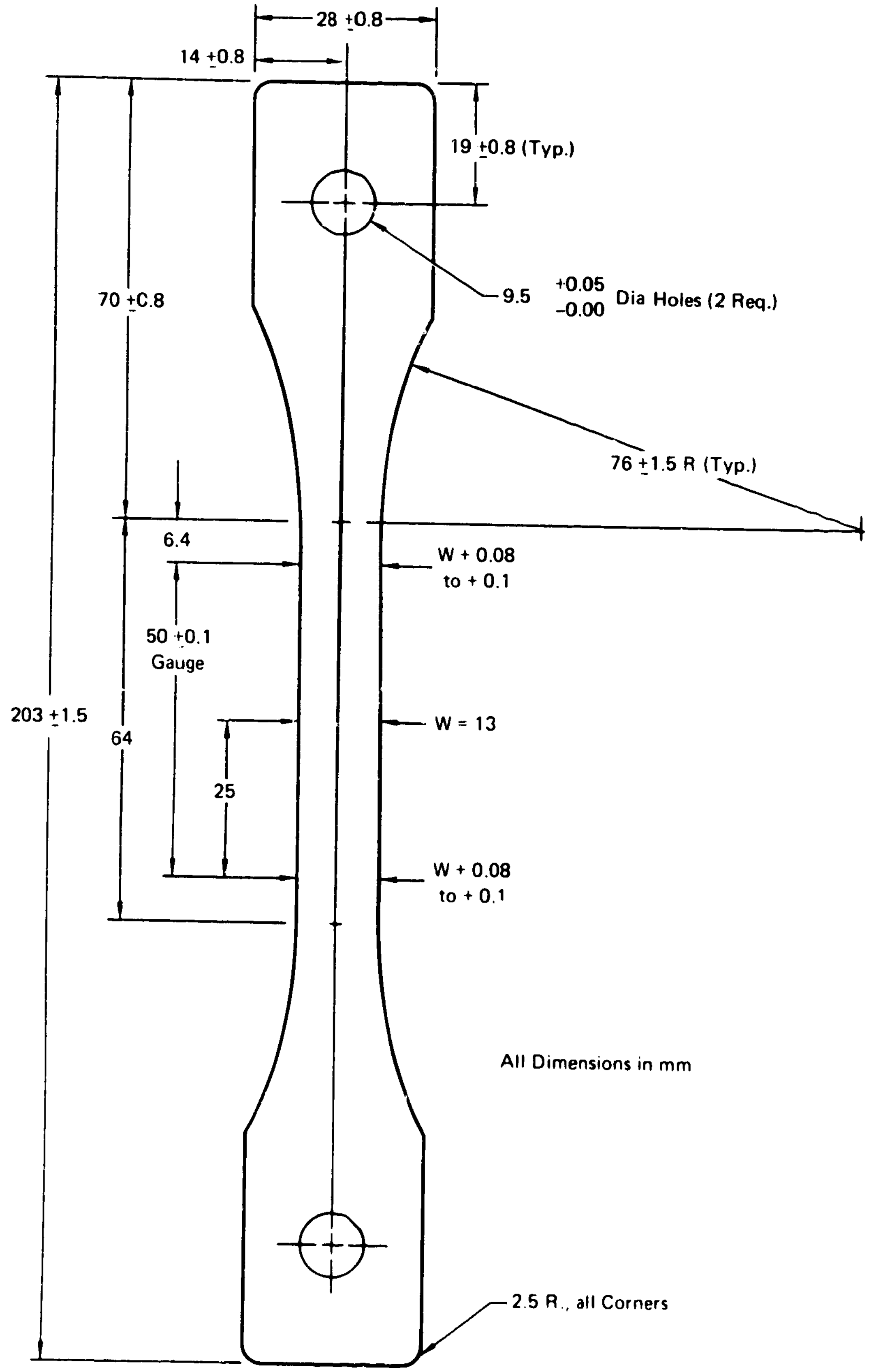

FIGURE 3-1
TENSILE SPECIMEN

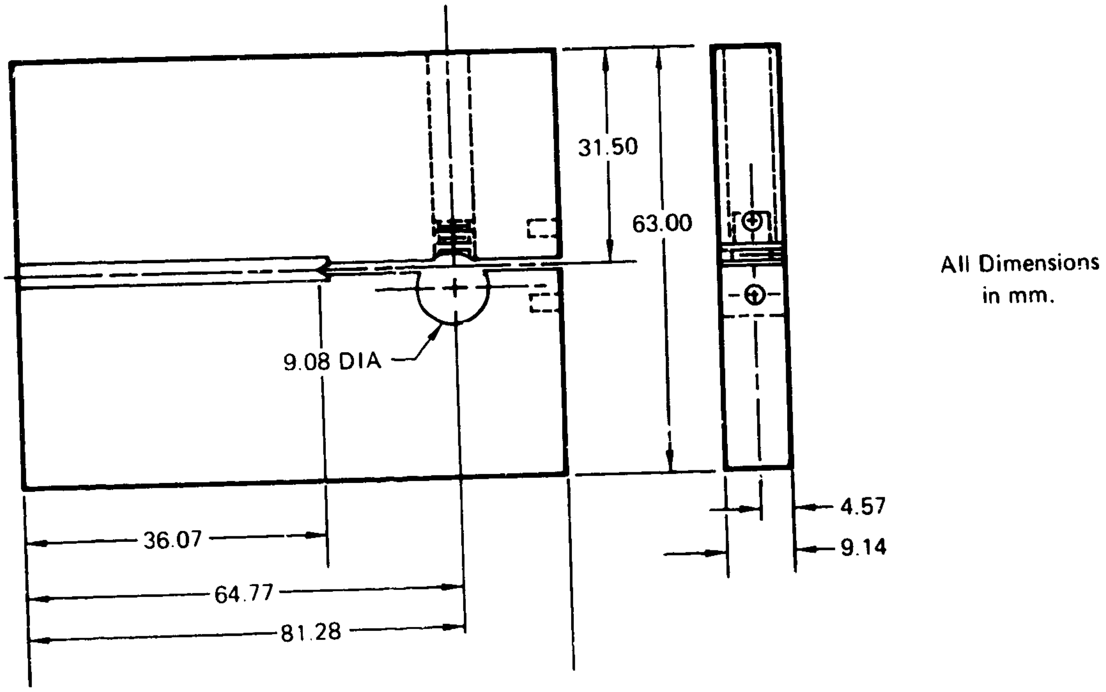

(a) Modified Wedge Opening Loading (MWOL) Specimen Configuration

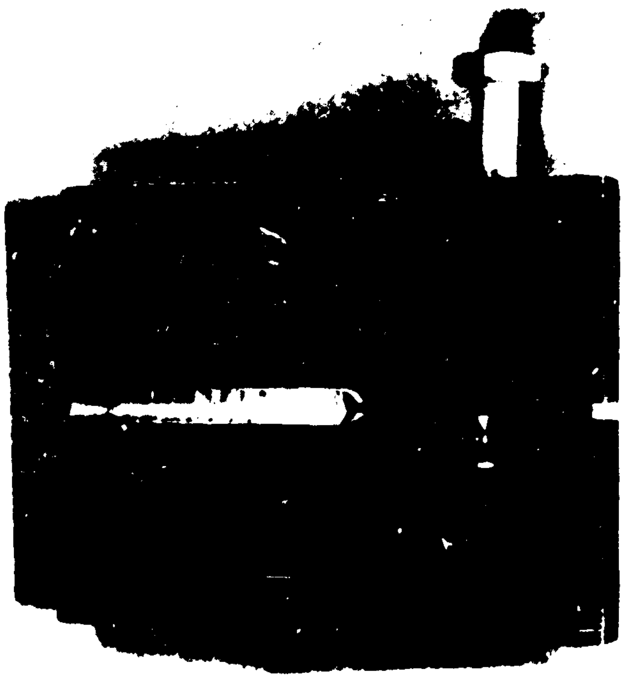

(b) MWOL Specimen Ready for Alternate Immersion Exposure

GP71 1177 9

FIGURE 3-2

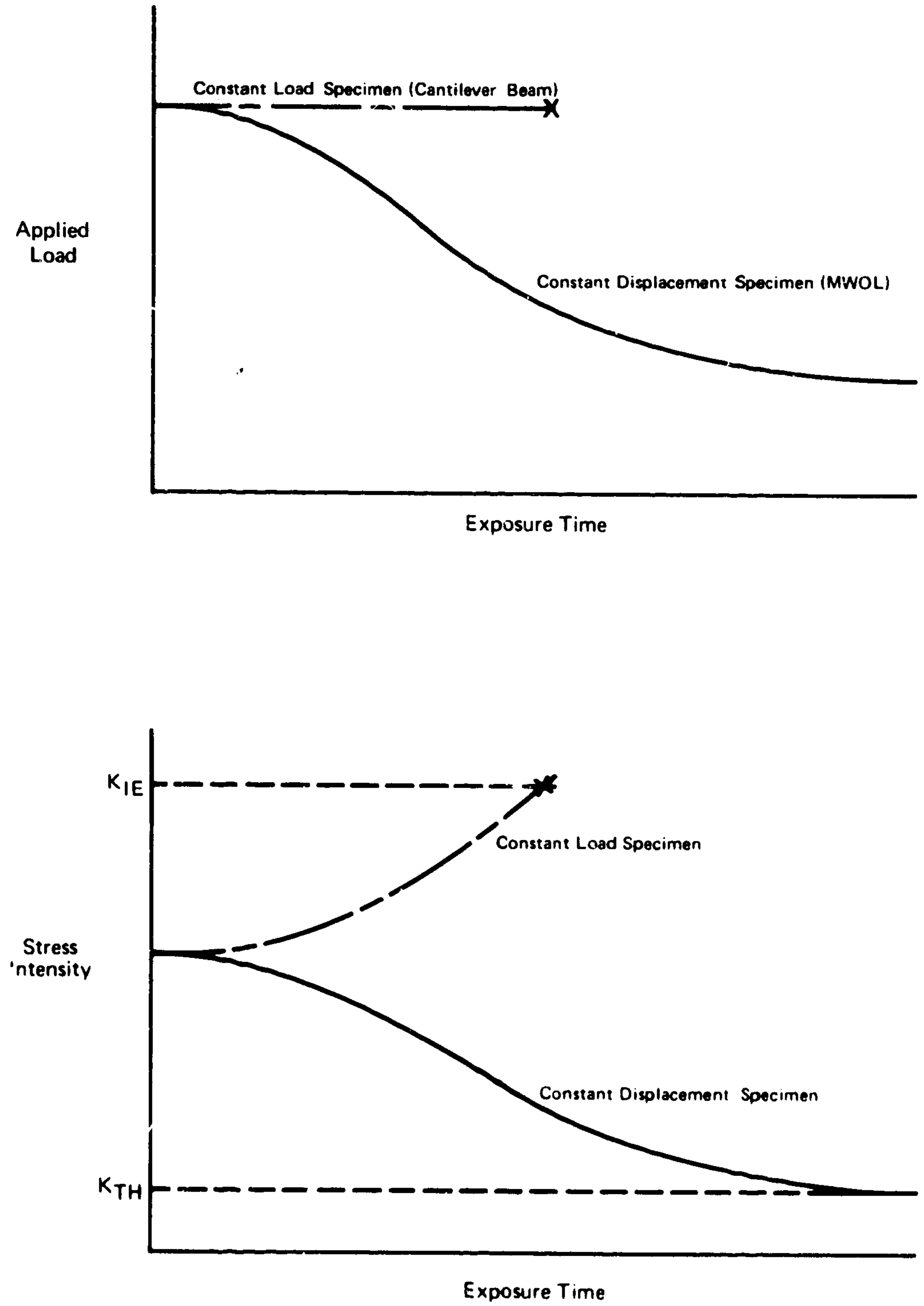

FIGURE 3-3
DIFFERENCE IN BEHAVIOR FOR MWOL AND CANTILEVER BEAM SPECIMENS

growth to a single plane. These side grooves were semicircular to aid in the monitoring of the crack tip; they reduced the nominal specimen thickness of 9.53 mm (.375 inch) by 50 percent. Such deep grooves are not usually recommended (Reference 7), but it was felt at the time of specimen manufacture that such grooving was necessary to achieve the degree of confinement required.

The specimen configurations selected for the investigation of the fatigue crack propagation behavior of D6AC and 18 Ni maraging steel are shown in Figures 3-4 and 3-5, respectively. Surface flaws were selected in order to simulate the type of flaws expected to occur during fabrication and service.

3.2 Fabrication and Heat Treatment of Test Specimens

The orientation of the loading axis for each specimen relative to the rolling direction of the original plate is summarized in the sectioning diagram of Figure 3-6.

The test specimens were heat treated in accordance with the schedules listed in Table 3-1. These heat treating schedules are designed to produce an ultimate tensile strength in the range of 1350-1550 MN/m^2 (195 - 225 ksi) for all the D6AC material and a nominal yield strength of 1380 MN/m^2 (200 ksi) for the 18 Ni maraging steel material.

In order to facilitate testing, the alternate immersion specimens were machined and heat treated before the fatigue crack propagation specimens. Smooth tensile coupons were heat treated with each group of test specimens to insure that the appropriate strength requirements were attained. Because of their large size, the fatigue crack propagation specimens were instrumented with thermocouples to insure that the required temperature/time parameters were achieved. The 18 Ni maraging steel specimens spent 4 hours and 20 minutes in the furnace, while the D6AC specimens spent 4 hours and 25 minutes.

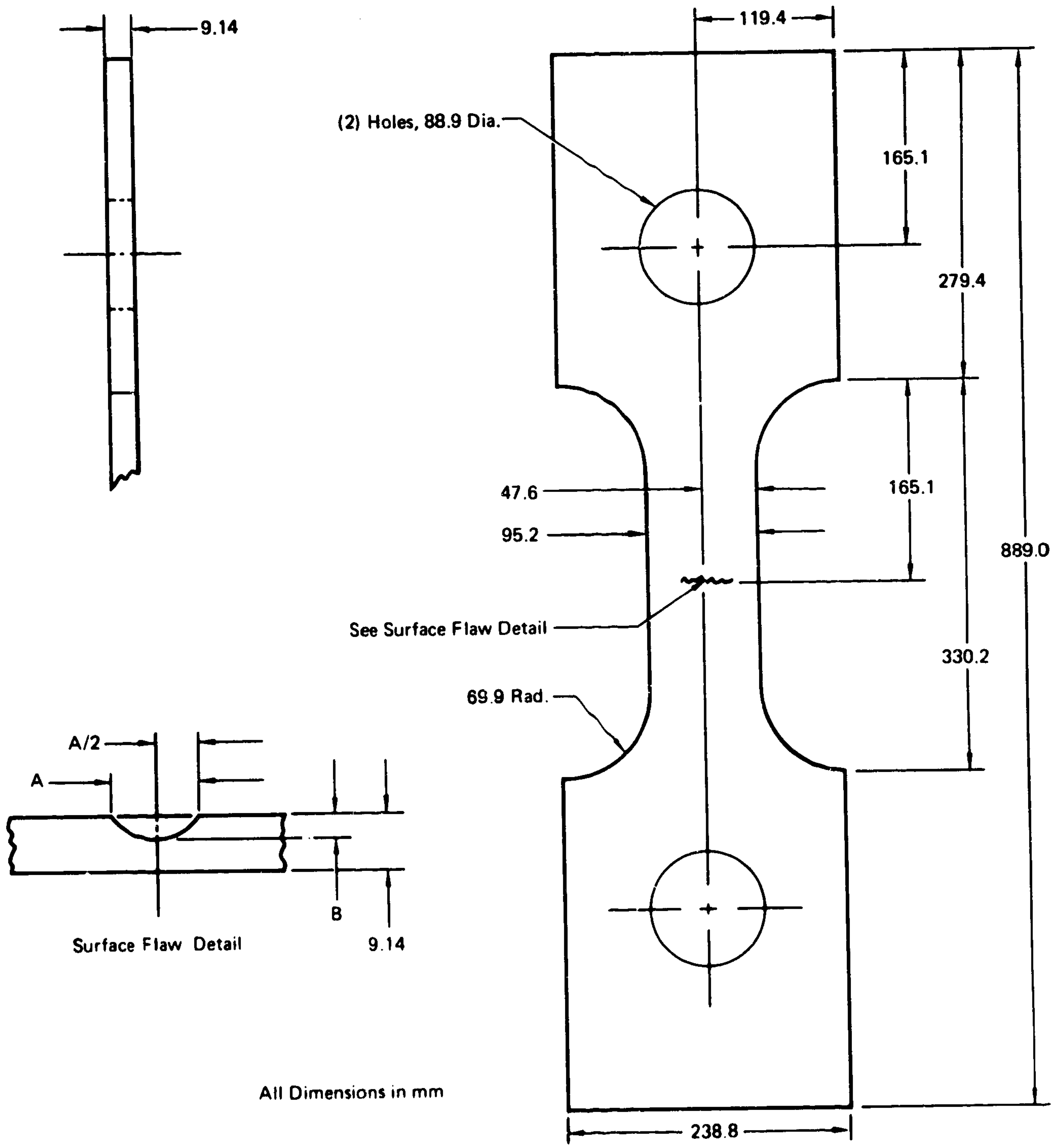

FIGURE 3-4
D6AC STEEL SURFACE FLAW SPECIMEN

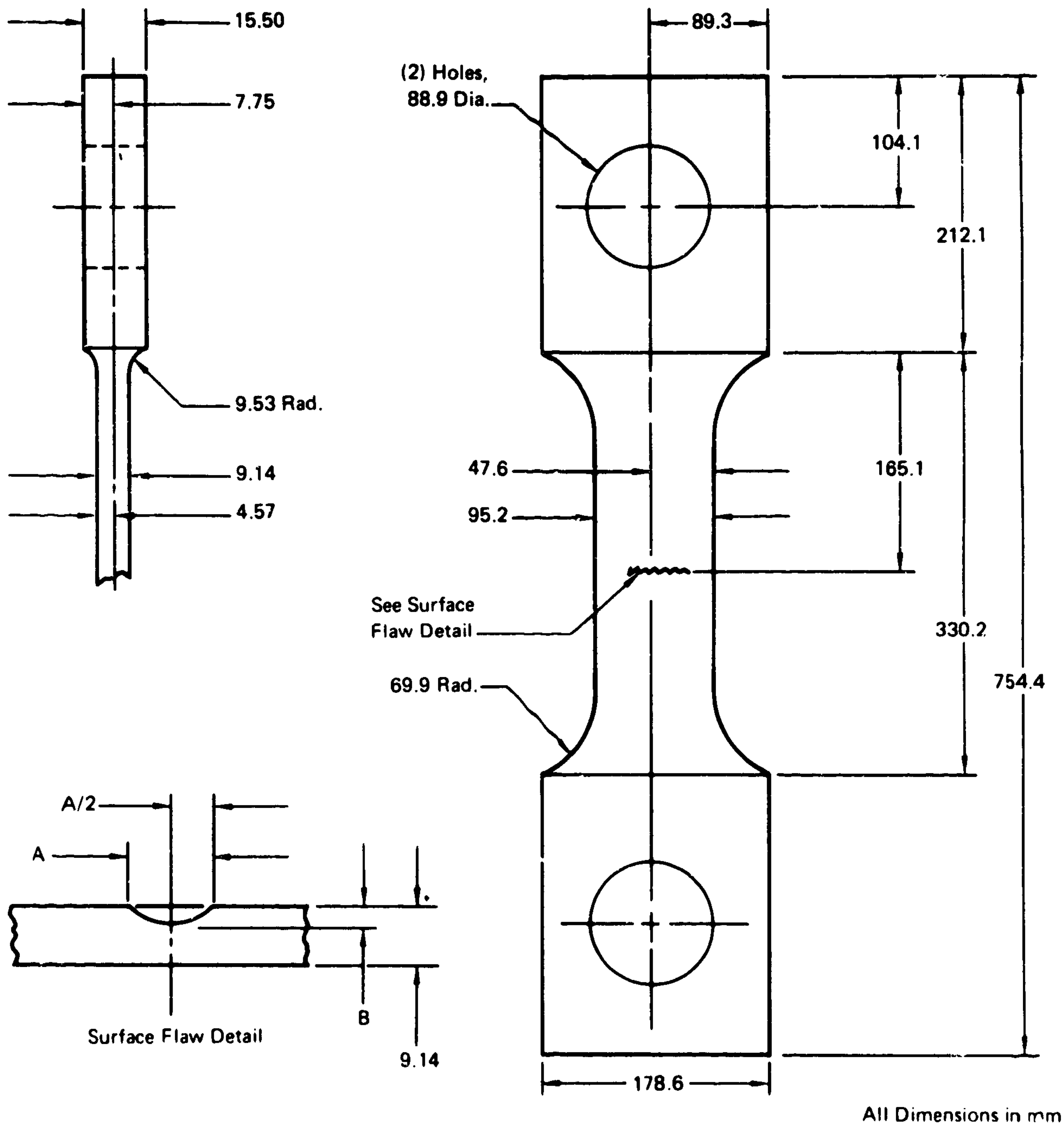

FIGURE 3-5
18 NICKEL MARAGING STEEL SURFACE FLAW SPECIMEN

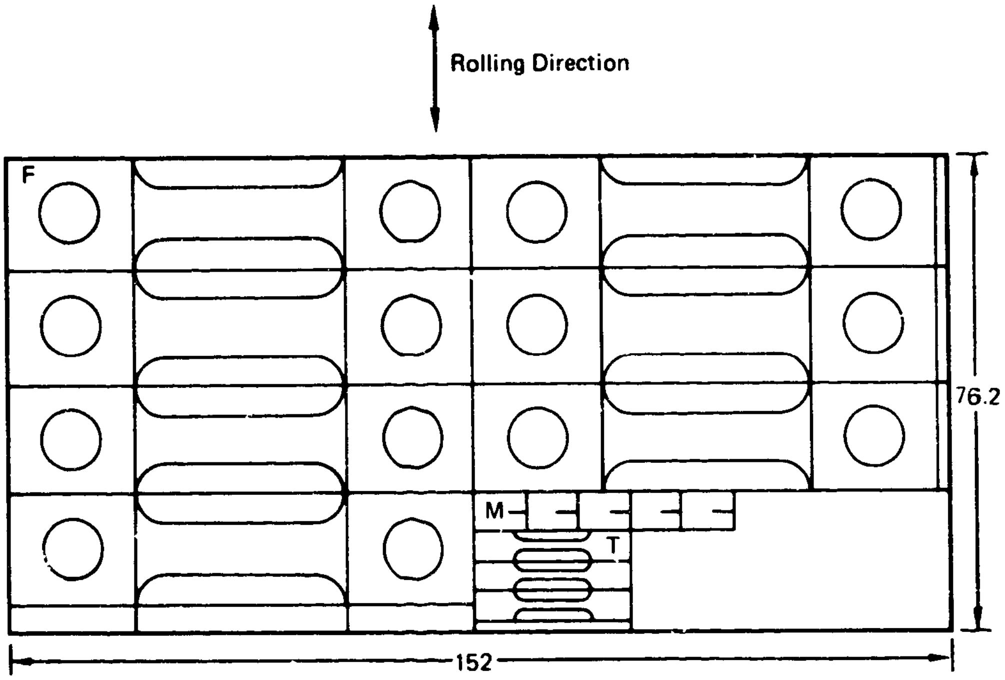

18 Nickel Maraging Steel Plate

All Dimensions in cm

F = Fatigue Specimen
M = Modified WOL Specimen
T = Smooth Tensile Specimen

Circumferential Direction
of Ring Rolled Case

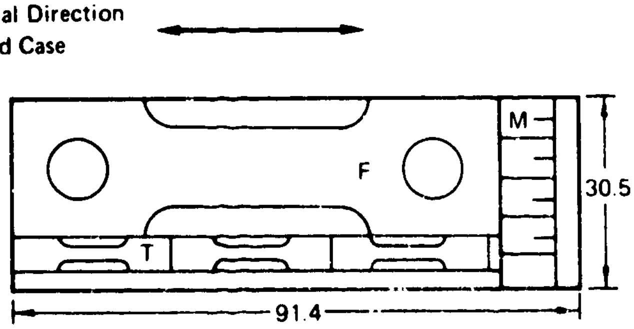

D6AC Steel Plate

FIGURE 3-6
SECTIONING DIAGRAM FOR D6AC AND 18 NICKEL MARAGING STEEL PLATE

TABLE 3-1

HEAT TREATING SCHEDULES FOR CANDIDATE CASE MATERIALS

MATERIAL	PROCESS	HEAT TREATMENT
D6AC-1625	Austenitize	1158°K (1625°F), 1 hour*
	Quench	477°K (400°F) salt
	Temper	872°K (1110°F), 4 hours
	Cooling	Air Cool
D6AC-1700	Austenitize	1200°K (1700°F), 1 hour**
	Quench	811°K (1000°F) salt 322°K (120°F) oil
	Temper	872°K (1110°F), 4 hours
	Cooling	Air Cool
18 Ni Maraging	Age	755°K (900°F), 4 hours
	Cooling	Air Cool

* Protective atmosphere (endothermic gas), dew point = 281 ± 1°K
** Protective atmosphere (endothermic gas), dew point = 276 ± 1°K

The results of the preliminary tensile testing, shown in Table 3-2, indicate that the strength requirements for this study were met for all groups of specimens. The microstructures of the heat treated alloys are shown in Figure 3-7.

TABLE 3-2. TENSILE PROPERTIES OF HIGH STRENGTH STEELS

ALLOY		F_{ty} MN/m^2	F_{ty} ksi	F_{tu} MN/m^2	F_{tu} ksi	E, modulus 10^3 MN/m^2	E, modulus 10^3 ksi	ELONGATION, % (5.08 cm gage length)
D6AC-1625		1360	197	1430	207	202	29.3	13
		1360	197	1420	206	199	28.9	14
		1360	197	1430	207	200	29.0	13
	Avg:	1360	197	1430	207	200	29.1	13
D6AC-1700		1350	196	1490	216	208	30.2	14
		1350	196	1500	217	205	29.8	15
		1360	197	1500	217	208	30.2	15
		1303	189	1420	206	201	29.2	11
	Avg:	1340	195	1480	214	206	29.9	14
18 Ni Maraging		1430	208	1500	217	181	26.3	12
		1420	206	1490	216	177	25.6	12
		1450	210	1500	218	179	25.9	12
		1440	209	1490	217	179	26.0	12
	Avg:	1430	208	1500	217	179	26.0	12

D6AC Steel
Austenitized at $1158^{\circ}K$
Tempered at $872^{\circ}K$
Mag. 500X

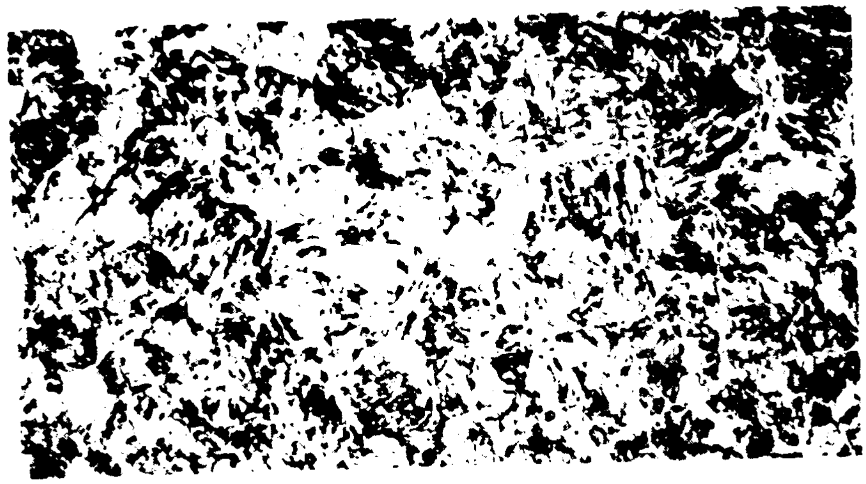

D6AC Steel
Austenitized at $1200^{\circ}K$
Tempered at $872^{\circ}K$
Mag: 500X

18 NI Maraging Steel
Aged at $758^{\circ}K$
Mag: 500X

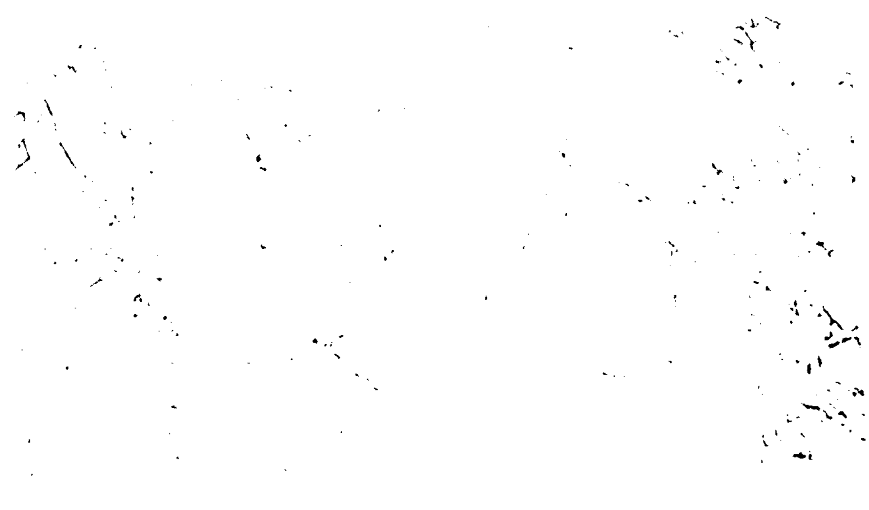

FIGURE 3-7
MICROSTRUCTURES OF HEAT TREATED HIGH STRENGTH STEELS
(ETCHANT: HCl & PICRAL)

4.0 ALTERNATE IMMERSION TESTING

4.1 Precracking of Test Specimens

The modified wedge opening loading (MWOL) specimens used in this program were machined with an initial slot length of 36.07 mm (1.420 inches). The slot width measured 2.29 mm (.090 inch), and had a terminating radius of approximately .20 mm (.008 inch). This slot was fatigue sharpened using a stress ratio of 0.10, a frequency of 30 Hz, and loads low enough to insure valid test results for each phase of testing. For all specimens, this extended crack length measured approximately 27.9 mm (1.1 inch). The apparatus used to precrack these specimens is shown in Figure 4-1.

4.2 Calibration of MWOL Specimens

Prior to alternate immersion testing, it was necessary to calibrate the particular MWOL specimen geometry used in this study in order to establish the relationship between stress intensity, crack length, applied load, and specimen deflection. The method used was similar to that described in Reference 8, in which measurements were made of the compliance (reciprocal of the stiffness) of specimens at successively longer crack lengths. Two specimens were calibrated, a D6AC specimen austenitized at 1158°K (1625°F) and an 18 Ni maraging steel specimen. The calibration was accomplished by incrementally extending a fatigue crack in the specimens. At each crack length, the specimens were incrementally loaded to some maximum static load. At each load level the displacement across the notched end of the specimen was measured with an instrumented clip-in displacement gage similar to that described in Reference 9. The fatigue loads and subsequent maximum static loads were chosen to form marker bands on the fracture surface, enabling exact measurements of the crack lengths where the calibrations were made. As the fatigue crack lengths

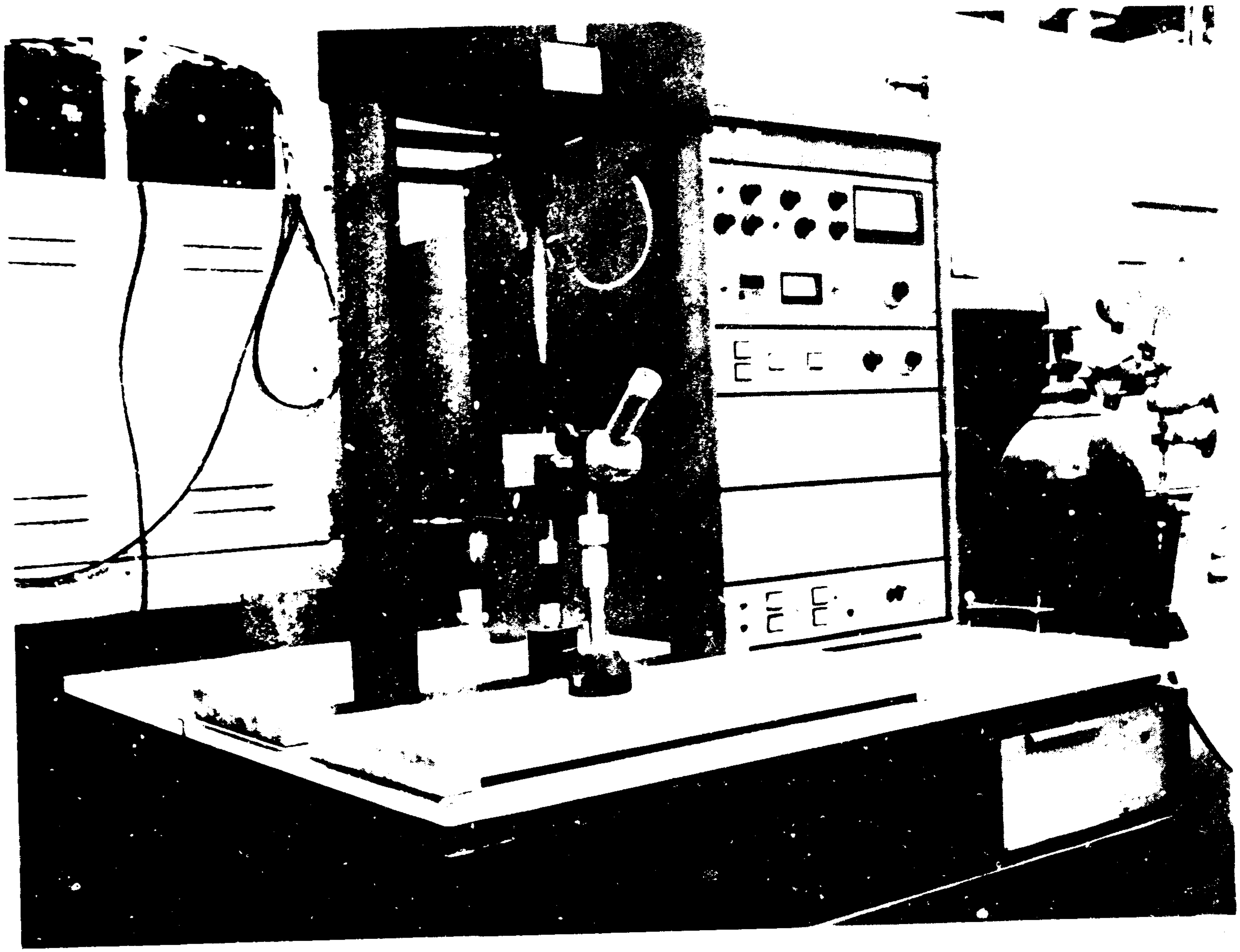

FIGURE 4-1
FATIGUE APPARATUS USED TO PRECRACK MWOL SPECIMENS

increased in the specimens, the fatigue loads and maximum static loads were reduced to prevent fracture of the specimens. In no instance did the fatigue precracking load exceed 50 percent of the maximum static load.

The compliance calibration data for the two specimens is presented in Table 4-1. The load deflection data for each crack length-to-specimen width ratio, a/W, was subjected to a least squares analysis to determine the compliance. To compare the data obtained from the specimens of the two different alloy steels, the compliance values were normalized by multiplying them by the modulus of elasticity (E). The relationship obtained between normalized compliance, expressed in units of mm^{-1}, and crack length for both specimens is shown in Figure 4-2. Excellent agreement was obtained between the two sets of data over the entire range of crack lengths studied.

Because compliance measurements ideally involved only that region of the specimen which includes the nonuniform stress field associated with the crack, load-displacement data should be obtained at the centerline of load application. However, for the MWOL specimen, such data is most conveniently and economically obtained at the end of the specimen. In order to compensate for the errors introduced by this technique, the displacement D_{END} obtained at the end of the specimen was converted to a displacement D_{CL} at the centerline of the load application by applying the linear correction factor described in Reference 6.
The correction factor used can be expressed as:

$$D_{CL} = \frac{c}{c + c_1} D_{END}$$

where c is the crack length and c_1 the distance between the centerline of load application and the point at which displacement measurements are taken. The corrected values of normalized compliance are presented in Table 4-2 and Figure 4-3.

TABLE 4-1 LOAD - DISPLACEMENT DATA FOR MWOL SPECIMENS

Alloy	a/W	Max. Applied Load, P (N)	Max. Applied Load, P (lbs)	Displacement at Each Applied Load: .2P (mm)	.2P (10^{-3} in)	.4P (mm)	.4P (10^{-3} in)	.6P (mm)	.6P (10^{-3} in)	.8P (mm)	.8P (10^{-3} in)	P (mm)	P (10^{-3} in)	Compliance, S (mm/N)	Compliance, S (10^{-6} in/lb)
[illegible]*	[illegible]	[illegible]	[illegible]	[illegible]	3.01	0.144	5.65	0.210	8.26	0.276	10.86	0.342	13.48	19.07	3.341
	[illegible]	[illegible]	[illegible]	[illegible]	3.02	0.166	6.52	0.252	9.91	0.333	13.09	0.412	16.20	23.36	4.093
	[illegible]	[illegible]	[illegible]	0.088	3.45	0.184	7.25	0.280	11.02	0.375	14.78	0.473	18.63	26.68	4.675
	[illegible]	[illegible]	[illegible]	0.094	3.70	0.196	[illegible]	0.297	11.70	0.396	15.59	0.498	19.61	32.08	5.620
	[illegible]	[illegible]	[illegible]	0.085	3.35	0.155	[illegible]	0.288	11.34	0.388	15.29	0.488	19.20	36.88	6.461
	[illegible]	[illegible]	[illegible]	0.106	4.17	0.226	8.89	0.349	13.72	0.467	18.37	0.585	23.01	44.16	7.737
	[illegible]	[illegible]	[illegible]	[illegible]	3.96	0.219	8.62	0.339	13.34	0.455	17.93	0.574	22.61	52.09	9.125
	[illegible]	[illegible]	[illegible]	0.092	3.62	0.209	8.23	0.325	12.80	0.442	17.39	0.558	21.96	63.47	11.12
	[illegible]	[illegible]	[illegible]	0.122	4.82	0.263	10.37	0.405	15.95	0.545	21.46	0.683	26.89	77.44	13.57
	[illegible]	[illegible]	[illegible]	[illegible]	4.32	0.245	9.66	0.381	15.00	0.518	20.41	0.655	25.78	99.22	17.38
	[illegible]	[illegible]	[illegible]	[illegible]	4.53	0.259	10.15	0.401	15.80	0.546	21.50	0.690	27.18	125.5	21.99
	[illegible]	[illegible]	[illegible]	[illegible]	[illegible]	0.285	[illegible]	0.444	17.45	0.601	23.67	0.761	29.95	172.4	30.21
	[illegible]	[illegible]	[illegible]	[illegible]	5.35	0.344	[illegible]	[illegible]	[illegible]	0.709	27.91	0.896	35.28	260.2	45.58
	[illegible]	[illegible]	[illegible]	0.142	[illegible]	0.319	12.55	0.496	19.54	0.672	26.45	0.851	33.51	386.9	67.77
	[illegible]	[illegible]	[illegible]	[illegible]	[illegible]	0.465	18.32	[illegible]	[illegible]	0.951	37.45	1.206	47.46	679.4	119.02
[illegible] Ni Maraging**	[illegible]	[illegible]	[illegible]	0.102	[illegible]	[illegible]	7.67	0.286	11.26	0.376	14.83	0.469	18.47	20.94	3.668
	[illegible]	[illegible]	[illegible]	0.124	4.55	0.241	[illegible]	0.351	13.82	0.461	18.16	0.571	22.48	25.53	4.473
	[illegible]	[illegible]	[illegible]	[illegible]	4.92	0.257	10.14	0.389	15.33	0.521	20.54	0.654	25.75	29.49	5.166
	[illegible]	[illegible]	[illegible]	[illegible]	[illegible]	0.300	11.83	0.455	17.93	0.611	24.09	0.769	30.30	34.66	6.073
	[illegible]	[illegible]	[illegible]	0.151	[illegible]	0.370	14.60	0.560	22.05	0.751	29.59	0.945	37.21	42.55	7.455
	[illegible]	[illegible]	[illegible]	[illegible]	[illegible]	0.339	13.35	0.519	20.46	0.698	27.50	0.881	34.72	48.82	8.728
	[illegible]	[illegible]	[illegible]	0.191	[illegible]	[illegible]	16.05	0.620	24.42	0.833	32.80	1.055	41.55	59.50	10.42
	[illegible]	[illegible]	[illegible]	0.156	6.14	0.346	13.63	0.537	21.16	0.730	28.76	0.920	36.25	69.75	12.22
	[illegible]	[illegible]	[illegible]	0.217	8.54	0.459	18.09	0.702	27.65	0.950	37.40	1.200	47.24	90.33	15.82
	[illegible]	[illegible]	[illegible]	0.154	6.05	0.346	[illegible]	0.552	21.76	0.759	29.90	0.964	37.97	109.88	19.25
	[illegible]	[illegible]	[illegible]	0.233	9.15	0.495	19.49	0.762	30.03	1.034	40.71	1.319	51.92	148.7	26.05
	[illegible]	[illegible]	[illegible]	0.215	8.57	0.495	19.52	0.777	30.59	1.053	41.46	1.350	53.13	204.0	35.75

* Heat Treatment: Austenitized at 1155°K (1620°F), 1 hour; quenched in 477°K (400°F) salt; tempered at 872°K (1110°F), 4 hours.

** Heat Treatment: Aged at [illegible] (900°F), 4 hours.

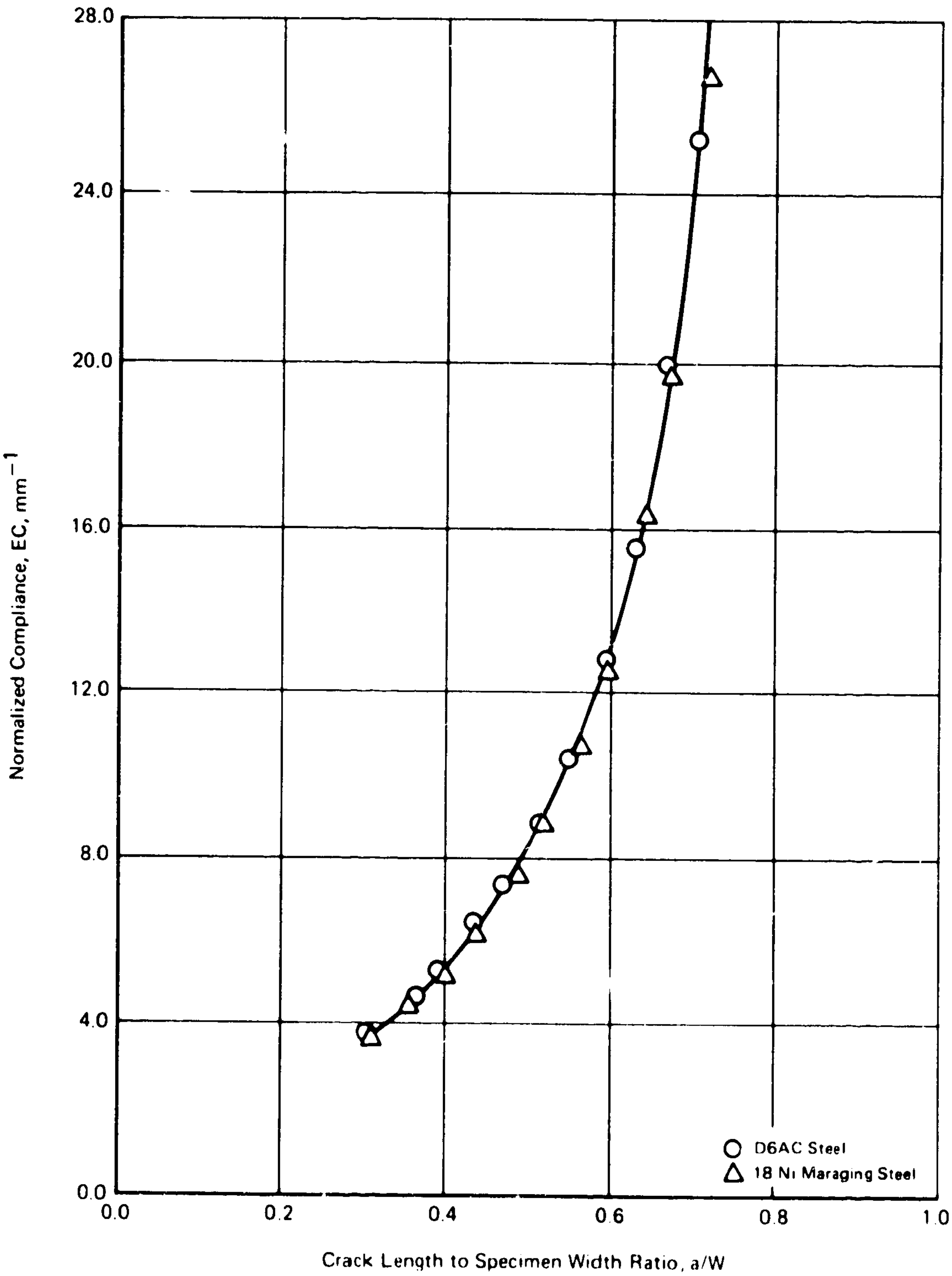

FIGURE 4-2
NORMALIZED COMPLIANCE (AT END OF SPECIMEN) vs CRACK LENGTH

TABLE 4-2. CORRECTED COMPLIANCE DATA FOR MWOL SPECIMENS

Alloy	a/w	Compliance @ End of Specimen		Compliance @ Centerline of Loading*	
		mm^{-1}	in^{-1}	mm^{-1}	in^{-1}
D6AC	0.307	3.8277	97.223	2.0019	50.848
	0.365	4.6892	119.10	2.6541	67.414
	0.390	5.3560	136.04	3.1172	79.177
	0.435	6.4386	163.54	3.9147	99.434
	0.471	7.4021	188.01	4.6411	117.88
	0.517	8.8640	225.14	5.7527	146.12
	0.551	10.4543	265.53	6.9311	176.05
	0.593	12.7398	323.59	8.6503	219.71
	0.630	15.5445	394.82	10.756	273.22
	0.670	19.9140	505.81	14.039	356.60
	0.707	25.1956	639.96	18.040	458.21
	0.746	34.6118	879.14	25.162	639.13
	0.786	52.2184	1326.3	38.485	977.51
	0.824	77.6374	1971.9	57.917	1471.10
	0.862	136.3587	3463.5	102.95	2614.9
18 Ni Maraging	0.312	3.7547	95.368	1.9787	50.259
	0.355	4.5786	116.29	2.5595	65.011
	0.400	5.2880	134.31	3.1094	78.978
	0.439	6.2164	157.89	3.7921	96.318
	0.488	7.6311	193.83	4.8457	123.08
	0.522	8.9341	226.92	5.8161	147.73
	0.565	10.6713	271.05	7.1283	181.06
	0.596	12.5097	317.74	8.5065	216.06
	0.643	16.1998	411.47	11.275	286.38
	0.678	19.7058	500.52	13.932	353.87
	0.718	26.6674	677.35	19.173	487.01
	0.758	36.5955	929.52	26.714	678.55

* Values obtained using a linear correction factor,

$$D_{CL} = \left[\frac{c}{c+c_1}\right] D_{END}$$

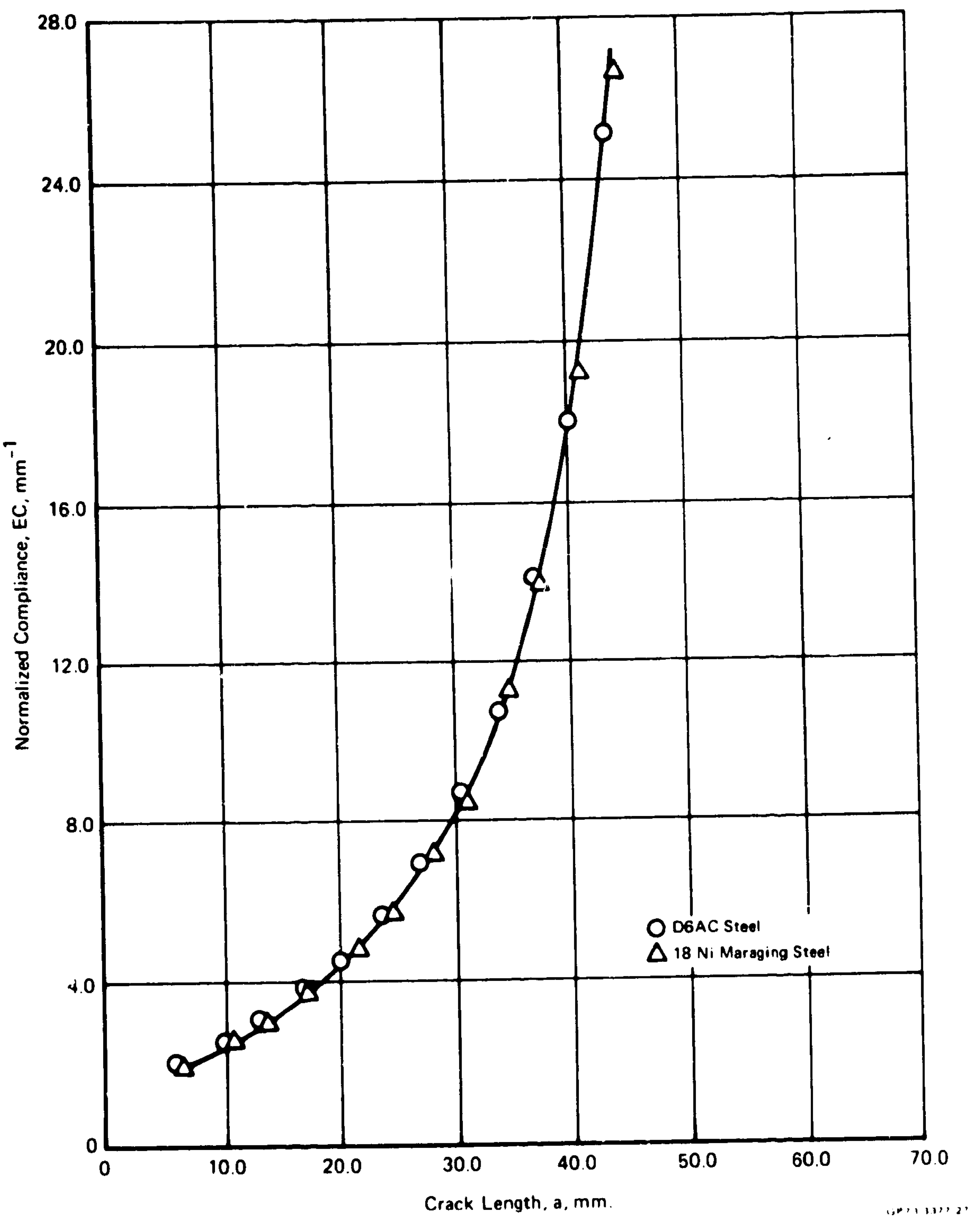

FIGURE 4-3
NORMALIZED COMPLIANCE (AT CENTERLINE OF LOADING) vs CRACK LENGTH

This correction factor has been found to be conservative in predicting centerline compliance values, particularly at the shorter crack lengths. However, for the shortest crack length used in the present study, the value of stress intensity calculated using this curve is overestimated by no more than 10 percent.

The stress intensity factor at each combination of applied load and crack length is related to specimen compliance in the following manner:

$$K = \sqrt{GE} \tag{2}$$

$$G = \frac{P^2}{2EB_n} \frac{d(ES)}{da} \tag{3}$$

In order to obtain an equation for (d(ES)/da), a least-squares-best-fit digital computer program was used to fit the data of Table 4-2 (expressed in English units) to a fifth degree polynominal in (a). This polynominal was found to be:

$$ES = 717.10 + 3550.8(a) - 6776(a^2) + 6503.9(a^3) - 3062.8(a^4) + 579.8(a^5) \tag{4}$$

where (a), E, and C are expressed in English units. Therefore,

$$\frac{d(ES)}{da} = 3550.8 - 13553(a) + 19511(a^2) - 12251(a^3) + 2899.1(a^4) \tag{5}$$

The coefficients in equations (4) and (5) are for use with English units.

4.3 Fracture Toughness Testing of MWOL Specimens

In order to establish critical stress intensity values for use as baseline data in the subsequent investigation of stress corrosion susceptibility, tests were conducted on MWOL specimens to obtain apparent fracture toughness (K_{IE}) values. Two MWOL specimens from each test material were precracked using a stress ratio ($\sigma_{min}/\sigma_{max}$) of 0.10, a cyclic rate of 30 cps, and a load which insured both the maximum stress intensity during terminal precrack extension, K_f (max), would be less than 50% of the K_{IE} value and that K_f (max)/E would not be greater than 0.0012.

After precracking, the specimens were fractured in a Baldwin universal testing machine. An autographic plot of the output of the load sensing transducer of the testing machine versus the output of the displacement gage attached to the specimen was obtained for each specimen.

After fracture, the depth of the fatigue crack in each specimen was measured at five locations across the thickness of each specimen in accordance with ASTM recommended practice. The secant intercept load, P_Q, used to calculate a conditional fracture toughness value, K_{IE}, was determined from the load displacement plots in accordance with the procedure specified in ASTM 399-72, Section 9.1.1. Equations (2), (3) and (5) were used to calculate an apparent fracture toughness, K_{IE}, for each specimen. The results of this testing are reported in Table 4-3.

The results of these fracture toughness tests follow the trends expected from other tests of these alloys, as shown in Table 4-4. However, because the thickness of the MWOL specimens used in the present study did not satisfy ASTM requirements for plane strain conditions*, the critical stress intensity values obtained in all cases are greater than the K_{Ic} values reported for the same alloys at similar strength levels. Such results can be attributed to a mixed-mode state of stress at the crack tip, involving both plane strain and plane stress conditions. The appearance of the fracture surfaces of these specimens, shown in Figure 4-4, supports this conclusion since shear lip formation is appreciable, even with the deep side grooves used on these specimens. According to Reference 10, plane strain conditions tend to be associated with fractures having shear lips that occupy less than 20 percent of the total fracture surface area.

---

* $B_n \geq 2.5\ (K_{Ic}/F_{ty})^2$

TABLE 4-3. CRITICAL STRESS INTENSITY DATA FOR HIGH STRENGTH STEELS (MWOL SPECIMENS)

ALLOY	Initial Flaw Size, c_o mm	in	Net Section Thickness, B_n mm	in	Secant Intercept Load, P_s * N	lb		Strain Energy Release Rate, G** N/mm	lb/in	Critical Stress Intensity, K_{IE}*** $(MN/m^2)\sqrt{m}$	ksi $\sqrt{in}$
D6AC+	28.73	1.131	4.37	0.172	19,500	4370		66.8	381	115	105
	28.27	1.113	4.27	0.167	17,900	4010		56.2	321	107	97
							Avg:	61.5	351	111	101
D6AC++	28.02	1.103	4.57	0.180	19,500	4390		59.4	339	111	101
	28.58	1.125	4.67	0.184	20,400	4590		65.9	376	116	106
							Avg:	62.7	358	114	104
18 Ni Maraging	27.89	1.098	4.62	0.182	21,900	4910		84.3	481	123	112
	28.25	1.112	4.55	0.179	22,800	5130		95.8	547	131	119
							Avg:	90.1	514	127	116

+ Austenitized at 1158°K (1625°F)

++ Austenitized at 1200°K (1700°F)

* Defined in ASTM E 399-72, Section 9.1.1

** Calculated in English units using equations (3) and (5).

*** Calculated in English units using equation (2).

TABLE 4-4. REPORTED K_{Ic} VALUES FOR HIGH STRENGTH STEELS

Alloy	Critical Stress Intensity $(MN/m^2)\sqrt{m}$	ksi $\sqrt{in}$	F_{ty} MN/m²	ksi	Heat Treatment Temperature: Austenitizing °K	Austenitizing °F	Tempering °K	Tempering °F	Reference
D6AC Steel	111	101 *	1330	193	1158	1625	872	1110	This study
	86.2	78.4 **	1450	210	1172	1650	825	1025	8
	70.9	64.5 **	1503	218	1172	1650	825	1025	9
	114	104 *	1350	196	1200	1700	872	1110	This study
	107	97.8 **	1410	204	1200	1700	866	1100	8
	104	94.8 **	1450	211	1200	1700	825	1025	9
18 Ni Maraging Steel	127	116 *	1430	207	----	----	755	900	This study
	110	100 **	1450	210	1172	1650	755	900	10

* K_{IE} values, MWOL specimens

** K_{Ic} values, compact tension specimens

D6AC Steel
Austenitized at 1158°K
Tempered at 872°K

D6AC Steel
Austenitized at 1200°K
Tempered at 872°K

18 Nickel Maraging Steel
Aged at 758°K

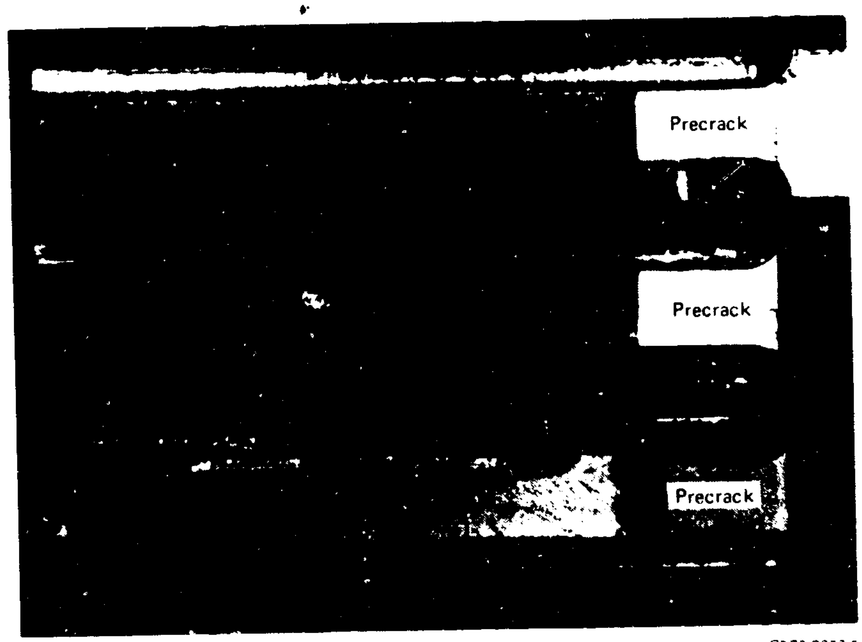

GP73 3377 5

FIGURE 4-4
FRACTURE SURFACES OF HIGH STRENGTH STEEL MWOL SPECIMENS AFTER FRACTURE TOUGHNESS TESTING

4.4 Test Procedure

Both stressed and unstressed specimens for each alloy were subjected to alternate immersion testing. The unstressed coupons, 6.4 x 25 x 51 mm (.25 x 1 x 2 inches), were ground using 600 grit paper and cleaned by rinsing in distilled water followed by rinsing in acetone. The coupons were then weighed to within ± 0.001 gram.

For the self-stressed MWOL specimens, a high strength steel bolt and a 17-7 PH stainless steel loading pin were used to apply an initial load to each specimen that corresponded to approximately 85% of the average K_{IE} value reported in Table 4-3. The displacement of each specimen required to give the desired stress intensity at the crack tip was determined from the calibration curve of Figure 4-3 and is tabulated in Table 4-5.

TABLE 4-5. INITIAL LOADS AND DEFLECTIONS FOR MWOL SPECIMENS SUBJECTED TO ALTERNATE IMMERSION EXPOSURE														
Alloy	Speci-men	c		B_N		C		D_{CL}		D_{End}		Load P	
		mm	in	mm	in	mm/N	in/lb x 10^{-6}	mm	in	mm	in	N	lbs
D6AC Austenitized at 1625°F	MD104	28.30	1.114	4.45	0.175	19.22	3.367	0.312	0.0123	0.513	0.0202	16,256	3653
	MD106	28.12	1.107	4.57	0.180	18.94	3.318	0.315	0.0124	0.518	0.0204	16,634	3738
D6AC Austenitized at 1700°F	LB104	28.30	1.114	4.72	0.186	18.56	3.251	0.320	0.0126	0.526	0.0207	17,244	3875
	LB105	28.19	1.110	4.70	0.185	18.43	3.229	0.318	0.0125	0.523	0.0206	17,244	3875
18 Ni Maraging	M114	27.92	1.099	4.57	0.180	20.86	3.654	0.399	0.0157	0.658	0.0259	19,046	4280
	M115	28.27	1.113	4.57	0.180	21.46	3.759	0.404	0.0159	0.663	0.0261	18,757	4215

(1) D_{CL} = Specimen deflection at centerline of loading

(2) D_{End} = Specimen deflection as measured at knife edges attached to specimens

(3) D_{End} is related to D_{CL} by the expression $D_{End} = [\frac{c + c_1}{c}] D_{CL}$

Prior to loading each specimen, a small amount of grease was applied to the bolt threads and bearing surface to facilitate load application. Each specimen was then held in a vise and a clip-in displacement gage attached to the end of the specimen. The bolt was torqued until the desired displacement was obtained. After loading, the bolt end of each specimen was masked with Unichrome 320 Stop-Off Compound to prevent possible galvanic corrosion around the bolt, specimen and loading pin.

Two bolt-loaded MWOL specimens and four unstressed coupons of each alloy were then subjected to alternate immersion in a 3.5% salt solution of simulated sea water, as specified in ASTM-D-114-52, Formula A. The sodium chloride content was checked daily with a salimeter, and regular adjustments were made to maintain the weight percentage of the sea salt in the solution of 3.5%. The specimens were subjected to repeated test cycles consisting of 10 minutes saline immersion followed by 50 minutes of air exposure for a total of 62 days (1488 hours).

4.5 Results of Exposure of Corrosion Coupons

Weight change measurements were made on all corrosion coupons after 15, 30, 44, and 62 days of exposure. Prior to weighing, the coupons were rinsed in distilled water and acetone. At each measurement interval, one specimen was retained for metallographic examination.

The results of the weight change measurements, listed in Table 4-6 and plotted in Figure 4-5, indicate that both heat treatments of D6AC steel are more susceptible to corrosion in synthetic sea water than the 18 Ni maraging steel. The heat treatment that includes austenitizing at 1158°K (1625°F) appears to produce a slightly more corrosion resistant material than does the 1200°K (1700°F) heat treatment. However, such results may be due to subtle differences in microstructure, such as the amount of retained austenite, the carbide distribution, or the prior austenite grain size. The D6AC steel austenitized at 1200°K (1700°F) was found to have a larger prior austenite grain size (i.e., ASTM 6), than the alloy austenitized at 1158°K (1625°F), which was determined to have a prior austenite grain size of ASTM 8.

The condition of the coupon surface of each alloy after 15 and 62 days exposure are shown in Figures 4-6 through 4-8. These photographs indicate that the D6AC steel is highly susceptible to general overall corrosion; little original surface was visible after 15 days' exposure. In contrast, the 18 Ni maraging steel exhibits excellent immunity to corrosive attack; there was very little evidence of general corrosion or pitting.

4.6 Results of Exposure of MWOL Specimens

The bolt-loaded MWOL specimens were temporarily removed from testing at various intervals for measurement of surface crack length. These measurements were obtained on both sides of the specimen using a Unitron measuring microscope.

TABLE 4-6. CORROSION DATA FOR HIGH STRENGTH STEELS

ALLOY	SPECIMEN	EXPOSURE TIME (DAYS)	WEIGHT CHANGE* mg	WEIGHT CHANGE* mg/cm^2
D6AC*	MD-201	15	61.8	1.67
	MD-202	15	65.2	1.76
		30	177.9	4.80
	MD-203	15	69.8	1.88
		30	176.9	4.77
		44	227.0	6.10
	MD-204	15	73.1	1.97
		30	182.1	4.92
		44	254.1	6.86
		62	308.0	8.32
D6AC**	LB-201	15	77.1	2.06
	LB-202	15	75.7	2.02
		30	229.7	6.13
	LB-203	15	86.9	2.32
		30	221.3	5.90
		44	296.5	7.91
	LB-204	15	98.6	2.63
		30	215.7	5.75
		44	349.0	9.31
		62	440.6	11.70
18 Ni Maraging	M-201	15	2.1	.06
	M-202	15	3.1	.08
		30	7.5	.20
	M-203	15	6.7	.18
		30	11.7	.31
		44	6.3	.17
	M-204	15	2.0	.05
		30	7.4	.20
		44	-8.0	-.21
		62	-5.7	-.15

* Negative values indicate weight loss
** Austenitized at 1200°K (1700°F)
*** Austenitized at 1158°K (1625°F)

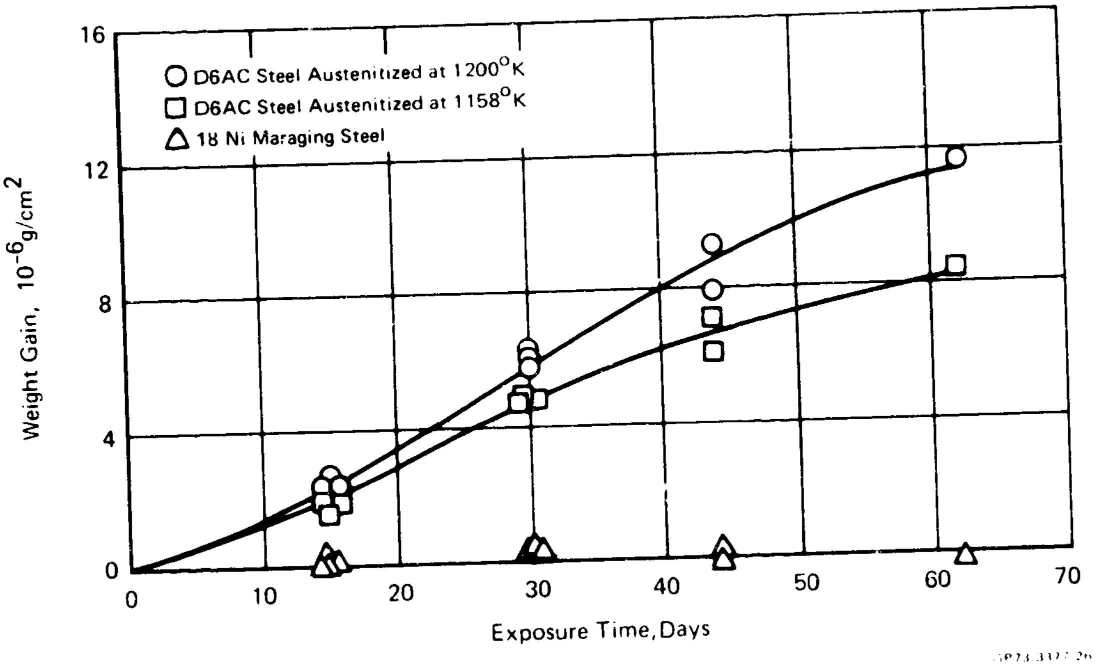

FIGURE 4-5
WEIGHT GAIN vs EXPOSURE TIME FOR HIGH STRENGTH STEELS SUBJECTED TO ALTERNATE IMMERSION IN SYNTHETIC SEA WATER

Equations (2), (3), and (5) were used in conjunction with the average surface crack length measurement to determine the variation of stress intensity with exposure time. Final crack length measurements at the end of the 62 day exposure period were obtained after the specimens were pulled to failure to measure the extent of stress corrosion crack growth. All crack length measurements and the calculated values of applied load and stress intensity are reported in Appendix A.

Throughout the 62 day exposure period, repeated measurements of surface crack length indicated that no stress corrosion crack growth had occurred in the 18 Ni maraging steel specimens. However, upon pulling these specimens to failure after exposure it was found that the stress corrosion cracks had tunnelled an appreciable distance below the surfaces of each specimen. For this reason, only the initial and final values of crack length are reported for these specimens in Appendix A.

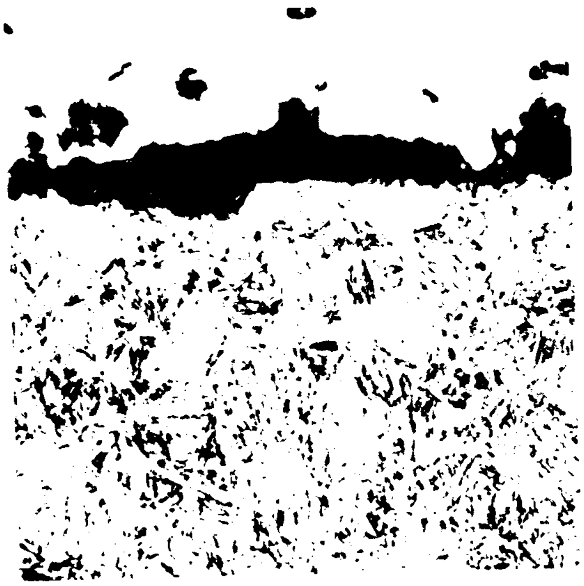

Cross-Section, X400

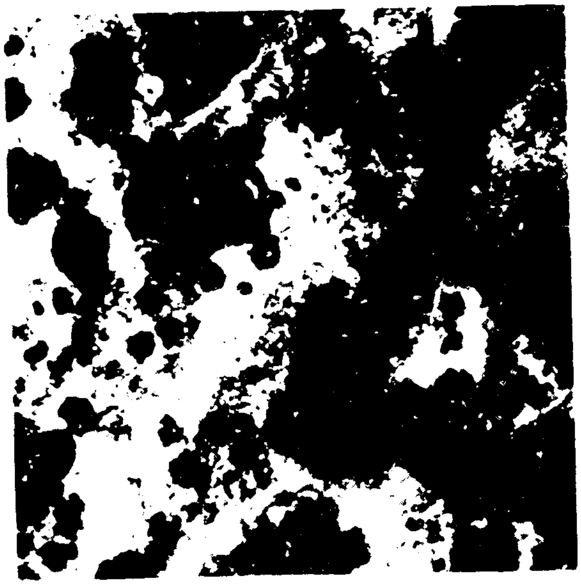

Surface, X13.5

(a) After 15 Days Alternate Immersion Exposure

Cross Section, X400

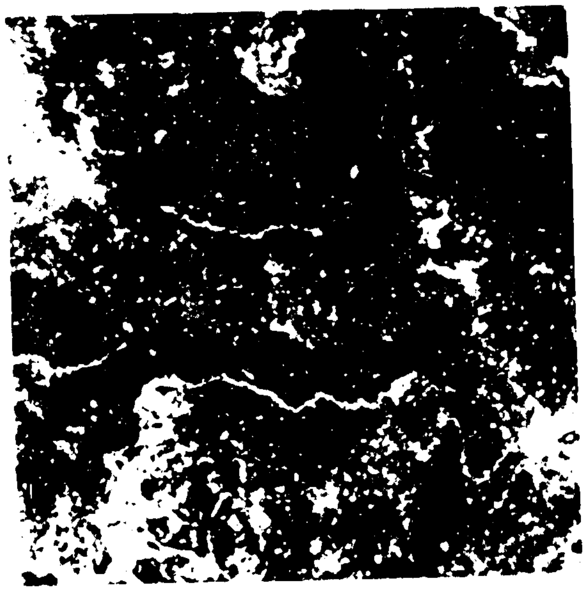

Surface, X13.5

(b) After 62 Days Alternate Immersion Exposure

FIGURE 4-6
EXTENT OF CORROSION ON D6AC STEEL SPECIMENS AUSTENITIZED AT 1158°K AFTER 15 AND 62 DAYS ALTERNATE IMMERSION EXPOSURE

Cross-Section, X400

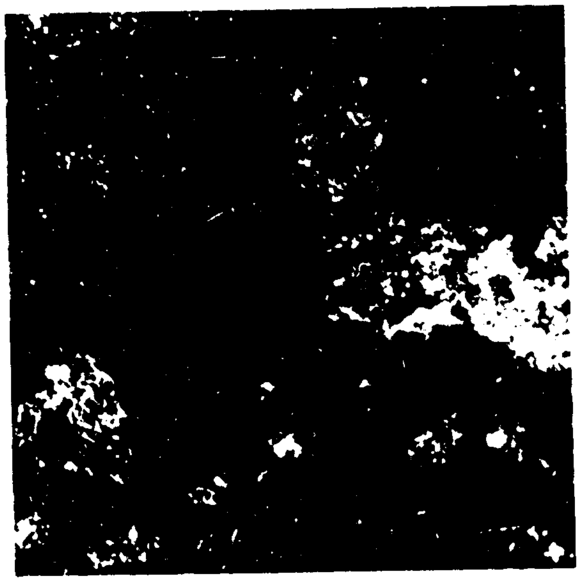

Surface, X13.5

(a) After 15 Days Alternate Immersion Exposure

Cross Section, X400

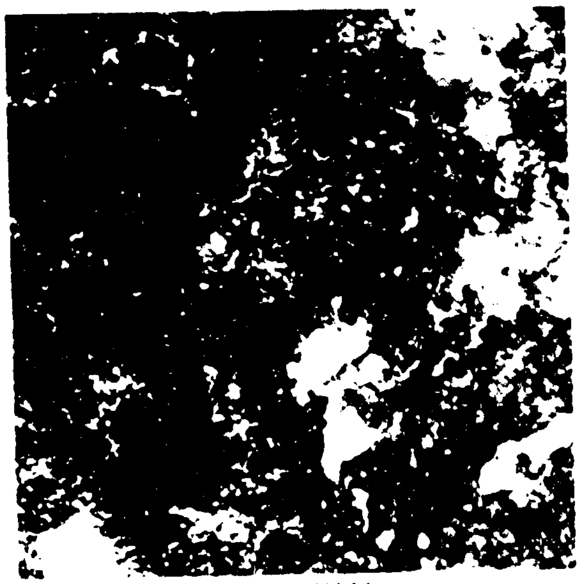

Surface, X13.5

(b) After 62 Days Alternate Immersion Exposure

FIGURE 4-7
EXTENT OF CORROSION ON D6AC STEEL SPECIMENS AUSTENITIZED AT $1200^{\circ}K$ AFTER 15 AND 62 DAYS EXPOSURE

Cross-Section, X400

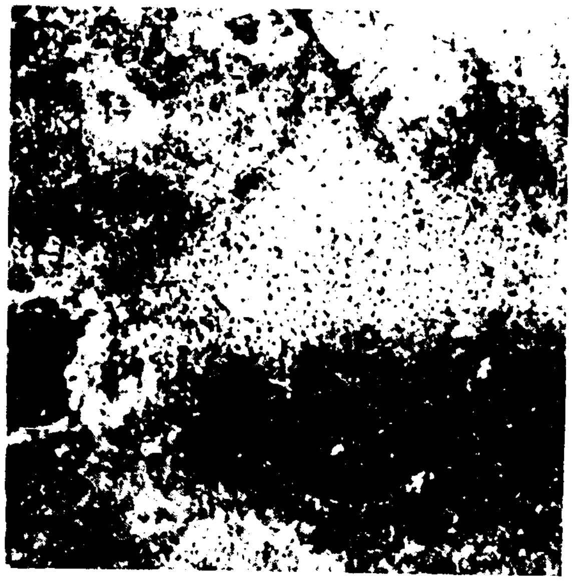

Surface, X13.5

(a) After 15 Days Alternate Immersion Exposure

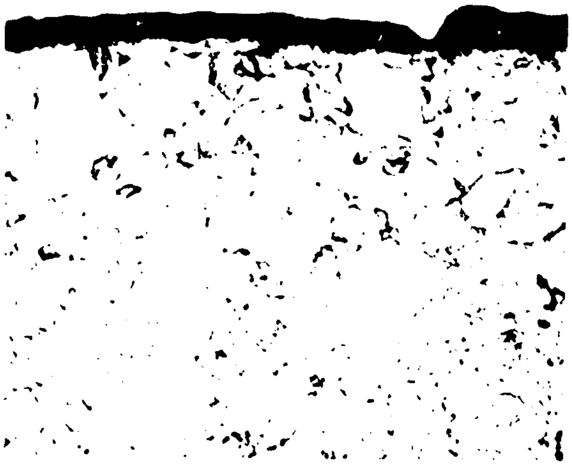

Cross-Section, X400

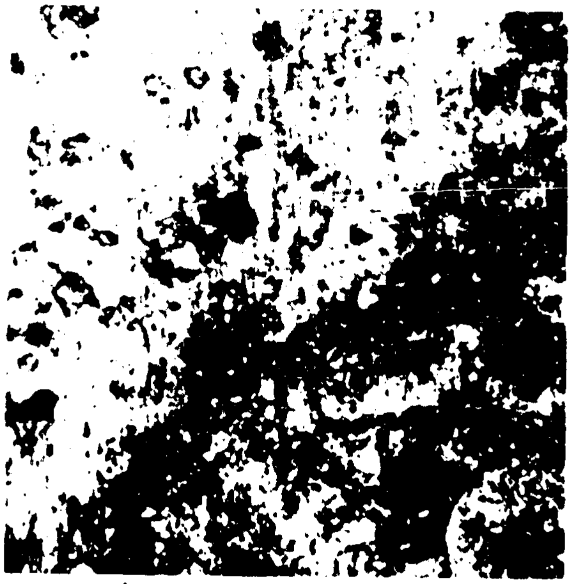

Surface, X13.5

(b) After 62 Days Alternate Immersion Exposure

FIGURE 4-8
EXTENT OF CORROSION ON 18 Ni MARAGING STEEL SPECIMENS
AFTER 15 AND 62 DAYS EXPOSURE

Photographs of the fracture surfaces of typical specimens of each alloy/heat treatment combination are shown in Figure 4-9; the nonlinear crack front observed in the 18 Ni maraging steel specimen is not present in any of the D6AC specimens.

The variation of stress intensity with exposure time for all specimens is illustrated in Figure 4-10. This figure shows that 18 Ni maraging steel has a much higher threshold stress intensity for stress corrosion cracking in synthetic sea water than either heat treatment of D6AC. Furthermore, this data indicates that the threshold stress intensity for D6AC steel at this strength level is independent of austenitizing temperature, since the data for both heat treatment conditions converges to the same value of stress intensity.

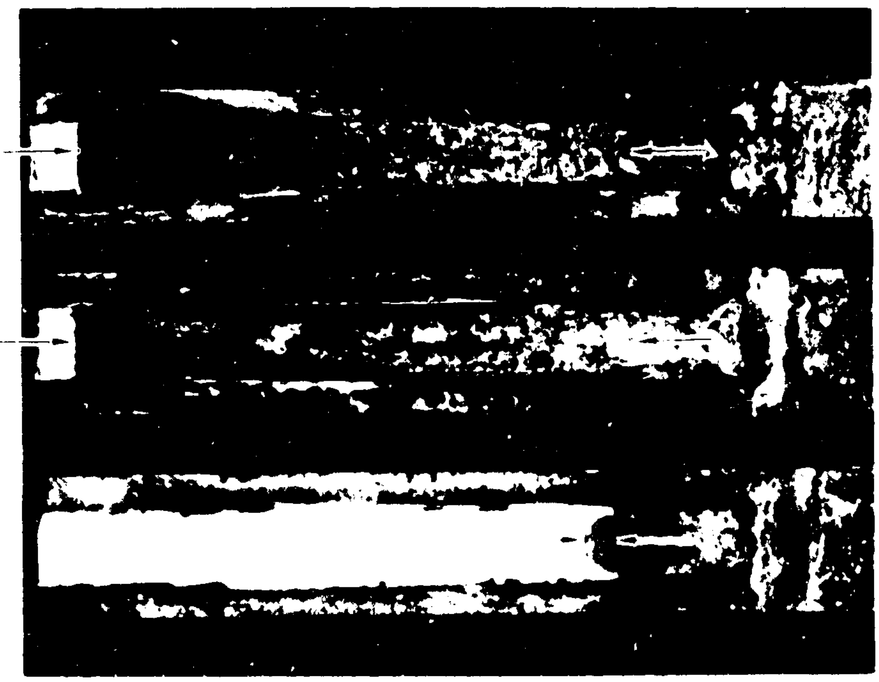

FIGURE 4-9
FRACTURE SURFACES OF HIGH STRENGTH STEEL MWOL SPECIMENS AFTER 62 DAYS ALTERNATE IMMERSION EXPOSURE

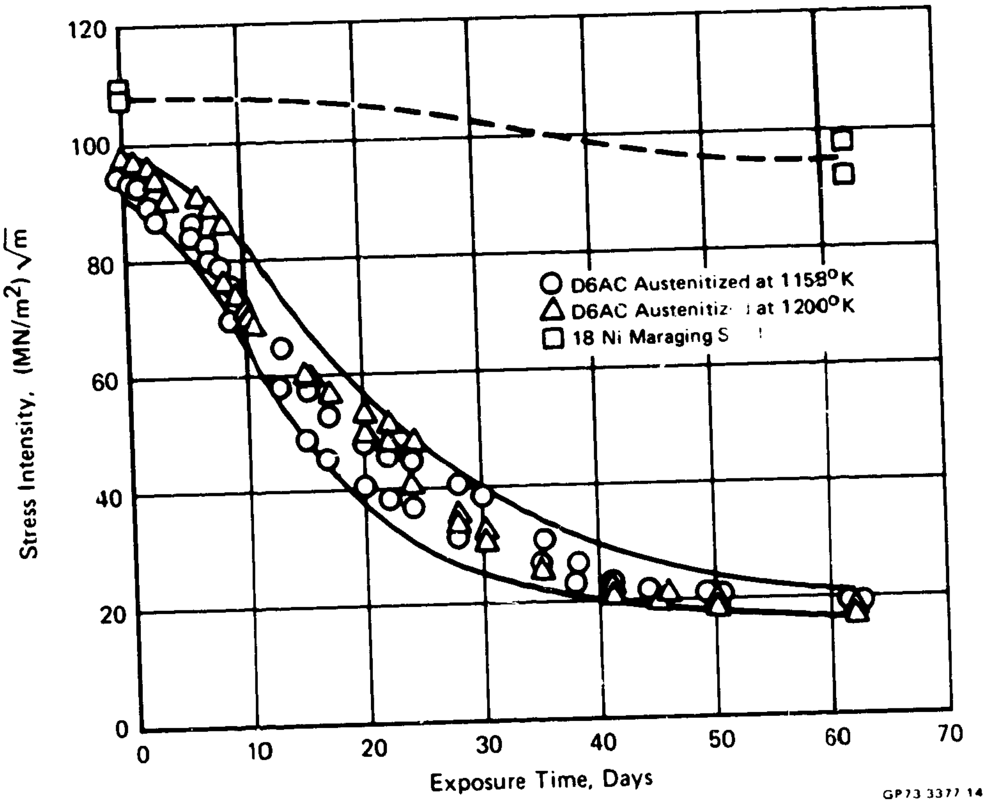

FIGURE 4-10
VARIATION OF STRESS INTENSITY WITH EXPOSURE TIME FOR HIGH STRENGTH STEEL MWOL SPECIMENS.

5.0 CRACK PROPAGATION TESTING

5.1 Precracking of Test Specimens

All flaws in the surface flawed specimens were prepared by using electrical discharge machining (EDM) to introduce the starter flaw. Tungsten sheet, 0.18 mm (.007 inch) thick, was used as an electrode material. The EDM starter flaw was then extended using the flexural fatigue apparatus shown in Figure 5-1. This technique involves cantilever loading the specimen over an anvil in such a way that the side containing the flaw is in tension. The specimens were fatigue precracked using this apparatus on a 44,500N (10,000 lb) capacity Sonntag fatigue machine at a frequency of 30 Hz. A cyclic stress ratio ($\sigma_{min}/\sigma_{max}$) of 0.8 was found to be necessary for this precracking technique. When lower stress ratios were used, excessive clatter developed and the specimen-fixture combination was observed to be under zero load. This behavior was determined to be a result of the stiffness of the specimen and fixture combination, which was such that its resonant frequency was at or near that of the Sonntag fatigue machine. Because of the invariance of the Sonntag's cyclic frequency, a single crack propagation rate was used, corresponding to .05 mm (.002 inch) per 1000 cycles. Maximum surface stress levels varied from 276 to 345 MN/m^2 (40 to 50 ksi). These stress levels were calculated using elastic beam theory, a procedure that has been experimentally confirmed in the calibration of similar specimens (References 11 and 12).

The number of cycles required to extend the starter flaws varied from specimen to specimen, depending on the EDM starter flaw size and the precracked flaw size required for subsequent testing. For D6AC, the number of cycles varied from 39,000 to 114,000; for 18 Ni maraging steel, the range varied from 76,000 to 444,000 cycles.

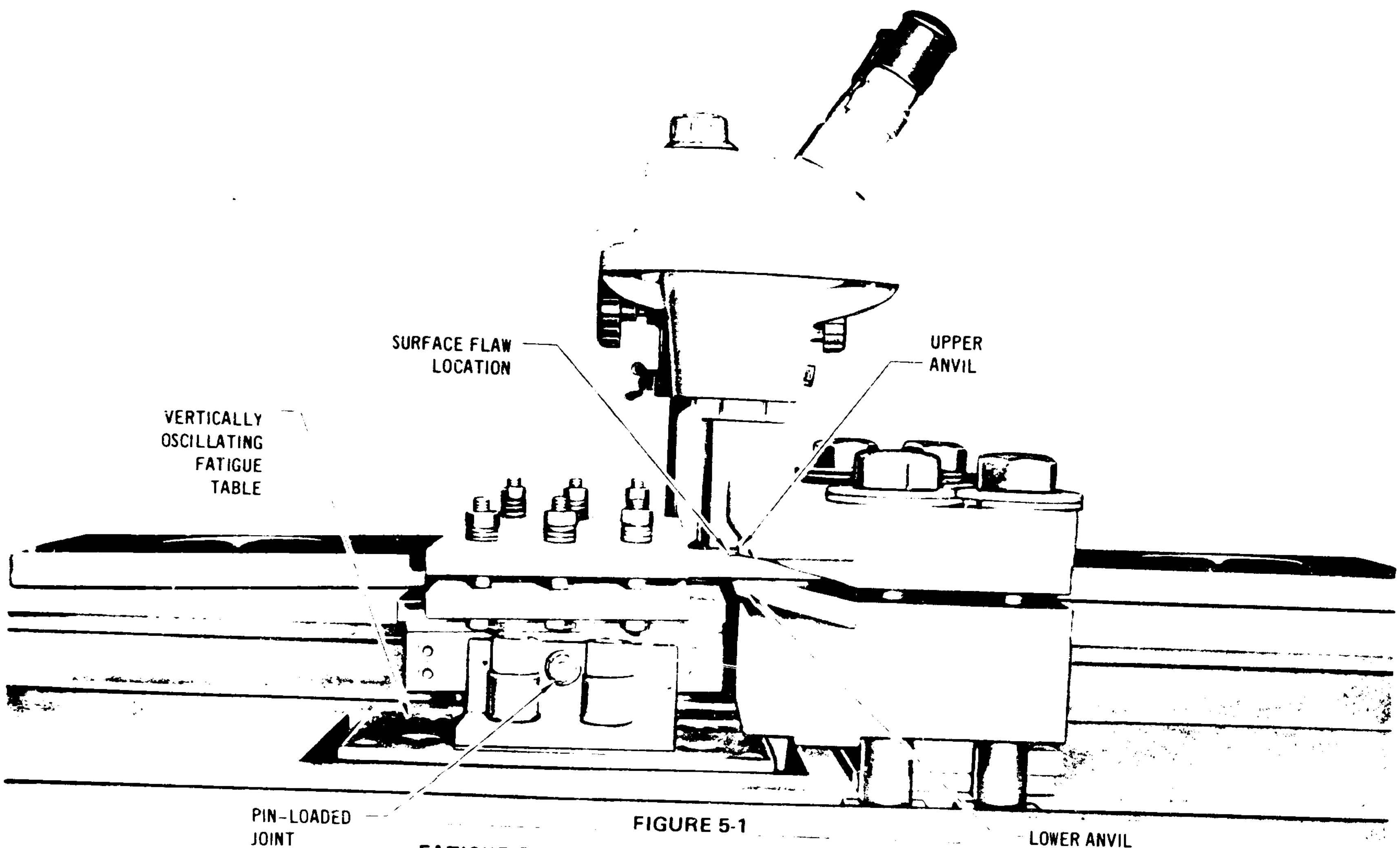

FIGURE 5-1

FATIGUE PRECRACKING APPARATUS FOR SURFACE FLAW SPECIMENS

5.2 Fracture Toughness Testing of Surface Flaw Specimens

In order to establish the initial flaw size for crack propagation testing, it was necessary to perform fracture toughness tests of each alloy to determine the relationship between room temperature gross section failure stress and normalized flaw size (a/Q). A loading rate of 266,880N (60,000 lbs) per minute was used. The results of this testing are shown in Table 5-1. The values of critical stress intensity, K_{IE}, were calculated using the relation,

$$K_{IE} = 1.1\sigma \sqrt{\pi (a/Q)}$$

The fracture surfaces of these specimens are shown in Figure 5-2.

5.3 Test Procedure

5.3.1 Determination of Initial Flaw Sizes

The crack propagation behavior of D6AC and 18 Ni maraging steel was investigated using multiple stress levels and a single flaw size. The cyclic stress levels were selected to provide a safety factor of approximately 1.4 on ultimate strength at the projected MEOP of 6900 MN/m^2 (1000 psi). Using the data of Table 3-2, this corresponds to a stress level of approximately 1080 MN/m^2 (156 ksi) for both alloys.

The single flaw size used for the cyclic tests of each alloy was defined by the proof test schedules to be used for the Shuttle SRB. The flaw size $(a/Q)_{max}$ required to cause failure in a motor case during an initial proof test of 1.15 MEOP can be determined from a curve of gross fracture stress vs. flaw size. For the alloys tested, such a curve is shown in Figure 5-3, which was plotted from the data of Table 5-1. For the D6AC steel, the flaw size $(a/Q)_{max}$ associated with the initial proof stress level is 2.64 mm (.104 inch). For the 18 Ni maraging steel, which has a higher fracture toughness, this flaw size is 4.80 mm (0.189 in),

TABLE 5-1 CRITICAL STRESS INTENSITY DATA, SURFACE FLAWED SPECIMENS												
ALLOY	SURFACE FLAW DIMENSIONS					a/Q		Failing Load		Gross Section Failure Stress		Critical Stress Intensity, K_{IE}
	DEPTH, a		LENGTH, 2c		a/2c							
	mm	in	mm	in		mm	in	MN	kips	MN/m^2	ksi	$(MN/m^2)\sqrt{m}$	ksi $\sqrt{in}$
18 Ni	4.11	.162	17.60	.693	.232	3.43	.135	1.203	270.5	1430	208	164	149
	4.67	.184	17.53	.690	.267	3.56	.140	1.257	282.5	1430	208	167	152
	5.10	.201	22.43	.883	.228	4.17	.164	1.148	258.0	1320	191	166	151
	5.36	.211	26.21	1.032	.204	4.57	.180	1.108	249.0	1270	184	168	153
	5.56	.219	30.35	1.195	.183	4.93	.194	1.083	243.5	1230	178	168	153
												AVG: 166	151
D6AC	3.35	.132	11.2	.442	.299	2.36	.093	1.160	261.6	1280	186	121	110
	3.81	.150	14.3	.561	.267	2.85	.112	1.080	243.5	1200	174	125	114
	4.67	.184	20.7	.813	.226	3.76	.148	.993	223.2	1110	160	132	120
	6.17	.243	32.6	1.285	.189	5.16	.203	0.805	181.0	887	129	124	113
												AVG: 126	114

indicative of the higher tolerance this material has for flaws. These (a/Q) values were transformed into actual flaw dimensions by linear interpolation of the data in Table 5-1. The flaw dimensions that correspond to the particular value of $(a/Q)_{max}$ for each alloy are listed in Table 5-2 for the precracking conditions employed.

Flaws less than this value of $(a/Q)_{max}$ would still be present in the structure and could, through subcritical flaw growth, cause failure during subsequent loading. Information as to the rate at which such subcritical flaw growth occurs was obtained by subjecting a series of specimens containing this particular flaw size to various cyclic stress profiles that simulate the expected service history of the SRB. The cyclic stress level was selected as the variable in the present study because the initial proof stress level of 1.15 MEOP is already quite near the guaranteed minimum yield strength for both alloys ($1.15_{MEOP}/F_{ty}$ = 0.970 for D6AC steel and 0.897 for 18 Ni maraging steel). For this reason, it was considered unrealistic to vary the initial proof stress level, and hence the value of $(a/Q)_{max}$, for crack propagation testing. Instead, the subsequent proof stress level was varied to measure its effect on cyclic life.

(a) 18 Ni Maraging Steel

σ_G = 1430 MN/m^2
a = 4.67 mm
2c = 17.53 mm
K_{IE} = 167 $(MN/m^2)\sqrt{m}$

σ_G = 1320 MN/m^2
a = 5.10 mm
2c = 22.43 mm
K_{IE} = 166 $(MN/m^2)\sqrt{m}$

σ_G = 1270 MN/m^2
a = 5.36 mm
2c = 26.21 mm
K_{IE} = 168 $(MN/m^2)\sqrt{m}$

σ_G = 1230 MN/m^2
a = 5.56 mm
2c = 30.35 mm
K_{IE} = 168 $(MN/m^2)\sqrt{m}$

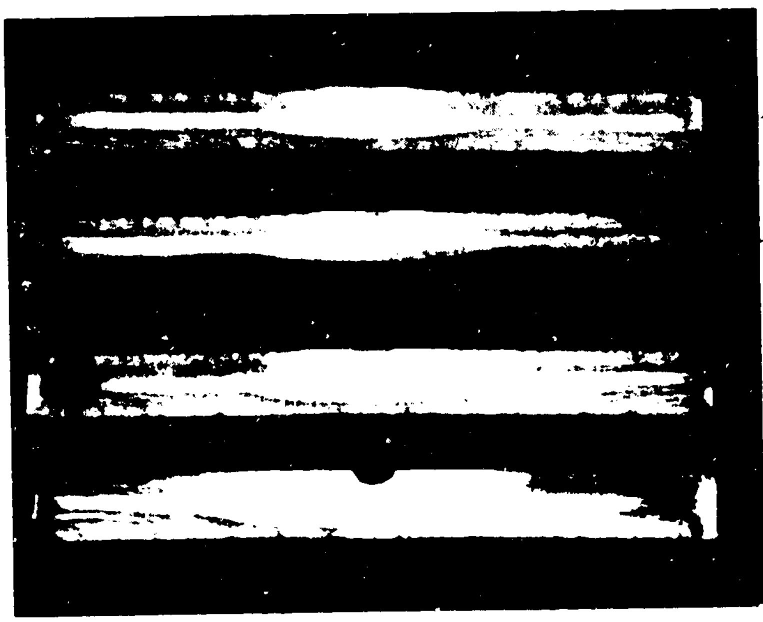

(b) D6AC Steel

σ_G = 1280 MN/m^2
a = 3.35 mm
2c = 11.2 mm
K_{IE} = 121 $(MN/m^2)\sqrt{m}$

σ_G = 1200 MN/m^2
a = 3.81 mm
2c = 14.3 mm
K_{IE} = 125 $(MN/m^2)\sqrt{m}$

σ_G = 1110 MN/m^2
a = 4.67 mm
2c = 20.7 mm
K_{IE} = 132 $(MN/m^2)\sqrt{m}$

σ_G = 887 MN/m^2
a = 6.17 mm
2c = 32.6 mm
K_{IE} = 124 $(MN/m^2)\sqrt{m}$

FIGURE 5-2
FRACTURE SURFACES OF HIGH STRENGTH STEEL SURFACE FLAW SPECIMENS AFTER FRACTURE TOUGHNESS TESTING

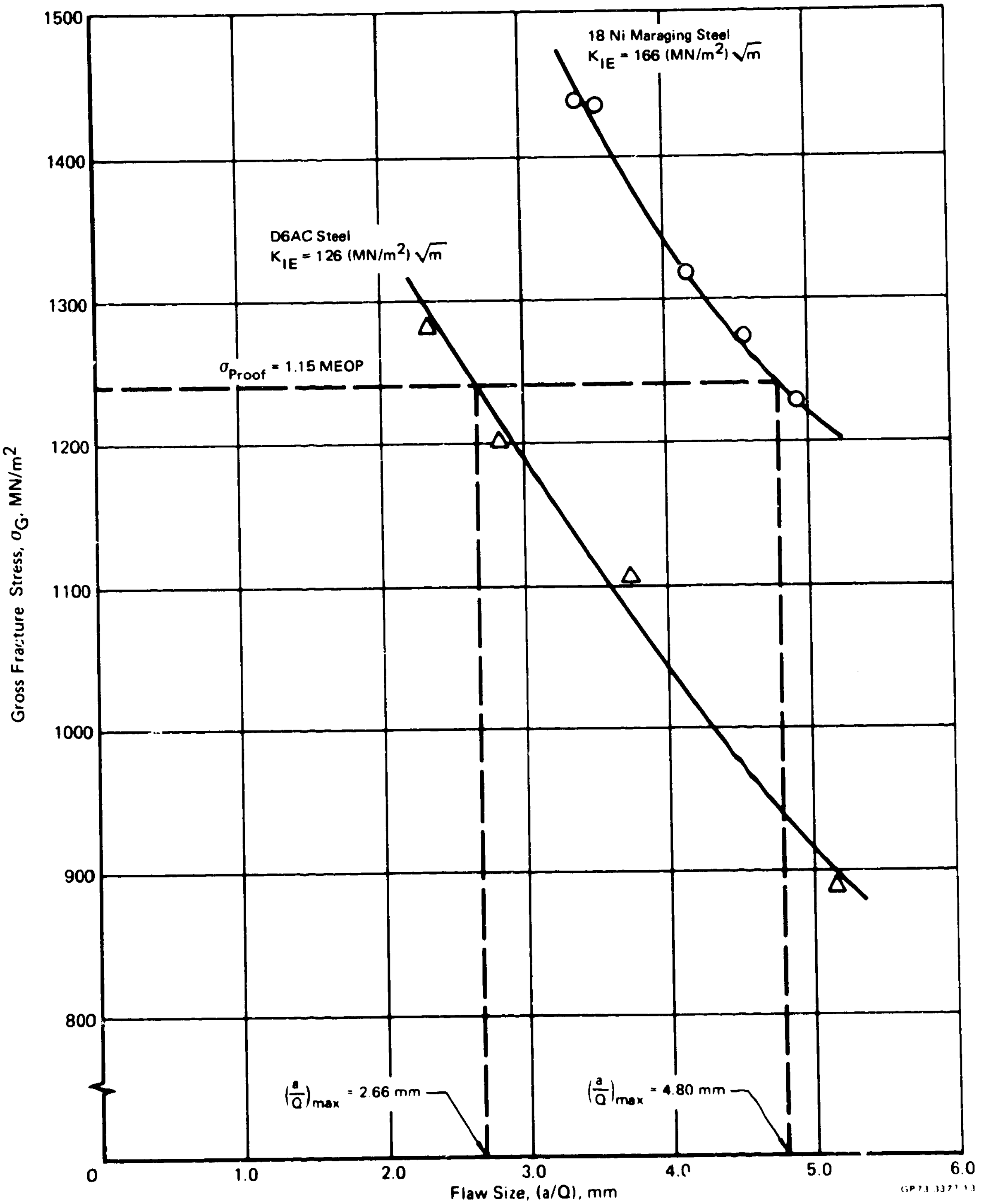

FIGURE 5-3
VARIATION OF GROSS SECTION FRACTURE STRESS WITH SURFACE FLAW SIZE

TABLE 5-2 FLAW SIZES USED FOR CYCLIC TESTING						
ALLOY	$(a/Q)_{max}$		FLAW LENGTH, 2c		FLAW DEPTH, a	
	mm	in	mm	in	mm	in
D6AC	2.66	.104	12.8	.500	3.50	.138
18 Ni Maraging	4.80	.189	28.70	1.130	5.46	.215

5.3.2 Cyclic Testing

The axial fatigue crack propagation testing was done in a 1.8 MN (400,000 lb) capacity Baldwin tensile machine on which the load was cycled manually. A calibrated strain link connected to a strip chart recorder was incorporated in the loading train during testing to supply a load-time history. The rate of loading was accomplished at the maximum capacity of the machine -- 0.89 MN/min (200,000 lbs/min). A sawtooth loading profile was used with a stress ratio of 0.1. Only the proof stress was varied; the operating stress was held constant at 1076 MN/m^2 (156 ksi) for all tests. The proof and operating stresses were applied alternately in order to simulate the loading history of the SRB.

Four specimens of each alloy were tested to failure using cyclic loading conditions only. Eight additional specimens of each alloy were tested using the combined load/temperature history shown in Figure 5-4. The 589°K (600°F) temperature cycle was introduced in order to simulate a liner removal method proposed for the refurbishment of the Shuttle SRB. Quartz heating lamps, located on each side of the specimen, served as the heat source for the tests. Temperature was monitored by thermocouples spot welded to the front and back surfaces of each specimen. These thermocouples were mounted 2.54 cm (1.0 in.) above and below the crack and indicated that good temperature uniformity was achieved throughout the test cycle; at no time did the temperature differ by more than 17°K (30°F).

During the temperature cycle, the applied stress was held constant at 108 MN/m^2 (15.6 ksi), corresponding to a stress ratio of 0.1. In order to maintain this stress level, the load was adjusted during the heating and cooling portion of the temperature cycle to offset the effects of thermal expansion. To minimize the time required to test each specimen, the fastest possible heating and cooling rates were used. No more than four minutes was required to heat the specimen to 589°K (600°F), and approximately eight minutes was required to achieve a temperature of 150°F using forced air cooling. Loading for the next test cycle was initiated once this temperature was achieved by all four thermocouples.

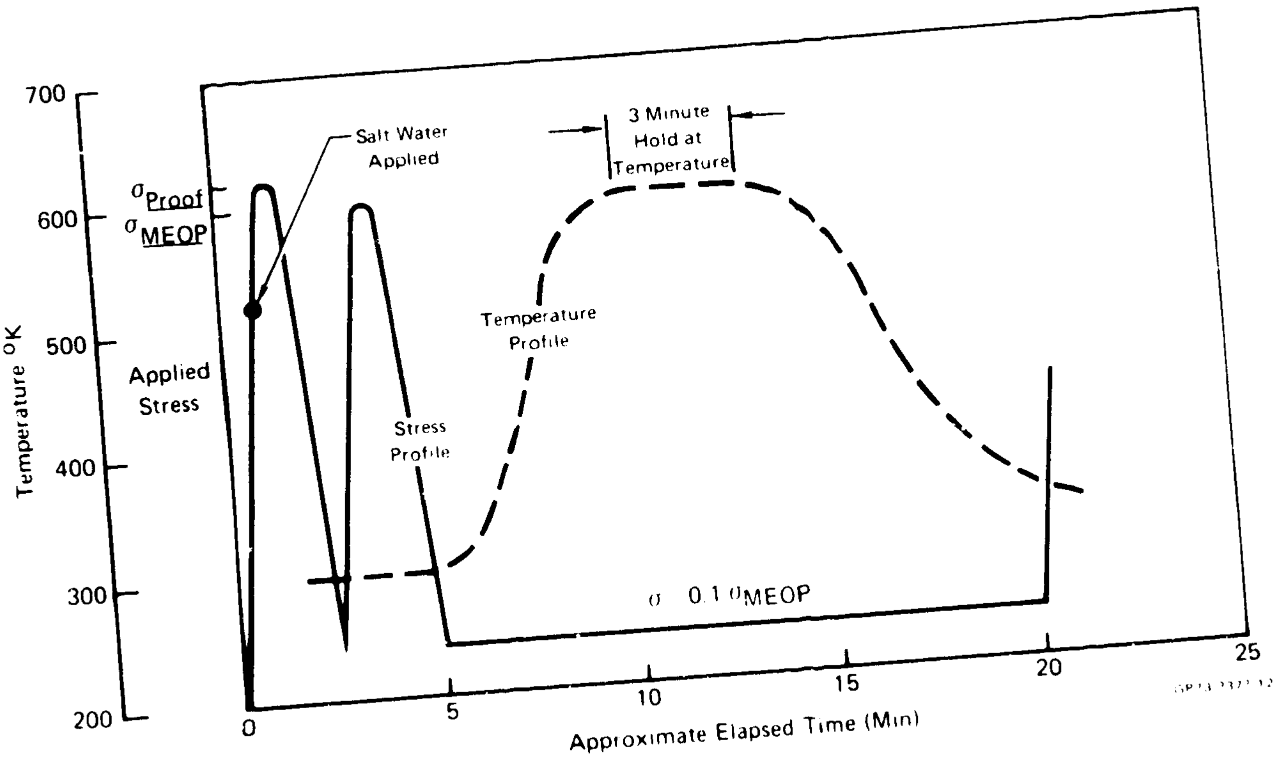

FIGURE 5-4
STRESS/TEMPERATURE CYCLE FOR CRACK PROPAGATION TESTING

Of the eight specimens of each alloy tested under cyclic load and temperature conditions, four were cycled in air and four were cycled with intermittant exposure to synthetic sea water. For these latter tests, five cubic centimeters of synthetic sea water was blown into the crack front using 1.38 MN/m^2 (200 psi) compressed air. The salt water was applied on each primary load cycle (i.e., the cycle corresponding to proof st ess) when the load reached 75% of the maximum value. All specimens subjected to cyclic load and temperature conditions were tested either to failure or until the specimen sustained 40 test cycles.

5.4 Results of Crack Propagation Testing

All pertinent data regarding the crack propagation tests of both alloys are reported in Appendix B. One of the 18 Ni maraging steel specimens, number M1, was tested under uniform cyclic stressconditons (1080 MN/m^2 or 156 ksi), in order to ascertain the effect of proof testing at the stress level associated with the maximum expected operating pressure of the SRB. After the specimen sustained the full 40 pairs of stress cycles, 200 cycles were applied to this specimen at a maximum stress of 690 MN/m^2 (100 ksi) and a stress ratio of 0.1 in order to mark the flaw front at this location. The test was then continued at a stress level corresponding to MEOP until fracture occurred. The multiple flaw depths reported in Table B-1 for this specimen reflect this loading history.

The cyclic test data of Appendix B, plotted in Figure 5-5 as initial stress intensity vs the number of cycles to failure, indicates that the cyclic flaw growth behavior of 18 Ni maraging steel is unaffected by expected liner removal temperatures. However, at longer exposure times, accelerated flaw growth appears to have occurred in the specimens exposed to synthetic sea water. In contrast, the cyclic test data for D6AC steel indicates that flaw growth is accelerated by temperature cycling to 589°K (600°F); subsequent exposure to synthetic sea water under similar cyclic load and temperature conditions produces no further decrease in cyclic life.

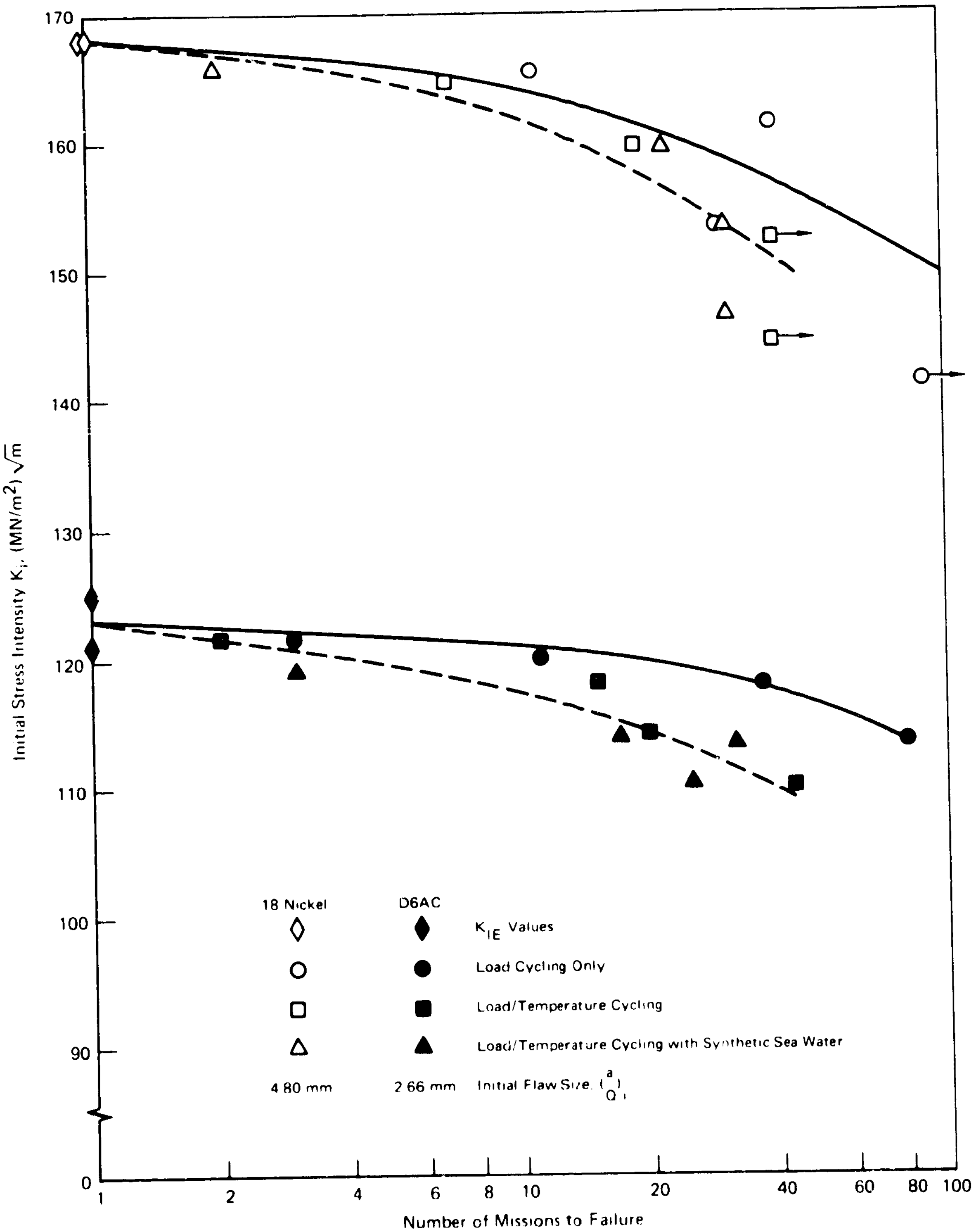

FIGURE 5-5
RESULTS OF CRACK PROPAGATION TESTING

An attempt was made to determine the mechanisms responsible for this accelerated flaw growth by examining selected specimens of both alloys with the scanning electron microscope (SEM). Two-stage plastic/carbon replicas of the fracture surfaces of selected D6AC specimens were also examined with the transmission electron microscope. The results of this examination, presented in Appendix B, revealed that the morphologies of the fatigue zones were so similar that it was impossible to determine which mechanisms were responsible for the observed decreases in cyclic life. Figures 5-6 and 5-7 show the salient features of the fracture surfaces of a D6AC and an 18 Ni maraging steel specimen, respectively; Figure 5-8 contains stereo photographs of these same specimens.

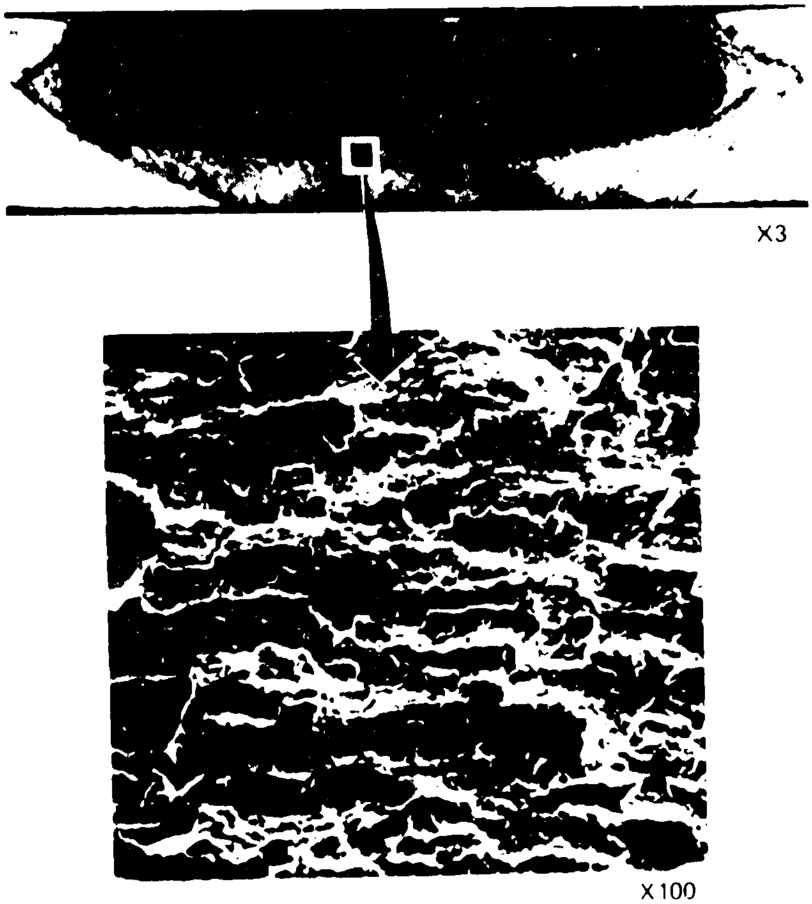

FIGURE 5-6
TYPICAL FRACTURE SURFACE OF MISSION CYCLED 18 NICKEL MARAGING STEEL SURFACE FLAWED SPECIMEN

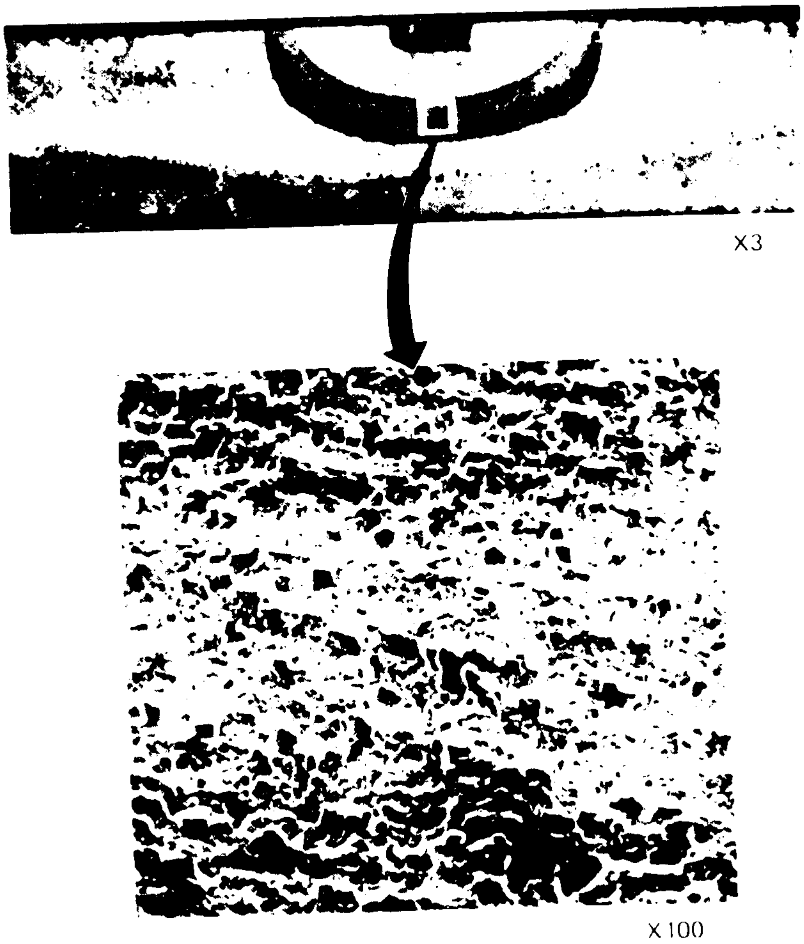

FIGURE 5-7
TYPICAL FRACTURE SURFACE OF MISSION
CYCLED D6AC STEEL SURFACE FLAWED SPECIMEN

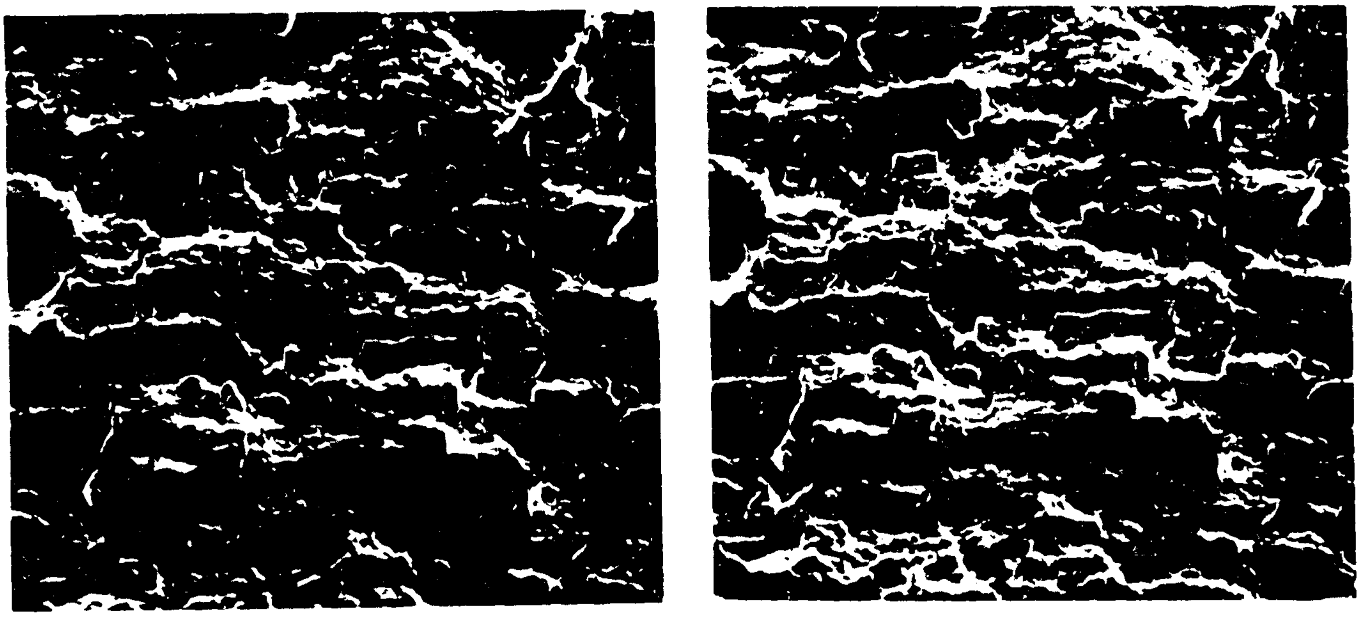

(a) 18 Nickel Maraging Steel

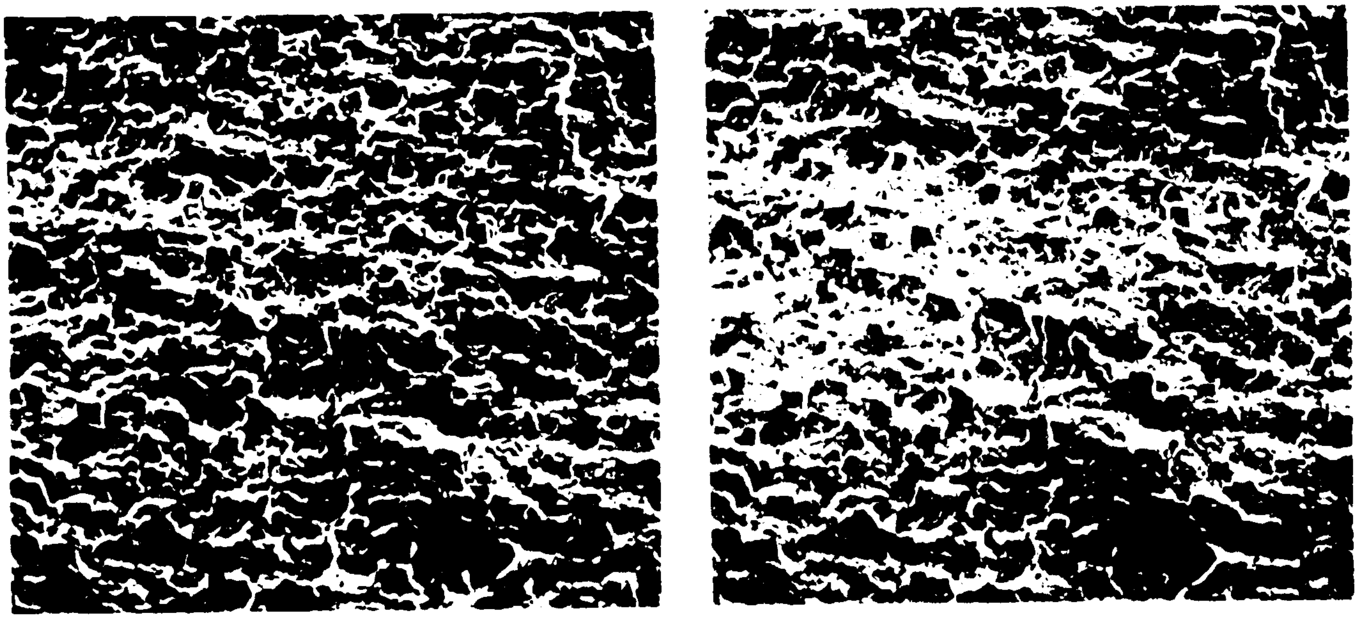

(b) D6AC Steel

FIGURE 5 8
STEREO PHOTOGRAPHS OF THE FRACTURE SURFACES OF SPECIMENS SUBJECTED TO LOAD AND TEMPERATURE CYCLING AT 1.05 MEOP (X100)

(THIS PAGE INTENTIONALLY LEFT BLANK)

5.4.1 Discussion of Test Results -- 18 Ni Maraging Steel

The accelerated flaw growth observed when 18 Ni maraging steel is exposed to mission cycling with synthetic sea water is probably a result of combined stress corrosion and fatigue crack growth. Such flaw growth would occur on each load cycle whenever the stress intensity exceeded the threshold value, and would be more pronounced in those specimens that were cycled at the lower stress levels (i.e., greater number of cycles to failure), where the total amount of sustained load crack growth was higher.

5.4.2 Discussion of Test Results -- D6AC Steel

For the cyclic tests of D6AC, accelerated crack growth was observed for all tests involving temperature cycling to 589°K (600°F). Periodic exposure to synthetic sea water under cyclic load and temperature conditions produced no further decrease in cyclic life, even though this alloy was found to be susceptible to stress corrosion cracking (Section 4.6). It appears that the mechanism is related to subtle microstructural changes that occurred as a result of load and temperature cycling. One such mechanism might be related to the strain tempering phenomenon observed in an earlier study of D6AC steel at a different strength level (Reference 13). In this study, the initial tempering and the retempering temperatures employed differed significantly from those used in the present study and no cyclic tests were performed. It was found, however, that the yield strength could be increased and, in some cases, fracture toughness decreased by prestraining and retempering specimens prior to test. It has been proposed (Reference 14) that this phenomenon may be associated with a martensite decomposition reaction. Although it is likely that strain tempering of martensite did occur in the D6AC specimens subjected to load and temperature cycling, such a hypothesis could only be confirmed by further testing.

5.4.3 Comparison of Test Results

The cyclic flaw growth data for D6AC and 18 Ni maraging steel obtained in the present study can be compared by normalizing the initial stress intensity to account for differences in fracture toughness (K_{IE}). This is done in Figure 5-9 by plotting the ratio of initial-to-critical stress intensity, K_i/K_{IE}, vs the number of missions to failure. This figure shows that the cyclic flaw growth behavior of these two alloys are remarkably similar when normalized to account for differences in fracture toughness. Furthermore, this data appears to indicate that an SRB fabricated from D6AC might survive more missions that one of 18 Ni maraging steel, since the K_i/K_{IE} ratio for the latter alloy is slightly higher. If such small differences are ignored and lower bound data is used, then an SRB fabricated from either alloy would survive approximately 15 missions before failure would occur. This estimation of cyclic life is based upon the preliminary design parameters quoted in Section 2.1 and can be increased by either decreasing the operating stress level of the case, keeping the initial proof stress constant, or by increasing the initial proof stress in order to decrease the initial flaw size present after fabrication.

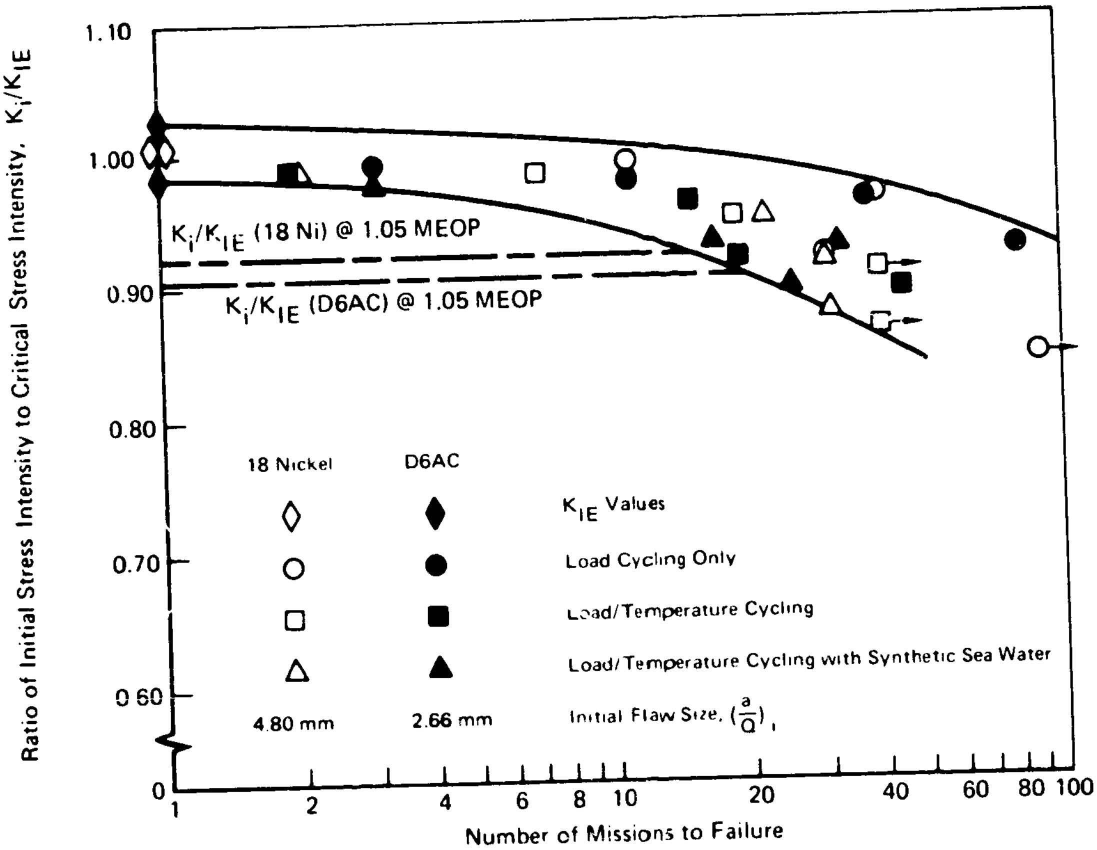

GP73 3377 7

FIGURE 5-9
RELATIONSHIP BETWEEN NORMALIZED STRESS INTENSITY AND MISSIONS TO FAILURE FOR D6AC AND 18 NICKEL MARAGING STEEL

6.0 CONCLUSIONS

The results of this study indicate that the corrosion and stress corrosion resistance of 18 Ni maraging steel is superior to that of D6AC steel when exposed to synthetic sea water. No benefit as regards resistance to corrosion or stress corrosion is obtained by austenitizing D6AC steel at 1200°K (1700°F) rather than the conventional temperature of 1158°K (1625°F).

Under fatigue conditions that simulate expected SRB service conditions, both D6AC and 18 Ni maraging steel will survive approximately 15 missions prior to failure, five more than current designs require. However, if a scatter factor of four is applied to the 10 mission minimum requirement, then neither alloy will satisfy current demands. This low cyclic life is primarily a result of the temperature and salt water environments imposed during testing, since tests conducted under cyclic loading conditions alone indicate that an actual lifetime of 40 missions is nearly obtained. For D6AC steel, liner removal operations that involve heating to 589°K (600°F) cause a decrease in cyclic life. For 18 Ni maraging steel, a decrease in cyclic life occurs upon intermittent exposure to synthetic sea water.

7.0 RECOMMENDATIONS FOR FURTHER STUDY

As a result of this study, several areas have been observed that require further investigation. These studies should be conducted in order to select a material for the SRB case that is both economical and reliable enough to satisfy the demand for reusability.

The present study has indicated that the cyclic life of D6AC steel is decreased by exposure to temperatures of 589°K (600°F) following the application of cyclic loads. Such thermal exposure, simulating a proposed liner removal method, is not mandatory, since alternative removal methods are available. Since the mechanism responsible for the accelerated crack growth in D6AC steel as a result of such exposure is not completely understood, the effect of the other thermal cycles experienced by the SRB cannot be predicted. Consequently, further studies should be undertaken to determine if other, lower temperature thermal cycles produce similar decreases in cyclic life.

The present study has provided data on the crack growth behavior of D6AC and 18Ni maraging steel under sustained and cyclic loading conditions. No such data, however, has been generated on these alloys in the welded condition, and it is certain that a large, complex vehicle like the SRB will contain welds. Such data should be obtained because accurate predictions of the performance of welded alloys cannot be made from data on parent metal. Any studies of the crack growth behavior of welds should include an evaluation of gas-tungsten arc (GTA) and gas-metal arc (GMA) welding processes. With respect to D6AC steel, such studies should include an evaluation of the effects of various postwelding heat treatments.

As a result of this study, crack growth data under simulated SRB service conditions is now available on two candidate case materials. It is possible that both alloys will not economically meet the requirements for reliability and reusability. Consequently, additional crack growth studies on such steels as 10Ni-Cr-Mo-V (HY-180) or HP-9-4-.20 would be required to determine if a more viable material exists for the SRB motor case.

8.0 REFERENCES

1. Aerojet Solid Propulsion Company, "Study of Solid Rocket Motor for a Space Shuttle Booster," Final Report 1917-FR1, 15 March 1972.

2. Conversations with C. Crockett, Astronautics Laboratory, and R. Eilerman, SRB Program Office, NASA, Marshall Space Flight Center, 13 October 1972.

3. Aerojet-General Corporation, "260 Inch Diameter Motor Feasibility Demonstration Program" Final Program Summary Report, NASA CR-72127, April 1966.

4. C. E. Fedderson, D. P. Moon, W. S. Hyler, "Crack Behavior in D6AC Steel," Metals and Ceramics Information Center Report No. MCIC-72-04, January 1972.

5. J. A. Klies, in Weld Imperfections, ed. by A. R. Fluges and R. E. Lewis, Addison-Wesley Publishing Company, Menlo Park, California, 1968, p. 333.

6. S. R. Novak, S. T. Rolfe, "Modified WOL Specimen for K_{Iscc} Environmental Testing" Journal of Materials, Vol. 4, No 3, September 1969, p. 701-728.

7. W. F. Brown, Jr., J. E. Srawley, "Review of Developments in Plane Strain Fracture Toughness Testing", ASTM STP 463, American Society for Testing and Materials, 1970, pp 216-247.

8. W. F. Brown, Jr., J. E. Srawley, "Plane Strain Crack Toughness Testing of High Strength Metallic Materials," ASTM STP 410, American Society for Testing and Materials, 1966, pp. 9-16.

9. D. M. Fisher, R. T. Bubsey, and J. E. Srawley, "Design and Use of a Displacement Gage for Crack Extension Measurements," National Aeronautics and Space Administration Technical Note D-3724, November 1966.

10. J. E. Srawley, W. F. Brown, Jr., "Fracture Toughness Testing and Its Applications," ASTM STP 381, American Society for Testing and Materials, 1965, p. 190.

11. Conversation with D. L. Corn of Aeroneutronics, Division of Philco-Ford, Newport Beach, California, 7 March 1973.

12. D. H. Killpatrick, D. L. Corn, G. R. Stoeckinger, "Cryogenic Fracture Toughness of 18 Nickel 200-Grade Maraging Steel Plate and Welds," presented at the 1973 Westec Conference, Los Angeles, California, 12 March 1973.

13. R. E. Yount, "Determination of Engineering Properties of Mar-Strained Steels," ASD-TDR-62-230, August 1962.

14. D. Kalish, M. Cohen, "Structural Changes and Strengthening in the Strain Tempering of Martensite," Material Science and Engineering, September 1970, Vol. 6 (3), pp. 156-166.

APPENDIX A

STRESS INTENSITY/TIME DATA FOR MWOL SPECIMENS

The following data tables incorporate the crack length, applied load, and stress intensity values obtained on MWOL specimens during alternate immersion testing. The applied load and stress intensity values were calculated using equations (2), (3), (4), and (5) and the following relationship between applied load (P), specimen compliance (S), and initial specimen deflection (D):

$$P = \frac{D}{S}$$

Because of the great number of calculations involved, a short computer program was written to transform the crack length measurements into the required load and stress intensity data. This program has been disclosed as a New Technology Report.

TABLE A-1 STRESS INTENSITY AS A FUNCTION OF EXPOSURE TIME FOR D6AC STEEL AUSTENITIZED AT 1158°K (1625°F)*

SPECIMEN	EXPOSURE TIME (DAYS)	CRACK LENGTH mm	CRACK LENGTH in.	APPLIED LOAD N	APPLIED LOAD LBS	STRESS INTENSITY $(MN/m^2)\sqrt{m}$	STRESS INTENSITY $ksi\sqrt{in}$
MD-104	0	28.3	1.114	16283	3661	94.7	86.2
MD-104	1	28.5	1.124	15963	3589	93.7	85.2
MD-104	2	29.5	1.163	14784	3324	89.7	81.6
MD-104	3	30.4	1.196	13862	3116	86.5	78.7
MD-104	6	30.9	1.217	13309	2992	84.6	77.0
MD-104	7	32.3	1.270	12017	2702	80.1	72.9
MD-104	8	33.5	1.317	10979	2468	76.7	69.8
MD-104	9	36.6	1.442	8582	1929	69.8	63.5
MD-104	10	37.4	1.473	8050	1810	68.4	62.3
MD-104	13	43.8	1.724	4389	987	58.3	53.0
MD-104	15	47.9	1.886	2698	607	48.9	44.5
MD-104	17	49.1	1.932	2325	523	45.9	41.8
MD-104	20	51.4	2.022	1725	388	40.1	36.5
MD-104	22	51.6	2.033	1662	374	39.4	35.9
MD-104	24	52.4	2.064	1498	337	37.5	34.1
MD-104	28	54.6	2.150	1120	252	32.4	29.5
MD-104	30	55.6	2.188	986	222	30.3	27.6
MD-104	35	57.5	2.263	768	173	26.5	24.2
MD-104	38	59.8	2.353	572	129	22.6	20.6
MD-104	41	60.7	2.390	509	114	21.2	19.3
MD-104	45	60.7	2.390	509	114	21.2	19.3
MD-104	50	60.9	2.396	499	112	21.0	19.1
MD-104	62	61.8	2.435	441	99	19.6	17.8
MD-106	0	28.1	1.107	16643	3742	94.9	86.3
MD-106	1	28.5	1.121	16189	3640	93.4	85.0
MD-106	2	28.5	1.123	16125	3625	93.2	84.8
MD-106	3	29.3	1.154	15169	3410	90.0	81.9
MD-106	6	30.4	1.196	13975	3142	86.0	78.3
MD-106	7	31.3	1.233	13010	2925	82.7	75.2
MD-106	8	32.5	1.280	11884	2672	78.9	71.8
MD-106	9	33.5	1.320	11004	2474	76.0	69.2
MD-106	10	35.0	1.378	9832	2210	72.5	66.0
MD-106	13	39.6	1.560	6708	1508	64.8	58.9
MD-106	15	43.5	1.712	4575	1028	58.5	53.3
MD-106	17	45.9	1.806	3488	784	53.5	48.7
MD-106	20	48.0	1.888	2703	608	48.5	44.1
MD-106	22	48.6	1.914	2486	559	46.8	42.6
MD-106	24	49.4	1.944	2254	507	44.9	40.8
MD-106	28	51.0	2.006	1835	413	40.9	37.2
MD-106	30	51.7	2.034	1670	376	39.1	35.0
MD-106	35	55.3	2.176	1035	233	30.8	28.0
MD-106	38	57.6	2.266	766	172	26.2	23.9
MD-106	41	59.4	2.338	606	136	23.1	21.0
MD-106	45	60.8	2.395	505	113	20.9	19.0
MD-106	50	60.8	2.395	505	113	20.9	19.0
MD-106	62	62.1	2.445	431	97	19.1	17.4

*Exposure Conditions: 1 hour cycles, consisting of 10 minutes immersion in synthetic sea water, ASTM-D-114-52, Formula A, followed by 50 minutes of air exposure.

TABLE A-2 STRESS INTENSITY AS A FUNCTION OF EXPOSURE TIME FOR D6AC STEEL AUSTENITIZED AT 1200°K (1700°F) *

SPECIMEN NO.	EXPOSURE TIME (DAYS)	CRACK LENGTH mm.	CRACK LENGTH in.	APPLIED LOAD N	APPLIED LOAD LBS	STRESS INTENSITY $(MN/m^2)\sqrt{m}$	STRESS INTENSITY $ksi\sqrt{in}$
LB-104	0	28.3	1.114	17253	3879	97.3	88.6
LB-104	1	28.3	1.116	17184	3863	97.1	88.4
LB-104	2	28.6	1.126	16847	3788	96.0	87.4
LB-104	3	30.1	1.186	15006	3374	90.0	81.9
LB-104	6	30.8	1.211	14268	3208	87.5	79.6
LB-104	7	31.9	1.254	13131	2952	83.7	76.1
LB-104	8	34.1	1.344	11042	2482	77.0	70.1
LB-104	9	35.8	1.409	9720	2185	73.3	66.7
LB-104	10	37.0	1.457	8818	1982	71.0	64.6
LB-104	13	41.7	1.640	5814	1307	63.8	58.1
LB-104	15	43.7	1.721	4690	1054	60.1	54.7
LB-104	17	45.6	1.796	3777	849	55.9	50.9
LB-104	20	46.7	1.837	3335	750	53.4	48.6
LB-104	22	47.8	1.880	2914	655	50.7	46.1
LB-104	24	48.6	1.912	2629	591	48.5	44.2
LB-104	28	53.7	2.113	1345	302	35.5	32.3
LB-104	30	55.0	2.164	1132	255	32.5	29.6
LB-104	35	57.8	2.274	785	176	26.8	24.3
LB-104	38	57.9	2.281	767	172	26.4	24.0
LB-104	41	59.9	2.358	597	134	23.0	21.0
LB-104	45	60.9	2.398	525	118	21.5	19.5
LB-104	50	62.3	2.452	443	100	19.5	17.8
LB-104	62	63.0	2.482	404	91	18.5	16.9
LB-105	0	28.2	1.110	17252	3879	97.2	88.5
LB-105	1	28.2	1.112	17184	3863	97.0	88.3
LB-105	2	28.9	1.136	16387	3684	94.5	86.0
LB-105	3	29.1	1.147	16036	3605	93.3	84.9
LB-105	6	29.8	1.172	15270	3433	90.8	82.6
LB-105	7	30.2	1.190	14743	3314	89.0	81.0
LB-105	8	31.2	1.228	13696	3079	85.5	77.8
LB-105	9	34.1	1.344	10954	2463	76.6	69.7
LB-105	10	37.9	1.494	8094	1820	69.1	62.9
LB-105	13	39.6	1.560	6994	1572	66.6	60.6
LB-105	15	43.6	1.715	4731	1064	60.0	54.6
LB-105	17	45.2	1.780	3930	883	56.6	51.5
LB-105	20	47.9	1.885	2845	640	50.1	45.6
LB-105	22	48.8	1.922	2525	568	47.6	43.3
LB-105	24	51.3	2.020	1826	410	41.1	37.4
LB-105	28	54.5	2.145	1197	289	33.4	30.4
LB-105	30	56.0	2.204	982	221	30.1	27.4
LB-105	35	58.8	2.315	681	153	24.7	22.5
LB-105	38	60.4	2.377	557	125	22.2	20.2
LB-105	41	60.3	2.413	497	112	20.8	18.9
LB-105	45	61.6	2.427	476	107	20.3	18.5
LB-105	50	61.9	2.436	462	104	20.0	18.2
LB-105	62	62.5	2.462	427	96	19.1	17.4

*Exposure Conditions: 1 hour cycles, consisting of 10 minutes immersion in synthetic sea water, ASTM-D 114-52, Formula A, followed by 50 minutes of air exposure.

TABLE A-3. STRESS INTENSITY AS A FUNCTION OF EXPOSURE TIME FOR 18 Ni MARAGING STEEL *							
SPECIMEN NO.	EXPOSURE TIME (DAYS)	CRACK LENGTH		APPLIED LOAD		STRESS INTENSITY	
		mm.	in.	N	LBS	$(MN/m^2)\sqrt{m}$	ksi$\sqrt{in}$
M-114	0	27.9	1.099	19131	4301	108.3	98.5
M-114	62	31.5	1.239	14547	3270	92.9	84.6
M-115	0	28.3	1.113	18842	4236	108.0	98.3
M-115	62	30.7	1.208	15642	3517	97.2	88.5

* Exposure Conditions: 1 hour cycles, consisting of 10 minutes immersion in synthetic sea water, ASTM-D-114-52, Formula A, followed by 50 minutes of air exposure.

APPENDIX B

CRACK PROPAGATION DATA FOR SURFACE FLAW SPECIMENS

The following tables incorporate the crack propagation data obtained from tests of surface flawed specimens of D6AC and 18 Ni maraging steel under simulated SRB service conditions. The data has been separated into three tables for each alloy. One table lists the data for the baseline test condition, where specimens were subjected to pairs of stress cycles. These stress cycles included a primary stress that simulated a proof test prior to each mission and a secondary stress that simulated the pressurized portion of the SRB flight cycle. Another table lists the data obtained on those specimens that were tested under similar cyclic loading conditions but were also exposed to elevated temperature cycles. For these tests, a single temperature cycle that included a three minute hold at 589°K (600°F) was applied after each pair of stress cycles. The third table lists the data obtained on those specimens that were tested under similar cyclic load and temperature conditions but were also exposed to a synthetic sea water environment. For these tests, five cubic centimeters of sea water was blown into the crack front using compressed air; the solution was applied on each primary stress cycle when the load reached 75% of the maximum value.

TABLE B-1 CRACK PROPAGATION DATA FOR 18 NICKEL MARAGING STEEL--LOAD CYCLING ONLY

		M1*	M2	M3	M4
SPECIMEN NO.		M1*	M2	M3	M4
PROOF FACTOR, α		1.00	1.05	1.10	1.13
LABORATORY ENVIRONMENT o Temperature	°K °F	295-299 71-79	300 80	297 75	299 78
o Relative Humidity (%)		27-41	44	30	30
MAXIMUM APPLIED CYCLIC STRESS o Primary	MN/m^2 ksi	1080 156	1130 164	1190 172	1210 176
o Secondary	MN/m^2 ksi	1080 156	1080 156	1080 156	1080 156
FAILURE STRESS o Gross Section	MN/m^2 ksi	1070 155	1120 162	1180 172	1200 174
o Net Section (Approximate)	MN/m^2 ksi	1340 195	1330 193	1480 215	1435 208
PRIMARY INITIAL STRESS INTENSITY	$(MN/m^2)\sqrt{m}$ $ksi\sqrt{in}$	142 129	154 140	162 147	166 151
NUMBER OF MISSIONS TO FAILURE		>90	30	39	11
INITIAL FLAW DIMENSIONS o Flaw Length, 2c	mm in	28.09 1.106	28.47 1.121	29.49 1.161	28.63 1.128
o Flaw Depth, a	mm in	5.89 .212	5.92 .233	5.72 .225	5.74 .226
o $(a/2c)_i$		.192	.208	.194	.201
o Maximum Initial (a/Q)	mm in	4.55 .179	4.88 .192	4.90 .193	4.88 .192
FINAL FLAW DIMENSIONS o Flaw Length at Surface	mm in	31.22 1.229	22.67 1.168	31.90 1.256	29.34 1.155
o Maximum Flaw Length	mm in	34.98 1.377	30.71 1.209	33.05 1.301	30.56 1.203
o Flaw Depth, a	mm	6.22* 6.50 7.21	6.50	6.88	6.68
	in	.245 .256 .284	.256	.271	.263
o $(a/2c)_f$		.201	.219	.216	.228

* An additional 200 cycles were applied to this specimen at a stress level of 689.5 MN/m^2 (100ksi) to mark the location of the crack front after 40 pairs of stress cycles (i.e., 80 cycles at MEOP). The reported values of crack depth represent the position of the crack after this cyclic history.

TABLE B-2 CRACK PROPAGATION DATA FOR 18 NICKEL MARAGING STEEL - LOAD CYCLING WITH TEMPERATURE CYCLING TO 589°K

SPECIMEN NO.		TM1	TM2	TM3	TM4
PROOF FACTOR, α		1.00	1.05	1.10	1.13
LABORATORY ENVIRONMENT					
o Temperature	°K	299	297	298	300
	°F	78	76	77	80
o Relative Humidity (%)		63	34	45	50
MAXIMUM APPLIED CYCLIC STRESS					
o Primary	MN/m^2	1080	1130	1190	1210
	ksi	156	164	172	176
o Secondary	MN/m^2	1080	1080	1080	1080
	ksi	156	156	156	156
FAILURE STRESS					
o Gross Section	MN/m^2	1120	1170	1180	1210
	ksi	163	169	171	176
o Net Section (Approximate)	MN/m^2	1480	1510	1421	1450
	ksi	215	219	206	210
PRIMARY INITIAL STRESS INTENSITY	$(MN/m^2)\sqrt{m}$	145	153	160	165
	$ksi\sqrt{in}$	132	139	145	150
NUMBER OF MISSIONS TO FAILURE		>40	>40	19	7
INITIAL FLAW DIMENSIONS					
o Flaw Length, 2c	mm	28.65	28.25	28.02	28.45
	in				
o Flaw Depth, a	mm	5.74	5.84	5.69	5.61
	in	.225	.230	.224	.221
o $(a/2c)_i$		.200	.207	.203	.197
o Maximum Initial (a/Q)	mm	4.75	4.83	4.78	4.83
	in	.187	.190	.188	.190
FINAL FLAW DIMENSIONS					
o Flaw Length at Surface	mm	30.35	30.15	29.11	28.75
	in	1.195	1.187	1.146	1.132
o Maximum Flaw Length	mm	31.57	31.42	31.39	31.01
	in	1.243	1.237	1.236	1.221
o Flaw Depth, a	mm	7.19	7.24	6.63	6.43
	in	.283	.285	.261	.253
o $(a/2c)_f$		.237	.240	.228	.224

TABLE B-3 CRACK PROPAGATION DATA FOR 18 NICKEL MARAGING STEEL - LOAD CYCLING WITH TEMPERATURE CYCLING TO 589°K AND WITH 3.5% SYNTHETIC SEA WATER

SPECIMEN NO.		STM1	STM2	STM3	STM4
PROOF FACTOR, α		1.00	1.05	1.10	1.13
LABORATORY ENVIRONMENT					
o Temperature	°K	300	NA	300	297
	°F	80	NA	80	76
o Relative Humidity (%)		23	NA	51	34
MAXIMUM APPLIED CYCLIC STRESS					
o Primary	MN/m^2	1080	1130	1190	1210
	ksi	156	164	172	176
o Secondary	MN/m^2	1080	1080	1080	1080
	ksi	156	156	156	156
FAILURE STRESS					
o Gross Section	MN/m^2	1060	1120	1180	1210
	ksi	154	162	171	176
o Net Section (Approximate)	MN/m^2	1303	1350	1460	1440
	ksi	189	196	211	209
PRIMARY INITIAL STRESS INTENSITY	$(MN/m^2)\sqrt{m}$	147	154	160	166
	$ksi\sqrt{in}$	134	140	145	151
NUMBER OF MISSIONS TO FAILURE		31	30	22	2
INITIAL FLAW DIMENSIONS					
o Flaw Length, 2c	mm	28.88	28.63	28.65	28.63
	in	1.137	1.127	1.128	1.127
o Flaw Depth, a	mm	6.02	5.87	5.59	5.77
	in	.237	.231	.220	.227
o $(a/2c)_i$		.208	.205	.195	.201
o Maximum Initial (a/Q)	mm	4.90	4.88	4.78	4.90
	in	.193	.192	.188	.193
FINAL FLAW DIMENSIONS					
o Flaw Length at Surface	mm	30.53	30.00	29.62	28.63
	in	1.202	1.181	1.166	1.127
o Maximum Flaw Length	mm	31.75	31.32	34.32	32.54
	in	1.250	1.233	1.351	1.281
o Flaw Depth, a	mm	7.09	6.96	6.73	5.99
	in	.279	.274	.265	.236
o $(a/2c)_f$		.232	.232	.227	.209

TABLE B-4 CRACK PROPAGATION DATA FOR D6AC STEEL - LOAD CYCLING ONLY					
SPECIMEN NO.		D1	D2	D3	D4
PROOF FACTOR, α		1.05	1.10	1.115	1.13
LABORATORY ENVIRONMENT o Temperature o Relative Humidity	°K °F	301-304 83-87 51-59	303 86 53	302 85 53	304 87 51
MAXIMUM APPLIED CYCLIC STRESS o Primary o Secondary	MN/m^2 ksi MN/m^2 ksi	1130 164 1080 156	1190 172 1080 156	1200 174 1080 156	1210 176 1080 156
FAILURE STRESS o Gross Section o Net Section (Approximate)	MN/m^2 ksi MN/m^2 ksi	1130 164 1170 169	1181 171 1210 175	1194 173 1220 177	1213 176 1230 179
PRIMARY INITIAL STRESS INTENSITY	$(MN/m^2)\sqrt{m}$ $ksi\sqrt{in}$	113 103	118 107	120 109	122 111
NUMBER OF MISSIONS TO FAILURE		80	37	11	3
INITIAL FLAW DIMENSIONS o Flaw Length, 2c o Flaw Depth, a o $(a/2c)_i$ o Maximum Initial (a/Q)	mm in mm in mm in	13.17 0.519 3.76 0.148 0.285 2.65 0.104	12.84 0.506 3.71 0.146 0.289 2.62 0.103	13.04 0.513 3.61 0.142 0.277 2.63 0.104	12.88 0.507 3.66 0.144 0.284 2.63 0.104
FINAL FLAW DIMENSIONS o Flaw Length at Surface o Flaw Depth, a o $(a/2c)_f$	mm in mm in	17.87 0.704 6.25 0.246 0.350	15.68 0.617 5.57 0.219 0.355	14.75 0.581 5.13 0.202 0.348	13.71 0.540 4.55 0.179 0.332

TABLE B-5 CRACK PROPAGATION DATA FOR D6AC STEEL - LOAD CYCLING WITH TEMPERATURE CYCLING TO 589°K					
SPECIMEN NO.		TD1	TD2	TD3	TD4
PROOF FACTOR, α		1.03	1.05	1.10	1.113
LABORATORY ENVIRONMENT					
o Temperature	°K	304-305	304	301	299
	°F	87-89	88	82	79
o Relative Humidity (%)		49-57	48	45	47
MAXIMUM APPLIED CYCLIC STRESS					
o Primary	MN/m^2	1110	1130	1190	1200
	ksi	161	164	172	174
o Secondary	MN/m^2	1080	1080	1080	1080
	ksi	156	156	156	156
FAILURE STRESS					
o Gross Section	MN/m^2	1107	1121	1183	1182
	ksi	160	162	171	171
o Net Section (Approximate)	MN/m^2	1140	1150	1210	1200
	ksi	165	167	175	175
PRIMARY INITIAL STRESS INTENSITY	$(MN/m^2)\sqrt{m}$	110	114	118	122
	ksi $\sqrt{in}$	99.9	104	107	111
NUMBER OF MISSIONS TO FAILURE		44	20	15	2
INITIAL FLAW DIMENSIONS					
o Flaw Length, 2c	mm	12.96	13.51	12.98	13.39
	in	0.510	0.532	0.511	0.527
o Flaw Depth, a	mm	3.58	3.70	3.62	3.73
	in	0.141	0.146	0.143	0.147
o $(a/2c)_i$		0.276	0.274	0.279	0.279
o Maximum Initial (a/Q)	mm	2.57	2.68	2.62	2.71
	in	0.101	0.105	0.103	0.101
FINAL FLAW DIMENSIONS					
o Flaw Length at Surface	mm	16.88	16.51	15.07	14.09
	in	0.665	0.650	0.593	0.555
o Flaw Depth, a	mm	6.62	5.52	5.01	4.70
	in	0.261	0.217	0.197	0.185
o $(a/2c)_f$		0.392	0.334	0.332	0.333

TABLE B-6 CRACK PROPAGATION DATA FOR D6AC STEEL - LOAD CYCLING WITH TEMPERATURE CYCLING TO 589°K AND WITH 3.5% SYNTHETIC SEA WATER

SPECIMEN NO.		STD1	STD2	STD3	STD4
PROOF FACTOR, α		1.03	1.05	1.075	1.10
LABORATORY ENVIRONMENT					
o Temperature	°K	302	302-304	300	299
	°F	85	84-88	80	78
o Relative Humidity (%)		41	48-66	47	63
MAXIMUM APPLIED CYCLIC STRESS					
o Primary	MN/m^2	1110	1130	1160	1190
	ksi	161	164	168	172
o Secondary	MN/m^2	1080	1080	1080	1080
	ksi	156	156	156	156
FAILURE STRESS					
o Gross Section	MN/m^2	1103	1129	1143	1177
	ksi	160	164	166	171
o Net Section (Approximate)	MN/m^2	1140	1160	1170	1200
	ksi	165	168	170	174
PRIMARY INITIAL STRESS INTENSITY	$(MN/m^2)\sqrt{m}$	110	114	114	119
	$ksi\sqrt{in}$	100	103	104	108
NUMBER OF MISSIONS TO FAILURE		25	32	17	3
INITIAL FLAW DIMENSIONS					
o Flaw Length, 2c	mm	13.12	13.12	12.80	13.32
	in	0.516	0.517	0.504	0.524
o Flaw Depth, a	mm	3.66	3.66	3.56	3.64
	in	0.144	0.151	0.140	0.143
o $(a/2c)_i$		0.279	0.292	0.278	0.273
o Maximum Initial (a/Q)	mm	2.60	2.65	2.56	2.67
	in	0.103	0.105	0.101	0.105
FINAL FLAW DIMENSIONS					
o Flaw Length at Surface	mm	17.35	17.34	15.22	14.00
	in	0.683	0.683	0.599	0.551
o Flaw Depth, a	mm	5.87	6.00	5.39	4.34
	in	0.231	0.236	0.212	0.171
o $(a/2c)_f$		0.338	0.346	0.354	0.310

APPENDIX C

FRACTOGRAPHS OF SURFACE FLAW SPECIMENS

The fracture surfaces of surfaced flawed specimens subjected to cyclic loading are shown in the following photographs. All specimens were photographed using a conventional macrocamera, and three specimens of each alloy were selected for examination with the SEM. The specimens selected are listed in Table C-1. These three specimens represented each of the following test conditions: load cycling; load plus temperature cycling; and load plus temperature cycling plus salt water. All three specimens were cycled at the same primary applied stress level - - i.e., 1.05 MEOP.

The predominant feature of all the axial fatigue zones was dimpled fracture, regardless of alloy type or test condition. The low magnification photographs do suggest that classical fatigue striations are present on all fracture surfaces; this type of morphology is typical of materials subjected to high strain amplitudes.

Of the two alloys examined with the SEM, the specimens of 18 Ni maraging steel exhibited a more dimpled and smaller fatigue zone than those of the lower toughness D6AC steel. The morphologies of the fatigue zones of all specimens of each alloy are strikingly similar.

TABLE C-1. SPECIMENS SELECTED FOR SEM EXAMINATION			
ALLOY	SPECIMEN NO.	MISSION CYCLES TO FAILURE	EXPOSURE CONDITION
18 Ni Maraging	M2	30	Load cycling*
	TM2	40	Load and temperature cycling
	STM2	30	Load and temperature cycling and salt water
D6AC	D1	80	Load cycling
	TD2	20	Load and temperature cycling
	STD2	32	Load and temperature cycling and salt water

* The maximum cyclic load was identical for all specimens examined - i.e., 1.05 MEOP (1130 MN/m^2 or 164 ksi)

Specimen M1
- Cycled @ MEOP
- >90 Missions to Failure

Specimen M2
- Cycled @ 1.05 MEOP
- 30 Missions to Failure

Specimen M3
- Cycled @1.10 MEOP
- 39 Missions to Failure

Specimen M4
- Cycled @ 1.13 MEOP
- 11 Missions to Failure

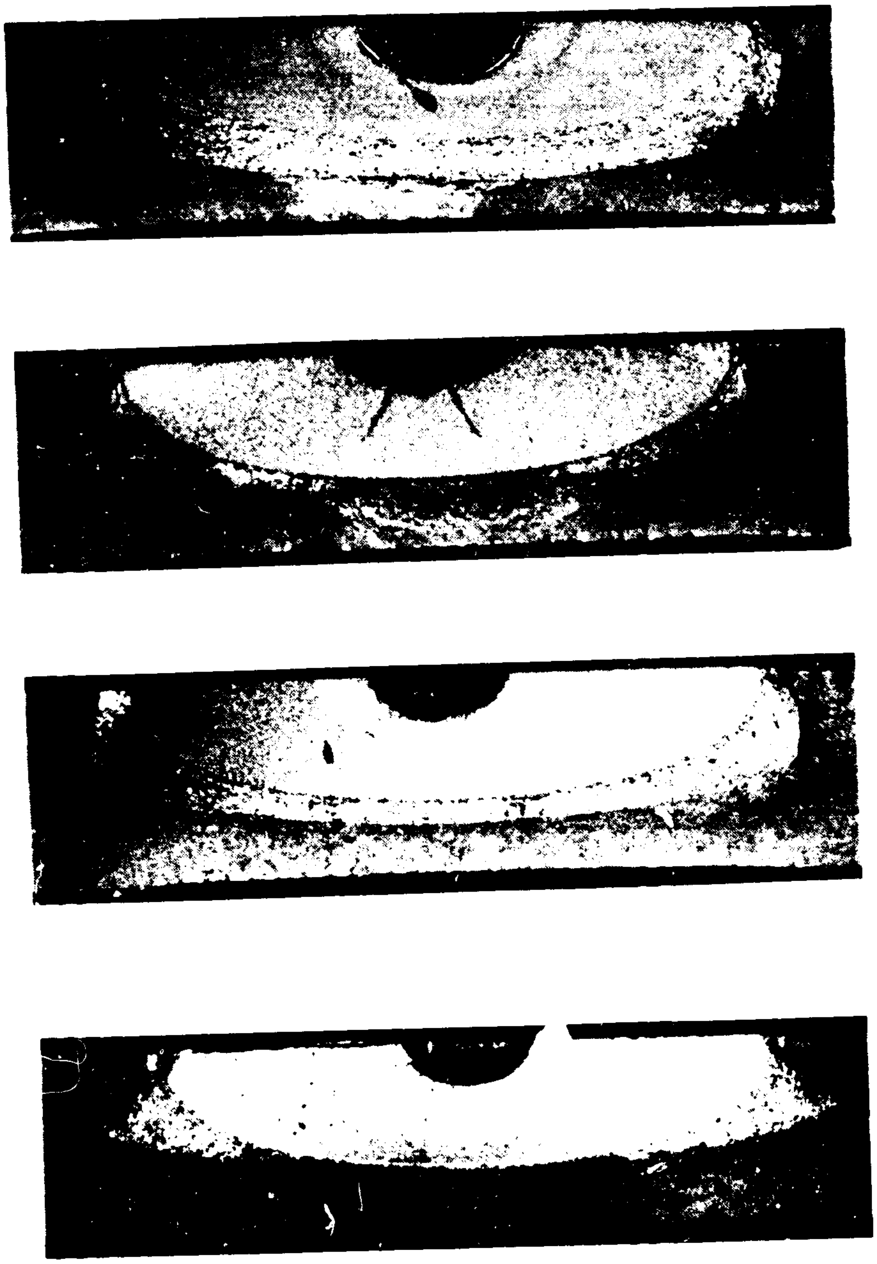

FIGURE C-1
FRACTURE SURFACES OF 18 NICKEL MARAGING STEEL SPECIMENS AFTER LOAD CYCLING (X3)

Specimen TM1

- Load Cycling @ MEOP
- Temperature Cycling to 589°K
- >40 Missions to Failure

Specimen TM2

- Load Cycling @ 1.05 MEOP
- Temperature Cycling to 589°K
- >40 Missions to Failure

Specimen TM3

- Load Cycling @ 1.10 MEOP
- Temperature Cycling to 589°K
- 19 Missions to Failure

Specimen TM4

- Load Cycling @ 1.13 MEOP
- Temperatue Cycling to 589°K
- 7 Missions to Failure

FIGURE C-2
FRACTURE SURFACES OF 18 NICKEL MARAGING STEEL SPECIMENS AFTER LOAD AND TEMPERATURE CYCLING (X3)

Specimen STM1
- Load Cycling @ MEOP
- Temperature Cycling to 589^{o}K
- Exposed to Synthetic Sea Water
- 31 Missions to Failure

Specimen STM2
- Load Cycling @ 1.05 MEOP
- Temperature Cycling to 589^{o}K
- Exposed to Synthetic Sea Water
- 30 [illegible]sions to Failure

Specimen STM3
- Load Cycling @ 1.10 MEOP
- Temperature Cycling to 589^{o}K
- Exposed to Synthetic Sea Water
- 22 Missions to Failure

Specimen STM4
- Load Cycling @ 1.13 MEOP
- Temperature Cycling to 589^{o}K
- Exposed to Synthetic Sea Water
- 2 Missions to Failure

FIGURE C-3
FRACTURE SURFACES OF 18 NICKEL MARAGING STEEL AFTER LOAD AND TEMPERATURE CYCLING WITH SALT WATER (X3)

Specimen D1
- Cycled @ 1.05 MEOP
- 80 Missions to Failure

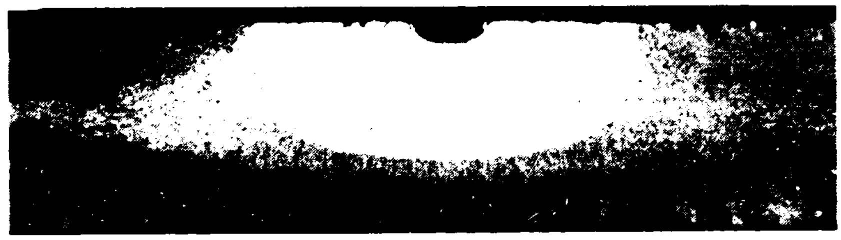

Specimen D2
- Cycled @ 1.10 MEOP
- 37 Missions to Failure

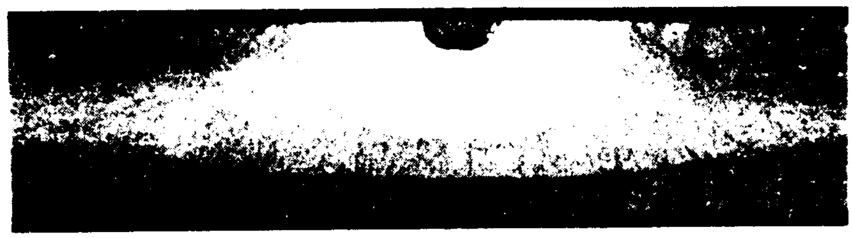

Specimen D3
- Cycled @ 1.115 MEOP
- 11 Missions to Failure

Specimen D4
- Cycled @ 1.13 MEOP
- 3 Missions to Failure

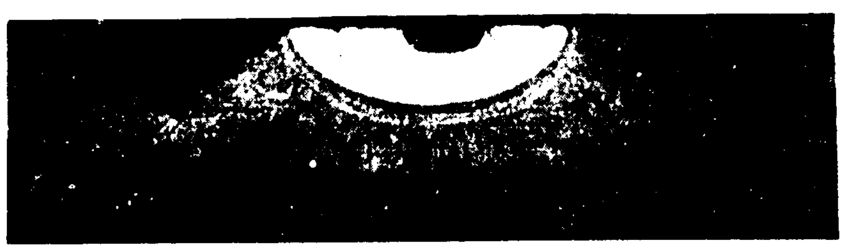

FIGURE C 4
FRACTURE SURFACES OF D6AC STEEL SPECIMENS
AFTER LOAD CYCLING (X3)

Specimen TD1
- Load Cycling @ 1.03 MEOP
- Temperature Cycling to 589°K
- 44 Missions to Failure

Specimen TD2
- Load Cycling @ 1.05 MEOP
- Temperature Cycling to 589°K
- 20 Missions to Failure

Specimen TD3
- Load Cycling @ 1.10 MEOP
- Temperature Cycling to 589°K
- 15 Missions to Failure

Specimen TD4
- Load Cycling @ 1.115 MEOP
- Temperature Cycling to 589°K
- 2 Missions to Failure

FIGURE C-5
FRACTURE SURFACES OF D6AC STEEL SPECIMENS AFTER LOAD AND TEMPERATURE CYCLING (X3)

Specimen STD1

- Load Cycling @ 1.03 MEOP
- Temperature Cycling to 589°K
- Exposed to Synthetic Sea Water
- 25 Missions to Failure

Specimen STD 2

- Load Cycling @ 1.05 MEOP
- Temperature Cycling to 589°K
- Exposed to Synthetic Sea Water
- 32 Missions to Failure

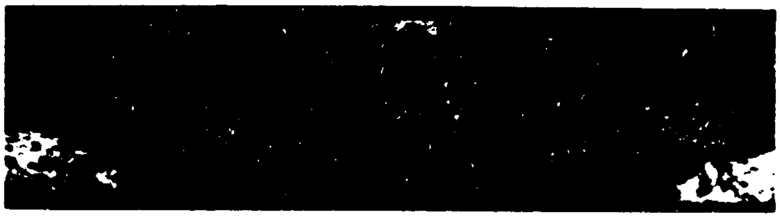

Specimen STD3

- Load Cycling @ 1.075 MEOP
- Temperature Cycling to 589°K
- Exposed to Synthetic Sea Water
- 17 Missions to Failure

Specimen STD4

- Load Cycling @ 1.10 MEOP
- Temperature Cycling to 589°K
- Exposed to Synthetic Sea Water
- 3 Missions to Failure

FIGURE C-6
FRACTURE SURFACES OF D6AC STEEL SPECIMENS AFTER LOAD AND TEMPERATURE CYCLING WITH SALT WATER (X3)

Specimen M2
- Load Cycling Only
- 30 Missions to Failure

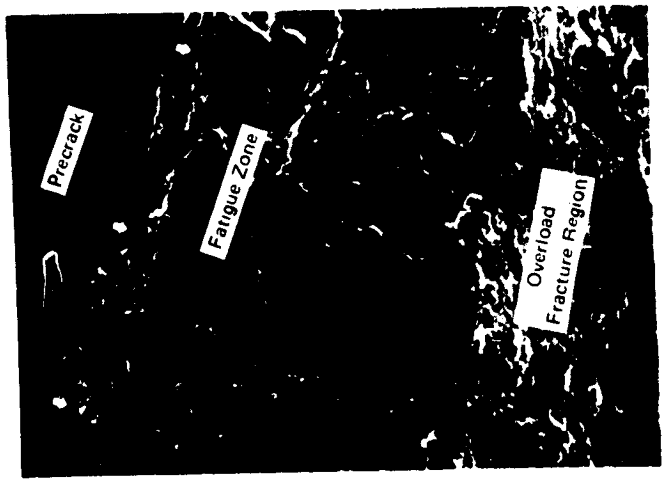

Specimen TM2
- Load and Temperature Cycling
- >40 Missions to Failure

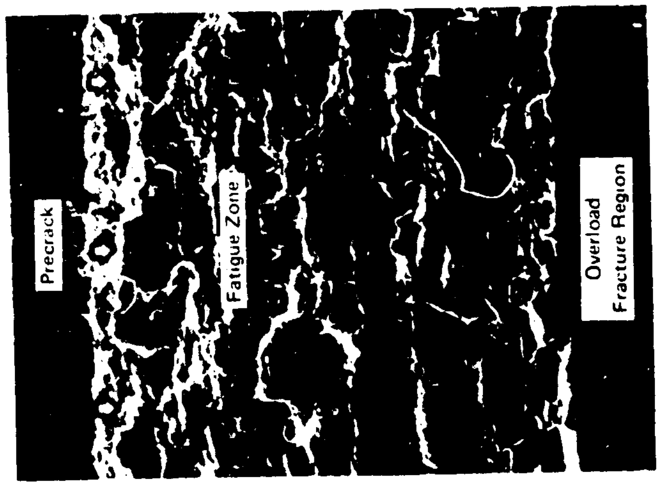

Specimen STM2
- Load and Temperature Cycling with Salt Water
- 30 Missions to Failure

Note: The arrows indicate the direction of crack propagation

FIGURE C-7
FRACTURE SURFACES OF 18 NICKEL MARAGING STEEL SPECIMENS AFTER MISSION CYCLING AT 1.05 MEOF (X60)

Specimen M2
- Load Cycling Only
- 30 Missions to Failure

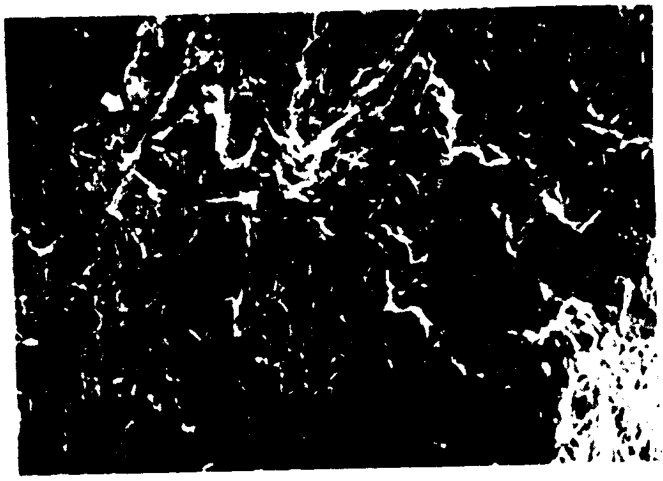

Specimen TM2
- Load and Temperature Cycling
- >40 Missions to Failure

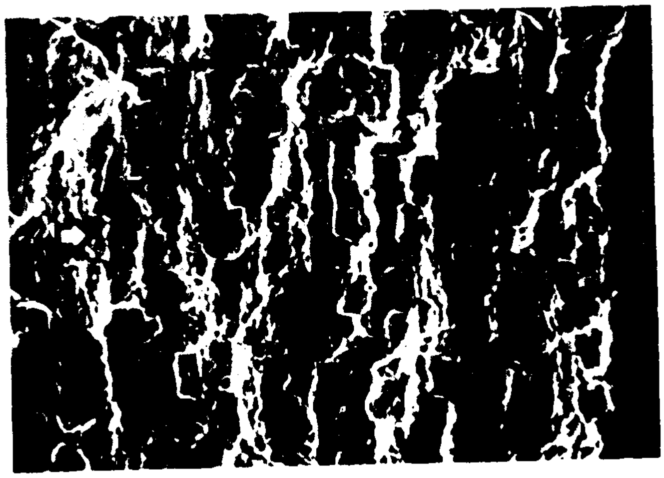

Specimen STM2
- Load and Temperature Cycling with Salt Water
- 30 Missions to Failure

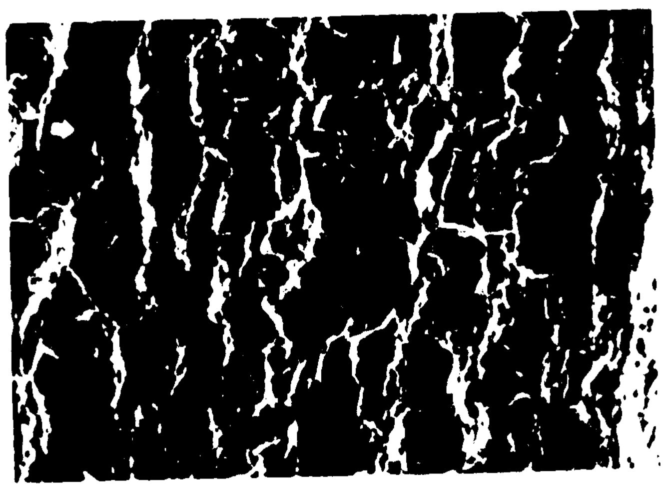

FIGURE C 8
FRACTURE SURFACES OF 18 NICKEL MARAGING STEEL SPECIMENS AFTER MISSION CYCLING AT 1.05 MEOP (X100)

Specimen M2
- Load Cycling Only
- 30 Missions to Failure

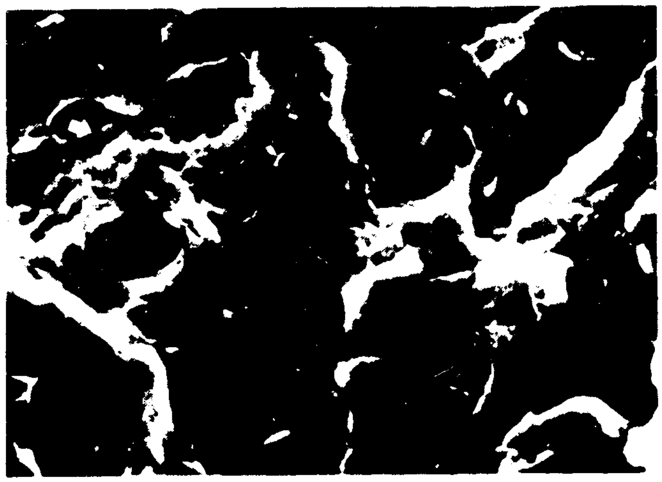

Specimen TM2
- Load and Temperature Cycling
- 40 Missions to Failure

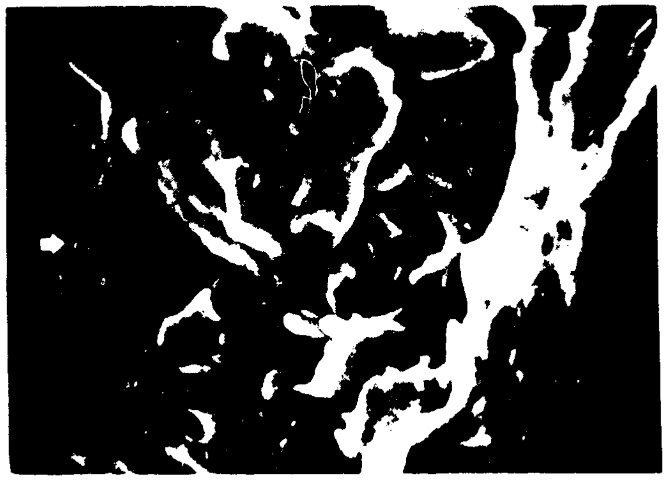

Specimen STM2
- Load and Temperature Cycling with Salt Water
- 30 Missions to Failure

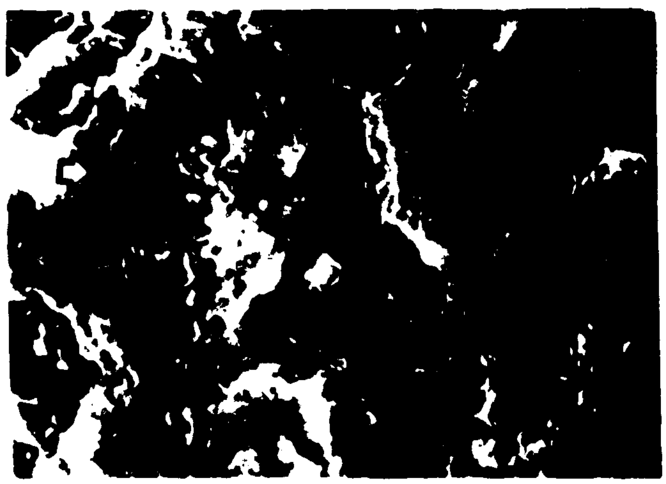

FIGURE C-10
FRACTURE SURFACES OF 18 NICKEL MARAGING STEEL SPECIMENS AFTER MISSION CYCLING AT 1.05 MEOP (X3000)

Specimen M2

- Load Cycling Only
- 30 Missions to Failure

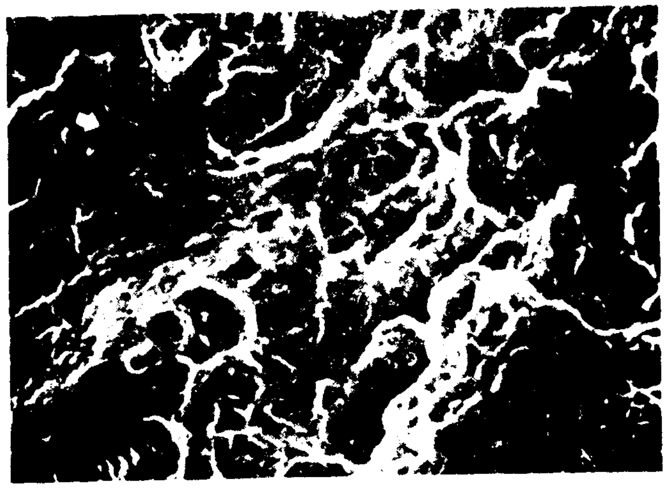

Specimen TM2

- Load and Temperature Cycling
- >40 Missions to Failure

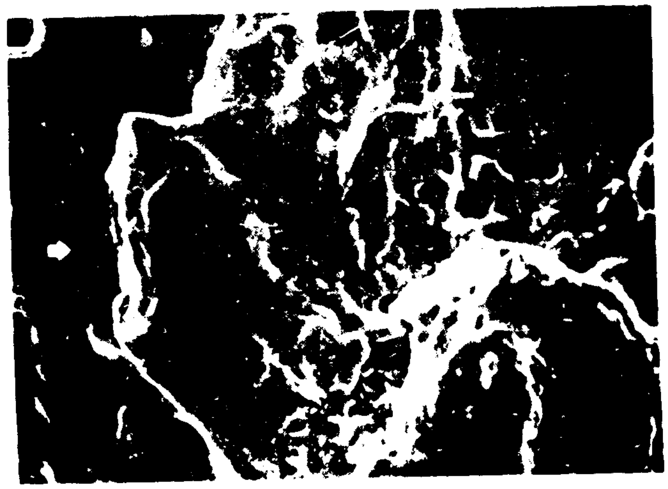

Specimen STM2

- Load and Temperature Cycling with Salt Water
- 30 Missions to Failure

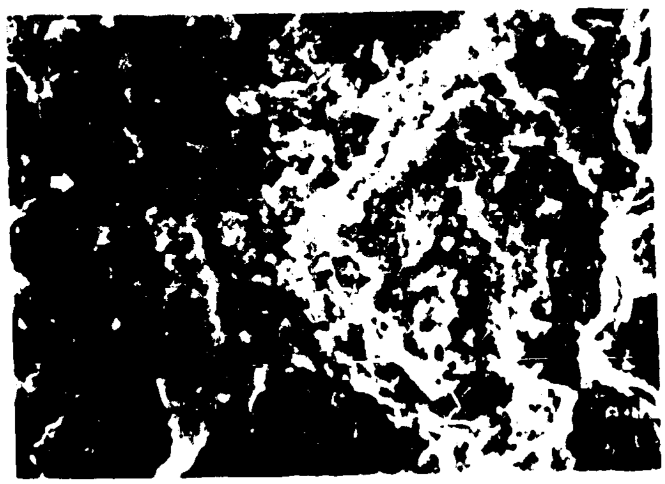

FIGURE C-9
FRACTURE SURFACES OF 18 NICKEL MARAGING STEEL SPECIMENS AFTER MISSION CYCLING AT 1.05 MEOP (X1000)

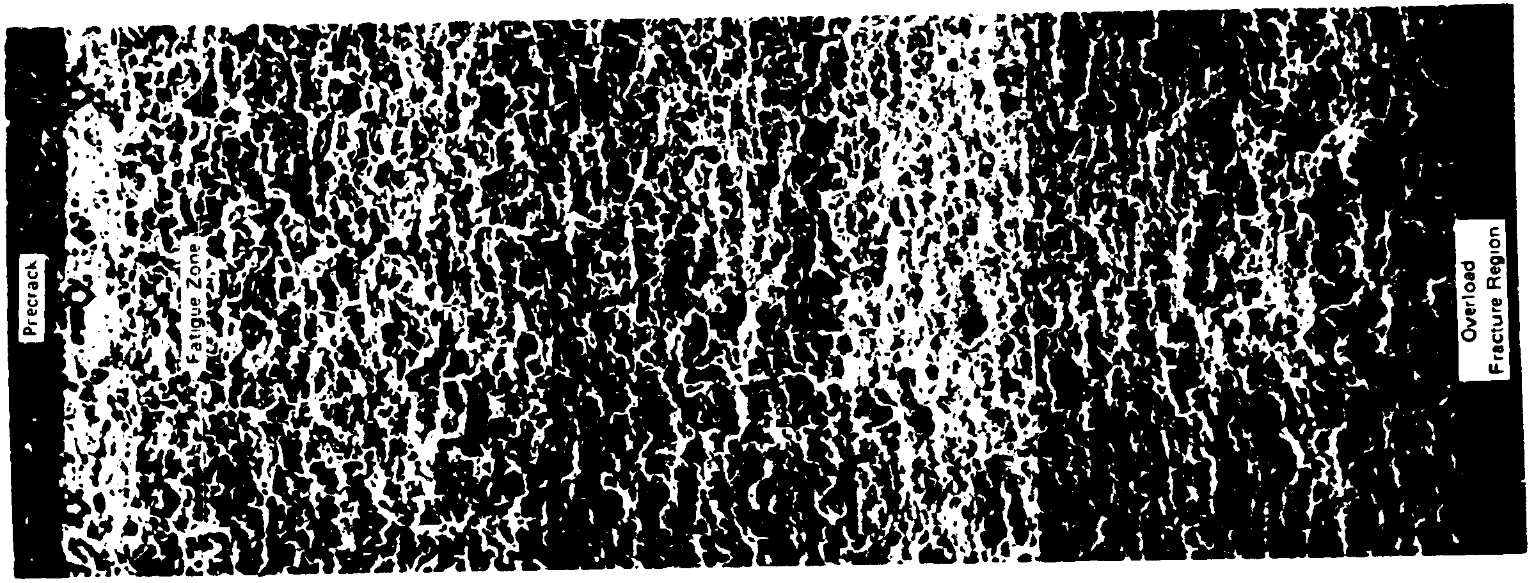

Specimen D1 – Load Cycling Only, 80
Missions to Failure

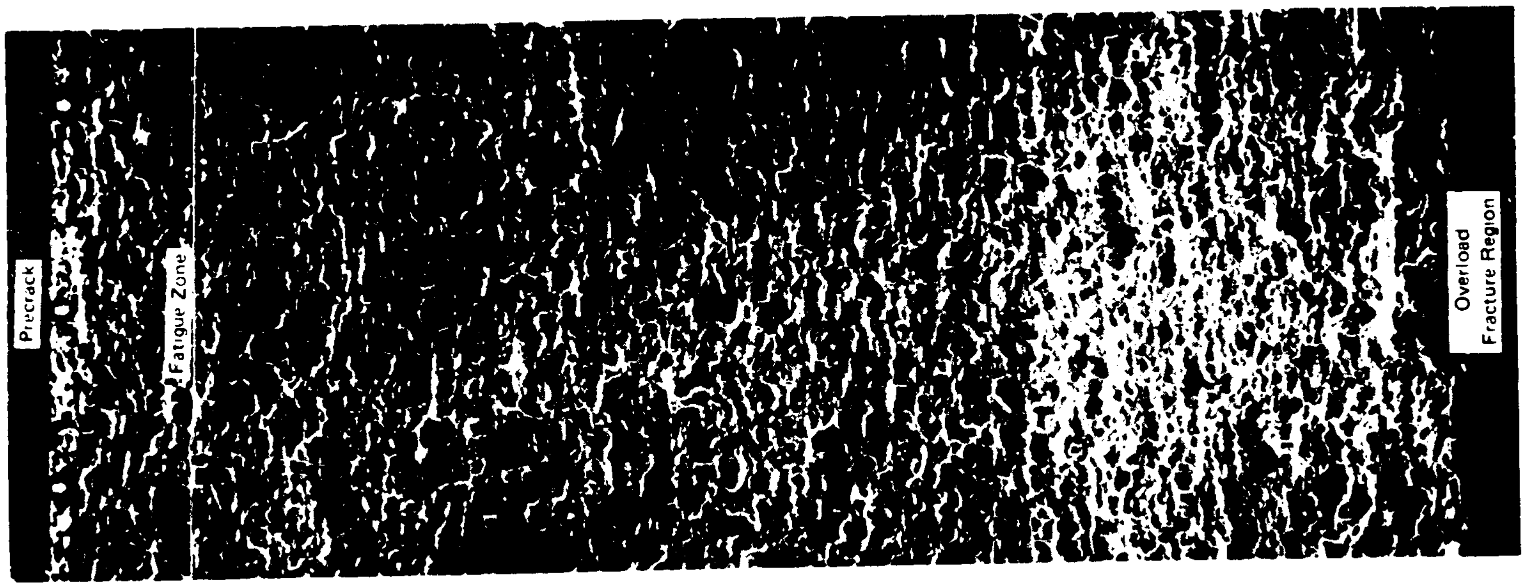

Specimen TD2 – Load and Temperature
Cycling, 20 Missions to Failure

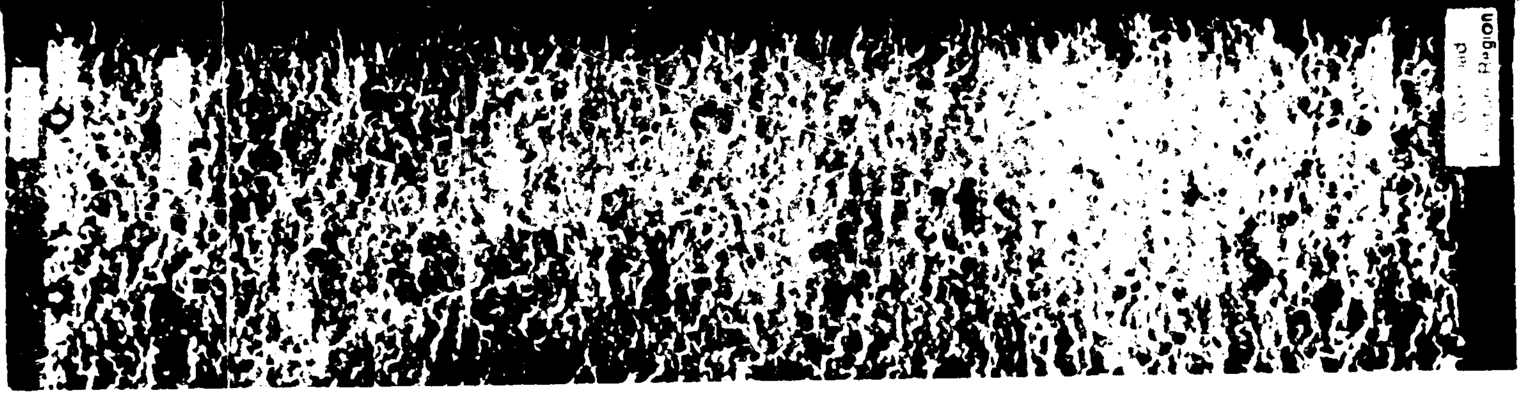

Specimen TD2 – Load and Temperature
Cycling, 20 Missions to Failure

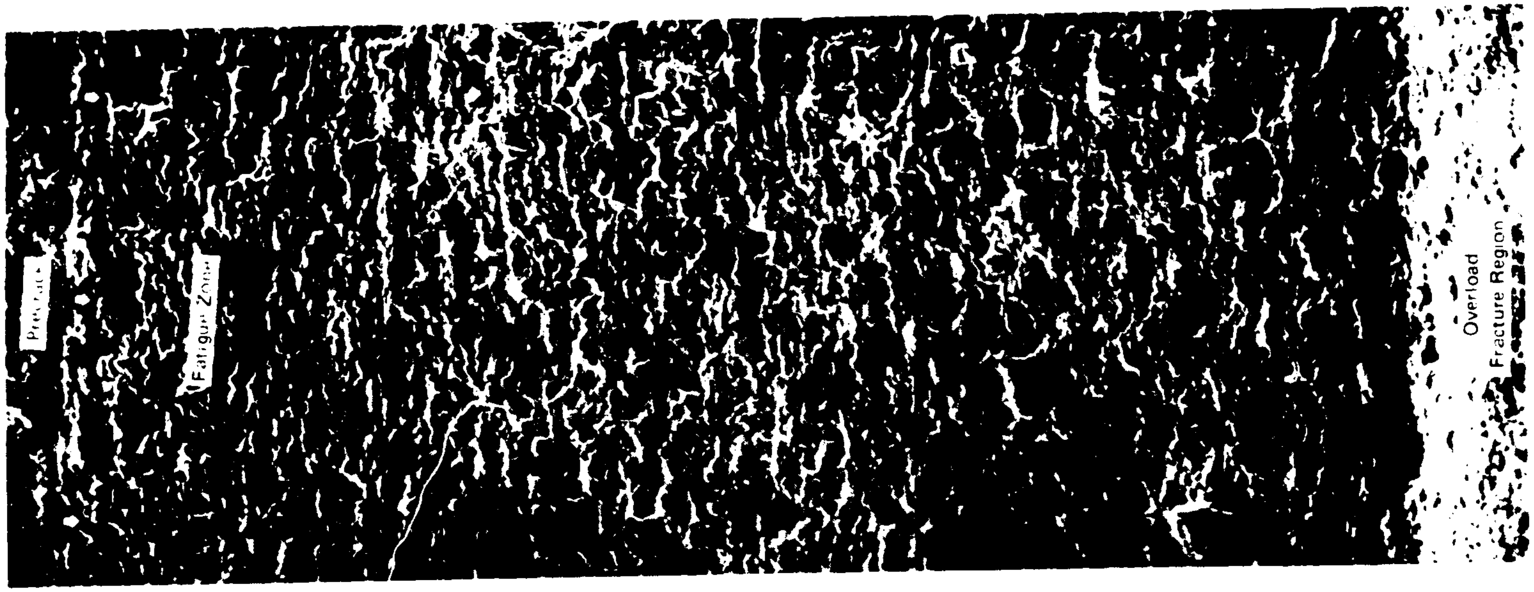

Specimen STD2 – Load and Temperature
Cycling, 32 Missions to Failure

FIGURE C-11
FRACTURE SURFACES OF D6AC STEEL SPECIMENS
AFTER MISSION CYCLING AT 1.05 MEOP (X60)

GP73 3377 42

FIGURE B-11

Specimen D1
- Load Cycling Only
- 80 Missions to Failure

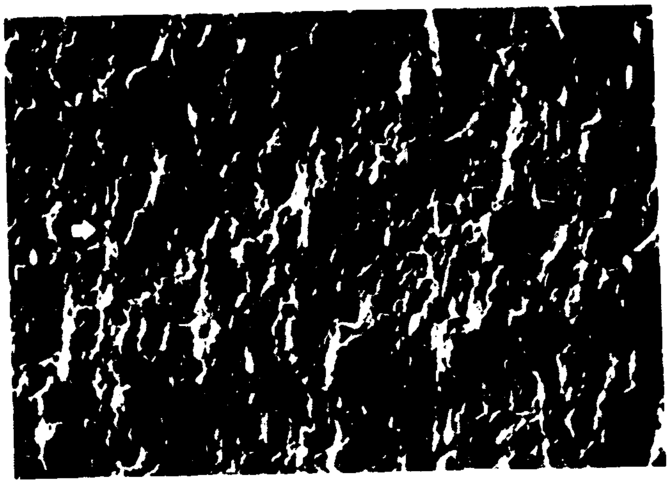

Specimen TD2
- Load and Temperature Cycling
- 20 Missions to Failure

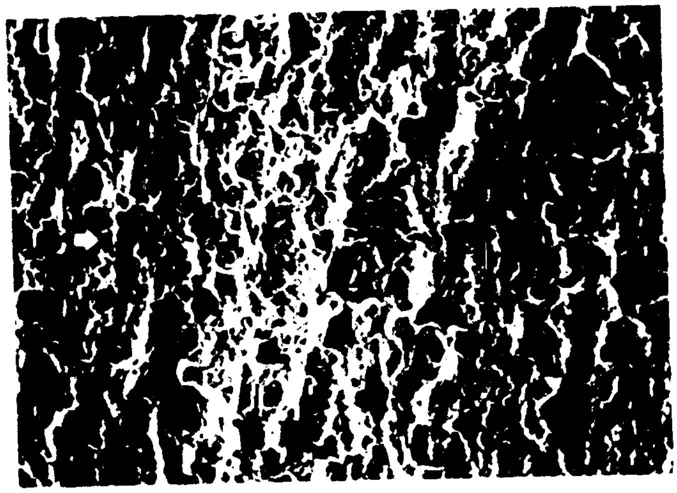

Specimen STD2
- Load and Temperature Cycling with Salt Water
- 32 Missions to Failure

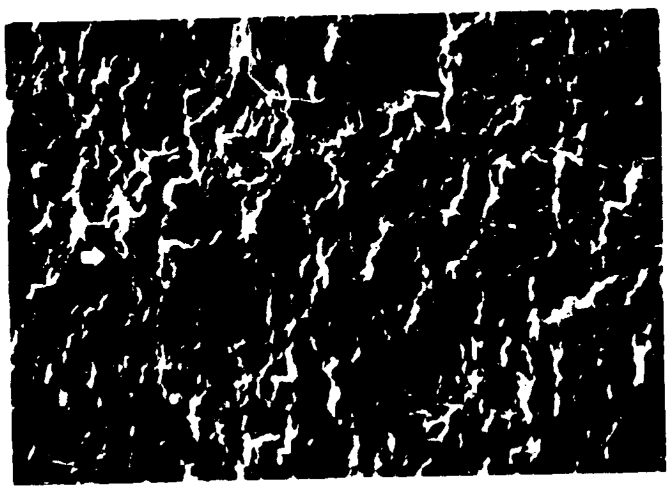

FIGURE C-12
FRACTURE SURFACES OF D6AC STEEL SPECIMENS AFTER MISSION CYCLING AT 1.05 MEOP (X100)

Specimen D1
- Load Cycling Only
- 80 Missions to Failure

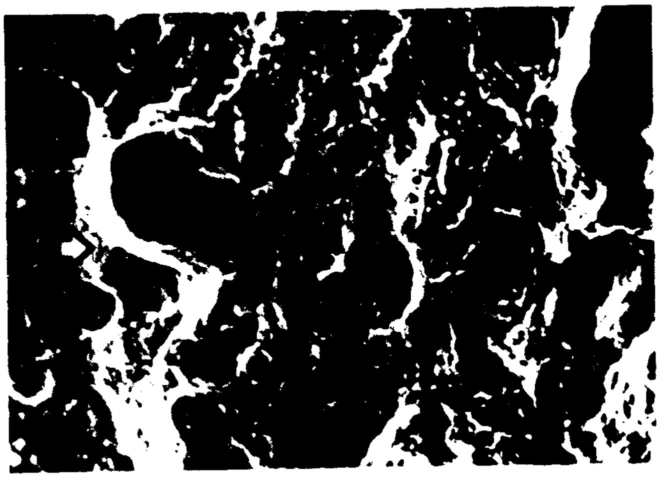

Specimen TD2
- Load and Temperature Cycling
- 20 Missions to Failure

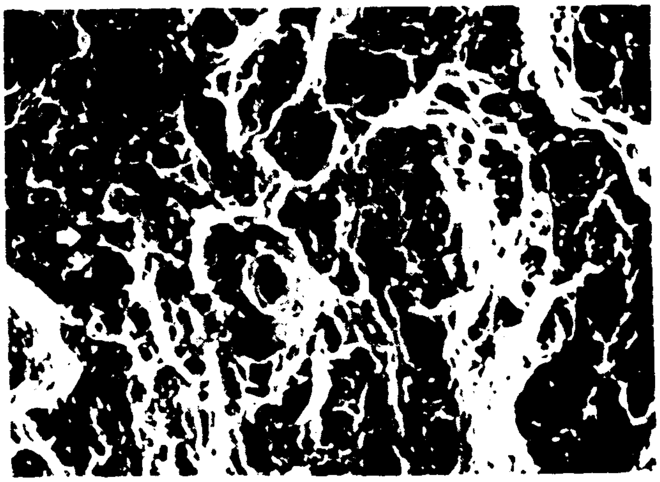

Specimen STD2
- Load and Temperature Cycling with Salt Water
- 32 Missions to Failure

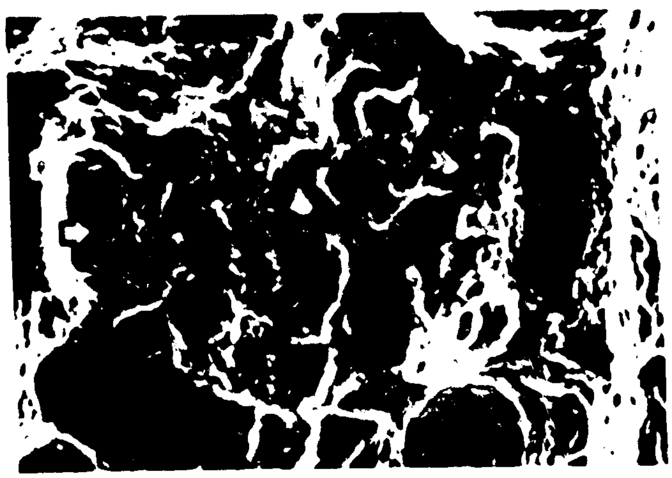

FIGURE C-13
FRACTURE SURFACES OF D6AC STEEL SPECIMENS AFTER MISSION CYCLING AT 1.05 MEOP (X1000)

Specimen D1
- Load Cycling Only
- 80 Missions to Failure

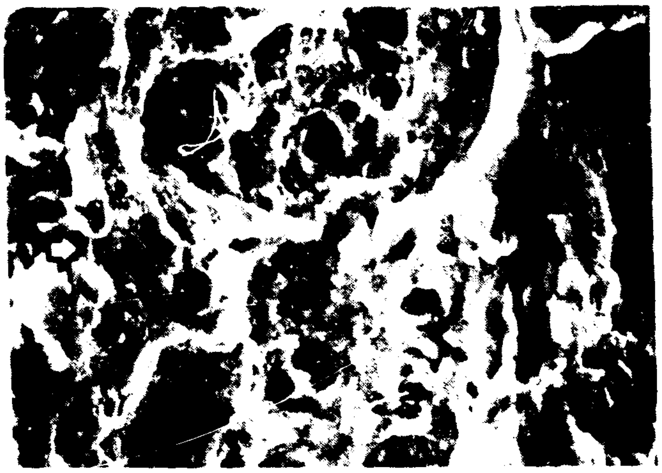

Specimen TD2
- Load and Temperature Cycling
- 20 Missions to Failure

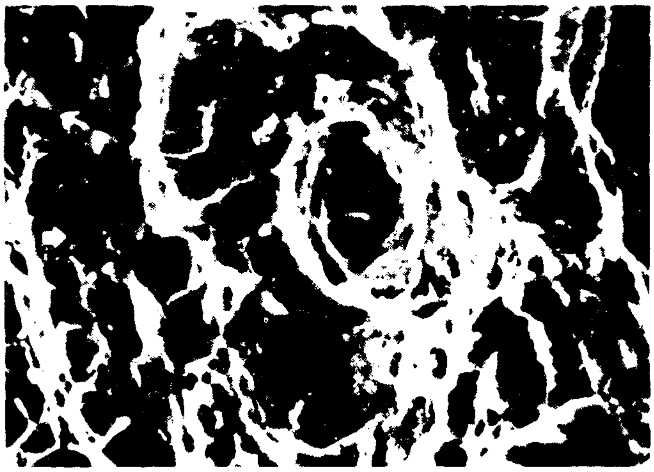

Specimen STD2
- Load and Temperature Cycling with Salt Water
- 32 Missions to Failure

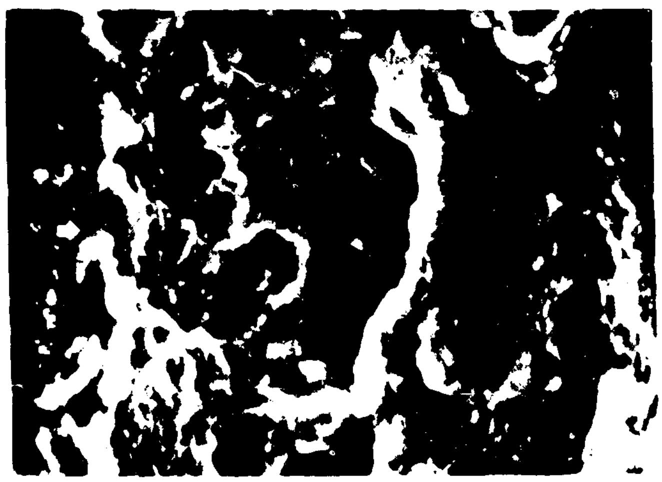

FIGURE C-14
FRACTURE SURFACES OF D6AC STEEL SPECIMENS AFTER MISSION CYCLING AT 1.05 MEOP (X3000)

Specimen D1
- Load Cycling Only
- 80 Missions to Failure

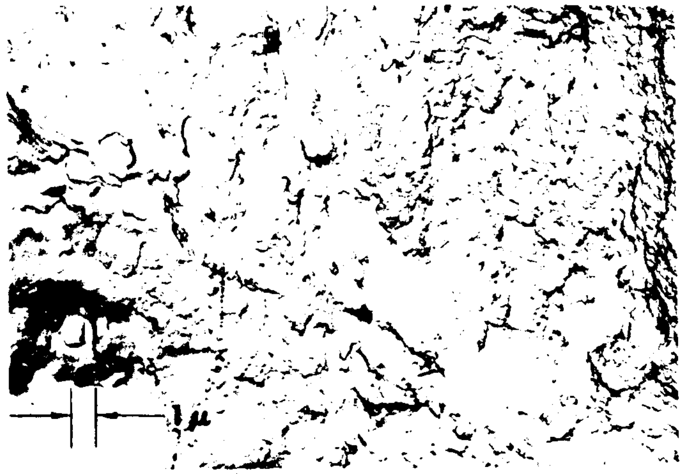

Specimen TD2
- Load and Temperature Cycling
- 20 Missions to Failure

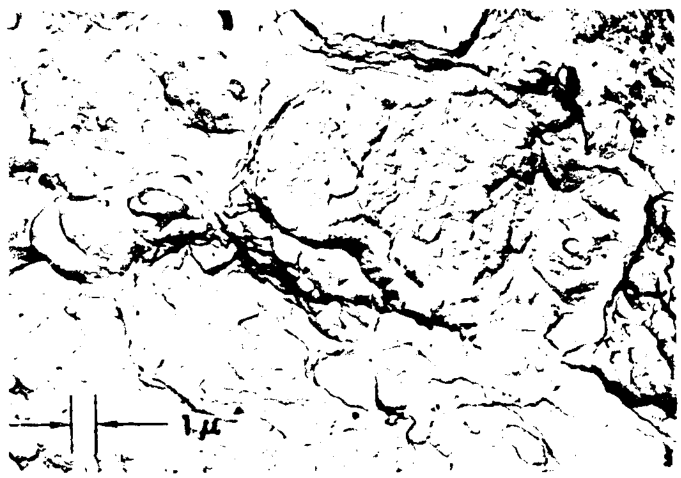

Specimen STD2
- Load and Temeprature Cycling with Salt Water
- 32 Missions to Failure

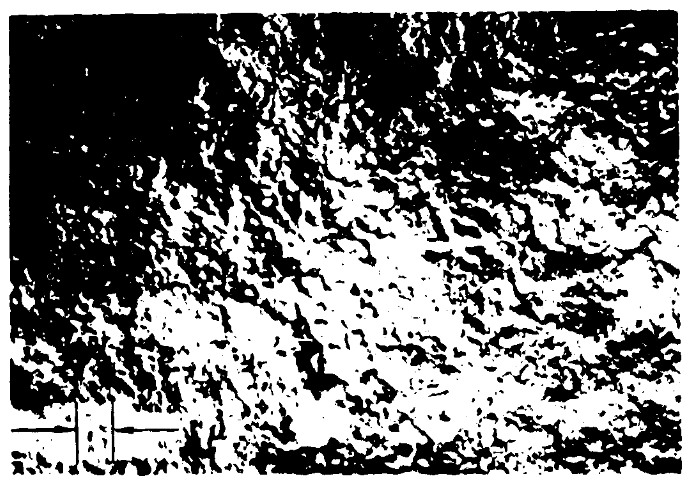

FIGURE C-15
TWO STAGE PLASTIC-CARBON REPLICAS OF D6AC STEEL SPECIMENS AFTER MISSION CYCLING AT 1.05 MEOP (X3300)

APPENDIX D

CONVERSION FACTORS

TO CONVERT FROM	TO	MULTIPLY BY
Fahrenheit	kelvin	$t_K = (5/9)(t_F + 459.67)$
foot	meter	3.048×10^{-1}
foot	kilometers	3.048×10^{-4}
inch	millimeter	$2.54 \times 10^{+1}$
lbf	newton	4.448
$lbf/inch^2$ (psi)	$newton/meter^2$	6.895×10^3
psi $\sqrt{in}$	$(MN/m^2)\sqrt{m}$	1.099